iScience

Drosophila parasitoids go to space: Unexpected effects of spaceflight on hosts and their parasitoids --Manuscript Draft--

Manuscript Number:	ISCIENCE-D-23-03001R4
Full Title:	Drosophila parasitoids go to space: Unexpected effects of spaceflight on hosts and their parasitoids
Article Type:	Research Article
Corresponding Author:	Shubha Govind, Ph.D. The City College of New York New York, New York UNITED STATES
First Author:	Jennifer Chou
Order of Authors:	Jennifer Chou
	Johnny R Ramroop
	Amanda M Saravia-Butler
	Brian Wey
	Matthew P Lera
	Medaya L Torres
	Mary Ellen Heavner
	Janani S Iyer
	Siddhita D Mhatre
	Sharmila Bhattacharya
	Shubha Govind, Ph.D.
Abstract:	While fruit flies (Drosophila melanogaster) and humans exhibit immune system dysfunction in space, studies examining their immune systems' interactions with natural parasites in space are lacking. Drosophila parasitoid wasps modify blood cell function to suppress host immunity. In this study, naïve and parasitized ground and space flies from a tumor-free control and a blood tumor-bearing mutant strain were examined. Inflammation-related genes were activated in space in both fly strains. Whereas control flies did not develop tumors, tumor burden increased in the space-returned tumor-bearing mutants. Surprisingly, control flies were more sensitive to spaceflight than mutant flies; many of their essential genes were downregulated. Parasitoids appeared more resilient than fly hosts, and spaceflight did not significantly impact wasp survival or the expression of their virulence genes. Previously undocumented mutant wasps with novel wing color, wing shape, and ovipositor morphology were isolated post-flight and will be invaluable for host-parasite studies on Earth.
Additional Information:	
Question	Response
Standardized datasets A list of datatypes considered standardized under Cell Press policy is	Yes
available <u>here</u> . Does this manuscript report new standardized datasets?	
Reviewers must have anonymous access to these standardized datasets that is free-of-cost. Please provide dataset	Data from bulk RNA-Seq experiments can be accessed from NASA's Open Science Data Repository (https://osdr.nasa.gov/bio/repo).

locations and instructions for access here. If applicable, include accession numbers and reviewer tokens.Please consult these Author's guides for more information: "Standardized datatypes, datatype-specific repositories, and general-purpose repositories recommended by Cell Press" and "How standardized datasets and original code accompany Cell Press manuscripts from submission through publication" or email us at iscience @cell.com.
emsp;as follow-up to "Standardized datasets

A list of datatypes considered

standardized under Cell Press policy is available https://marlin-prod.literatumonline.com/pb-

assets/journals/research/cellpress/data/R

ecommendRepositories.pdf" target="_blank">here. Does this manuscript report new standardized The preview links for the individual projects are as follows:

For Drosophila data: OSD-588, DOI: 10.26030/v9rh-5a70

https://osdr.nasa.gov/bio/repo/data/studies/OSD-588/preview/rujcL1mzrqCtvtX7hobE4OGbNSIy-Lvu

For L. heterotoma data: OSD-609, DOI: 10.26030/5rjq-a347

https://osdr.nasa.gov/bio/repo/data/studies/OSD609/preview/asoFANpyc2AYx0U6PiE1 OZ1MjGGaOPXU

For L. boulardi data OSD-610, DOI: 10.26030/9ee4-6s36

https://osdr.nasa.gov/bio/repo/data/studies/OSD610/preview/32jYx1SaXzpmdFMOW4 oro35diCUBdxoF

Original code

datasets?"

Does this manuscript report original code?

Reviewers must have anonymous access to these original code that is free-of-cost. Please provide code location and instructions for access here.Please consult this Author's guide for more information: "How standardized datasets and original code accompany Cell Press manuscripts from submission through publication" or email us at iscience @cell.com.
br/> as follow-up to "Original code

Does

this manuscript report original code?"

The link for the code is provided in KRT.

Yes



The City College of New York 160 Convent Ave. at 138th Street Marshak Science Bldg New York, NY 10031 212 650-8476 sgovind@ccny.cuny.edu



Department of Biology

PhD Programs in Biology & Biochemistry

Dec 10, 2023

Dr. Oscar Brusa Editor, *iScience*

Dear Dr. Brusa,

Re: "Drosophila parasitoids go to space: Unexpected effects of spaceflight on hosts and their parasitoids" (ISCIENCE-D-23-03001R3).

Responses to your requests for changes are as follows:

- 1. Track changes in the main word document have been accepted.
- 2. An alternative Figure 3 where the panels are rearranged is provided in this version. We prefer this rearranged version over the one submitted on 12-3-2023 as each panel and associated legend will be easier to visualize in this version.
- 3. Extra space on the top of the pages above figures has been removed.

Offer codes 21V2 and 22V3 for reviewing CURRENT-BIOLOGY-D-22-01321 and CURRENT-BIOLOGY-D-22-01321R1 are available to me to cover the Article Processing Charges. If this manuscript is accepted, I would like to use one or both these codes, if possible, as available funds to cover its publication costs are limited.

We look forward to a final decision on the manuscript.

Sincerely, Shubha Govind, PhD Professor of Biology; Member PhD Programs in Biology & Biochemistry Chou et al., "Drosophila parasitoids go to space: Unexpected effects of spaceflight on hosts and their parasitoids" (ISCIENCE-D-23-03001R3).

Please see cover letter.

- 1 Drosophila parasitoids go to space: Unexpected effects of spaceflight on hosts and their
- 2 parasitoids
- 3 Key words: Extracellular vesicles, chitin, Drosophila, gene expression, host, parasite, innate
- 4 immunity, inflammation, immune signaling, International Space Station, matrisome,
- 5 microgravity, mutants, ovipositor, transcriptomes, tumors, space radiation, wasp
- 6 Author List
- 7 Jennifer Chou¹, Johnny R. Ramroop¹, Amanda M. Saravia-Butler^{2,4}, Brian Wey^{1,3},
- 8 Matthew P. Lera⁴, Medaya L. Torres^{4,5}, Mary Ellen Heavner^{1,6}, Janani Iyer^{2,4,7},
- 9 Siddhita D. Mhatre^{2,4}, Sharmila Bhattacharya^{4,8}, Shubha Govind^{1,3,6,*}
- 11 Author affiliations
- ¹Biology Department, The City College of New York, 160 Convent Avenue, New York, NY
- 13 10031, USA

10

24

29

30

- ²KBR NASA Ames Research Center, Moffett Field, CA 94035, USA
- ³PhD Program in Biology, The Graduate Center of the City University of New York, 365 Fifth
- 16 Avenue, New York, NY 10016, USA
- ⁴Space Biosciences Division, NASA Ames Research Center, Moffett Field, CA 94035, USA
- ⁵Bionetics, NASA Ames Research Center, Moffett Field, CA 94035, USA
- ⁶PhD Program in Biochemistry, The Graduate Center of the City University of New York, 365
- 20 Fifth Avenue, New York, NY 10016, USA
- ⁷Universities Space Research Association, Mountain View, CA 94043, USA
- ⁸Present affiliation: Biological and Physical Sciences Division, NASA Headquarters,
- Washington DC 20024, USA
- 25 §Authors with equal contribution
- ^{*}Lead contact: Shubha Govind
- 27 Correspondence: e-mail: sgovind@ccny.cuny.edu
- 28 Telephone Number: +1 212 650 8476 and Fax: +1 212 650 8585

SUMMARY

While fruit flies (*Drosophila melanogaster*) and humans exhibit immune system dysfunction in space, studies examining their immune systems' interactions with natural parasites in space are lacking. *Drosophila* parasitoid wasps modify blood cell function to suppress host immunity. In this study, naïve and parasitized ground and space flies from a tumor-free control and a blood tumor-bearing mutant strain were examined. Inflammation-related genes were activated in space in both fly strains. Whereas control flies did not develop tumors, tumor burden increased in the space-returned tumor-bearing mutants. Surprisingly, control flies were more sensitive to spaceflight than mutant flies; many of their essential genes were downregulated. Parasitoids appeared more resilient than fly hosts, and spaceflight did not significantly impact wasp survival or the expression of their virulence genes. Previously undocumented mutant wasps with novel wing color, wing shape, and ovipositor morphology were isolated post-flight and will be invaluable for host-parasite studies on Earth.

INTRODUCTION

As humans become a space-faring species, they must confront the dual and long-term challenges of microgravity and radiation. Robust immune physiology and intact genomes are vital to the success of manned space exploration efforts. Animals and plants harbor a diverse array of microbial and metazoan pathogens and parasites. While the effects of the space environment in low Earth orbit are documented on many host species, with a focus on humans ¹, the effects of space on the accompanying pathogens and parasites are not known. This question is especially important as immune-compromised humans (and other animal hosts), or those with dysfunctional immunity, venture into space. Experiments with the *Drosophila* model organism and studies on astronauts over the last decade have revealed how highly conserved innate immune functions and mechanisms are altered in space ^{2,3}. These and earlier studies (reviewed in ⁴) also demonstrated that fruit flies can successfully develop in space, opening the system to further inquiry. In this study, we examined the effects of spaceflight on *D. melanogaster* infested with their natural parasitoid wasps that journeyed to and back from the International Space Station, aboard SpaceX-14, on a 34-day mission.

Parasitoid wasps represent a large class of obligate parasitic insects, and many are used in the biocontrol of agricultural pests. The term endoparasitoid refers to the wasp whose preimaginal stages develop within the host larva and pupa. The developing parasitoid (or parasite) eats the host as both continue to develop; the host builds a puparium that a parasite ultimately occupies and emerges from. *Drosophila* larvae and pupae serve as hosts to more than 60 species of such parasitic wasps ⁵. The female wasp's sharp ovipositor pierces the first line of host defense – the larval exoskeleton, made of cuticle – to introduce an egg and venom. This step triggers an encapsulation response in which larval blood cells (hemocytes) of the hosts' innate

immune system (macrophage-like plasmatocytes – called macrophages here – and their derivatives, lamellocytes) cooperate to recognize, surround, melanize, and destroy the wasp egg ⁶. This melanotic capsule itself, composed of dozens of macrophages and lamellocytes, shields the host from the dead parasite as it continues to become an adult fly. Encapsulation, an innate immune response, is conserved across many multicellular animals ^{6,7}.

Encapsulation of the parasite egg by Drosophila larvae is not always fatal to the parasite, as active and passive means to avoid encapsulation have evolved to assure that at least some percentage of parasitic wasp infections are successful. $Leptopilina\ heterotoma\ (Lh)$ is highly successful on many Drosophila species and is considered to be a generalist parasite 8 . Its venom contains spiked extracellular vesicle-like (EV) structures with immune-suppressive activities 9,10 . Lh EVs are surrounded by a phospholipid bilayer, and their protein composition is similar to that of mammalian extracellular vesicles 11,12 . $L.\ boulardi\ (Lb)$ is a specialist parasite and is successful on a narrower host range than $Lh\ ^{8,13}$. Lb EVs also bear spikes, are immune-suppressive, and have a protein profile similar to Lh EVs $^{13-16}$. There is no evidence that either Lb or Lh EV-like structures possess a genome or that they replicate in either the wasp or the host. The protein-coding genes of Lh EVs are present in the wasp genome 12 .

While the venom EVs from both *Lb* and *Lh* are immune suppressive, their effects on hemocytes differ greatly. *Lb* EVs enter lamellocytes and alter lamellocyte shape to suppress encapsulation without killing them ¹⁷. *Lh* EVs, on the other hand, lyse lamellocytes within a few hours after infection ^{18,19}. *Lh* EVs also kill circulating macrophages as well as hemocyte progenitors housed within a small hematopoietic organ called the lymph gland ^{18,20}. Thus, despite differing in the ways they attack host hemocytes, both wasps effectively create immune-deficient hosts, making it conducive for wasp development. In 20-25 days, one adult wasp emerges per fly

pupa; male and female wasps mate as free-living adults, and females then deposit eggs into fly larvae to initiate another generation ^{8,13,21}.

91

92

93

94

95

96

97

98

99

100

101

102

103

104

105

106

107

108

109

110

111

112

113

In this Fruit Fly-03 (FFL-03) spaceflight experiment, we compared the development of two fly strains: one healthy and another suffering from chronic inflammation (CI). The latter strain carries a dominant germline mutation in the Janus kinase (JAK) gene of the JAK-STAT signal transduction pathway. The mutation constitutively activates the fly's innate immune JAK-STAT and Toll signaling pathways ²²⁻²⁴. Components of both pathways are highly conserved in evolution, including humans. Both immune pathways also control hematopoietic development. Their genetic activation in the fly leads to the overgrowth of hematopoietic progenitors. As a result, small granuloma-like tumors form melanized structures that are observed in the larval hemolymph ²³⁻²⁶. In their physical properties, these small tumors are analogous to the hemocyte capsules formed around wasp eggs and are considered to be defective autoimmune reactions to self-tissue ^{27,28}. Tumor growth, inflammatory gene expression, and metabolic inflammation in hop^{Tum-l} larvae are sensitive to aspirin administration ²⁴. Thus, the hop^{Tum-l} background is a 'standin' disease model for animal leukemia and CI ²²⁻²⁴. In humans, aberrant JAK-STAT and Toll-NFkappa B signaling is linked to malignancies, immune deficiency, inflammation, autoimmunity, and cancer and is therefore the focus of therapeutic measures ^{29,30}.

The aims of this study were to: (a) compare how conditions in the International Space

Station (ISS) affect healthy control and CI fly hosts; (b) examine if the development of
endoparasites occurs normally in the ISS; and (c) study if parasite virulence is affected in space.

We report that fewer than expected tumor-free control fruit fly strain returned to Earth, but,
unexpectedly, the tumor-bearing CI strain succeeded in space just as well as ground controls. In
both strains, genes encoding extracellular matrix (ECM) proteins or ECM-associated proteins

(together, matrisome proteins) that contribute to cuticle and chorion structure and function were strongly affected in space, but genes essential for life were downregulated only in the control fruit fly strain. Orthologs of many of these genes have disease relevance in humans. However, inflammation-related genes were activated in both strains, and while the control flies remained free of tumors, the tumor burden in the space-returned CI strain increased. The effects of spaceflight on parasite emergence were minimal, if any, and changes in the expression of virulence genes were modest, at best. The venom activity of *Lh* from space wasps was comparable to that of ground wasps, and their virulence EV particles were normally distributed within the hosts. Visible mutations affecting wing shape, color, and ovipositor integrity were identified in the progeny of space *L. heterotoma*.

Pathogens and parasites pose a threat to astronaut's health during spaceflight. Bacteria reared under microgravity conditions exhibit an increase in virulence ^{31,32}. Thus, in addition to assessing changes in host immune mechanisms, it is important to evaluate changes in pathogen or parasite virulence in space in the context of their natural hosts. Our studies show that metazoan parasites can develop normally in space, retaining their infection strategies. Continued analysis of such systems will be important to help establish multigenerational studies and to obtain a fine-grained understanding of the long-term effects of space on diverse organisms.

RESULTS

Spaceflight compromises y w but not hop^{Tum-l} emergence

Lb and Lh females attack their larval hosts, introducing one or more egg and venom into the host's body cavity. Depending on the host's ability to defend itself and the wasp's ability to overcome host defenses, one of the two insects emerges alive from the host's puparium (Figure 1A). To study the effects of spaceflight on this host-parasite scuffle, naïve hosts or Lb17-/Lh14-infected hosts were held in ventilated fly boxes (VFBs); these fly boxes were then placed into a cargo transfer bag (CTB) aboard the ISS or at the ground facility tracking ISS conditions (Figure 1B, C). The FFL-03 experimental design consisted of two fly-only cultures (fly strains y w and y w, hop^{Tum-l}), and four fly/parasite co-cultures on each host strain (Figure 1D). Survival of animals was scored post-flight (see Methods and Materials).

We found that the overall yield of both male and female y w flies in each vial was roughly half of the ground-reared flies (**Figure 2A-C**; FFL-03 ground control and space samples retrieved post-flight are referred to as G0 and S0, respectively). The trend was somewhat different for the hop^{Tum-l} animals that did not appear to suffer from the effects of spaceflight; while spaceflight actually favored male viability slightly but significantly (average 44 versus 57 males/vial), female development remained unaffected (**Figure 2A-C**). Thus, under the FFL-03 experimental protocol, animals of the two genetic backgrounds responded differently to spaceflight, underscoring the complex interplay of these factors. There was no significant difference in the yields of flies and wasps from the fly/wasp co-culture vials (**Figure 2D, E**).

Effects of spaceflight on gene expression in adult flies

To understand the molecular basis of the effects of spaceflight on flies, we analyzed bulk RNA-Seq gene expression results in naïve adult flies. Differentially expressed genes (DEGs) were defined as adjusted p < 0.05 and |log 2FC| > 1. The close clustering of the four replicates and high variation among the four sample types in the Principal Component Analysis (PCA) show that the experiment was well-controlled (Figure S1A). Overall, the y w strain was more sensitive to spaceflight than hop^{Tum-l}, with 13.22% versus 6.78% DEGs (spaceflight versus ground control samples), respectively (Table S1), a difference that is also reflected in the PCA plot (Figure **S1A**). A separate RNA-Seq analysis of white-eyed (w^{1118}) flies, also on the SpaceX-14 mission, reported 6.49% and 3.25% DEGs in S0 versus G0 female and male fly heads, respectively (FDR adjusted p-values < 0.05; total number of genes expressed was 13,991 ³³). Although the sample types in the two studies are different, these results suggest that the y w strain is more sensitive to space conditions than the $y w hop^{Tum-l}$ and the w^{1118} strains. On Earth, the hop^{Tum-l} strain showed 9.69% DEGs relative to y w, with more than two-thirds of DEGs upregulated and the remaining DEGs downregulated. In space, this differential expression was enhanced (14.03% of genes affected), but the proportion of upregulated versus downregulated genes was roughly equal (Table S1).

154

155

156

157

158

159

160

161

162

163

164

165

166

167

168

169

170

171

172

173

174

175

176

Volcano plots of the four comparisons revealed distinct gene identity profiles in each comparison (**Figure S1B-E**). This distinction between the strains is also clearly evident from Gene Ontology-based Kyoto Encyclopedia of Genes and Genomes (KEGG) pathway analysis showing active Toll/Imd signaling not only in naïve G0 hop^{Tum-l} compared to y w flies, but, surprisingly, also in S0 y w and hop^{Tum-l} flies, relative to their G0 counterparts (**Figure S2A**). Furthermore, for these same three comparisons, the top 20 significantly enriched (adjusted p-value < 0.05) gene ontology terms in Biological Process enrichment analyses included host

defense terms such as response to bacterium, response to other organism, and response to biotic stimulus (**Figure S2B**). These four comparisons allowed us to decouple the effects of genetic strain differences in the S0/G0 culture conditions. We next examined changes in expression patterns of the most significantly DEGs (Top DEGs), genes essential to fly viability (Essential DEGs), and immune genes in the JAK/STAT and Toll/IMD pathways (Pathway DEGs), as summarized in **Figure S1F**.

Top DEGs in space include members of protease, endopeptidase, and matrisome gene

families

We analyzed 172 annotated Top DEGs (see Methods for selection of Top DEGs) and identified six profiles described here in two broad categories (**Figure 3A-F**): In the first category (**Figure 3A, B**), we consider the Top DEGs showing differential expression in the two fly strains as follows: (a) Top DEGs upregulated in G0 hop^{Tum-l} versus G0 y w that maintain their expression patterns in space (S0 hop^{Tum-l} versus S0 y w) include genes annotated for stress- and immunerelated peptides (Tot and Tep family members), proteases, and endopeptidases (**Figure 3A**). (b) The Top DEGs downregulated in G0 hop^{Tum-l} versus G0 y w that maintain their expression patterns in space (S0 hop^{Tum-l} versus S0 y w) include members of the lysozyme gene family, histone H4 genes, serine proteases, carboxypeptidases, and other enzymes (**Figure 3B**). Exceptions to both of these trends were also observed (**Figure 3A, B**). These results define strong differences in DEG patterns in hop^{Tum-l} and y w flies. They also show that the molecular gene expression differences between two genetic strains, for many but not all genes, are maintained in spaceflight conditions.

In the second broad category, we consider the effects of spaceflight on Top DEGs in individual strains as below (Figure 3C-F): (a) Top DEGs upregulated in S0 y w, when compared to the respective ground control group (i.e., G0 y w), encode (i) structural proteins for cuticle (e.g., chitin-binding domain-containing proteins of the Twdl, CPLCA, and Cpr families); (ii) proteins with the GYR/YLP domain or immune response-related proteins (Figure 3C). (b) Top DEGs downregulated in S0 y w flies but not in S0 hop^{Tum-l} flies, when compared to respective ground control groups, include members of the *yellow* gene family (*yellow-g*, *yellow-g*, *yellow-g* e3), bearded gene family (Brd, Tom, BobA), Histone H1s, and several genes for chorion constituents and chorion assembly (e.g., Cp7Fb, Cp7Fc, Cp16, Cp19, Cp36, Cp38, Mur11Da; Figure 3D). These Cp genes are clustered on the X and third chromosomes, and the gene clusters are selectively amplified in the follicle cells of the ovary ³⁴. (c) Top DEGs upregulated in S0 hop^{Tum-l} , when compared to the respective ground control group (G0 hop^{Tum-l}), include Cprfamily genes, Osiris family genes, tracheal-prostasin (tpr), a protein important for sleep regulation (nemuri, nur), and CG3108 (Figure 3E). (d) Top downregulated DEGs in S0 versus G0 flies of both genetic backgrounds include several cuticle-related (CPLCA, CPLCP) families and flight-related genes (e.g., flightin (fln) and Troponin C isoform 4 (TpnC4); Figure 3F). Chitin supports the epidermal and tracheal cuticles and the peritrophic matrices that line the gut while the chorion makes up the egg shell. These comparative RNA-Seq results suggest that matrisome genes of many multigene families that encode proteins of the *Drosophila* cuticle ³⁵ are sensitive to spaceflight.

219

220

199

200

201

202

203

204

205

206

207

208

209

210

211

212

213

214

215

216

217

218

Essential genes are downregulated in y w flies exposed to spaceflight

To further understand the differential effects of spaceflight on fly survival, we examined the expression of 1,024 essential genes that have been identified in genetic experiments as indispensable for life (see Methods). Across the four comparisons, we found 137 essential genes to be differentially expressed (adjusted p < 0.05 and |log2FC| > 1). Strikingly, the space environment had a profound effect on the differential expression of these genes between the two genetic backgrounds. For example, in G0 hop^{Tum-l} versus G0 y w samples, only 15 differentially expressed essential genes were either upregulated (11 genes) or downregulated (4 genes), whereas spaceflight conditions affected the transcription of 95 genes in the S0 hop^{Tum-l} versus S0 y w comparison (81 genes upregulated, 14 genes downregulated, **Figure 4A**).

The most striking effects of spaceflight were seen in y w flies: 96 genes were either upregulated (24 genes) or downregulated (72 genes) in y w space-flown samples compared to the respective ground control samples. The most strongly upregulated DEGs of these 96 DEGs, with $\log 2$ -(FC) > 2, include Cpr65Ec (cuticular protein), CG15784, and CG30457 (both latter genes lack annotation). The most highly downregulated genes are S1A serine protease Notopleural and histone H1 His1:CG31617, with $\log 2$ -(FC) < -1.9. Remarkably, gene expression changes were milder in space-flown hop^{Tum-l} samples, with the expression of only 10 genes significantly affected; either 2 genes were upregulated or 8 genes were downregulated, compared to respective ground control samples (**Figure 4A**). These results likely explain why y w flies are more sensitive to spaceflight than hop^{Tum-l} flies.

Differentially expressed essential genes reveal association with human disease conditions

To assess why S0 y w flies were sensitive to spaceflight and if they have relevance to human conditions, we filtered the 137 essential DEGs for a DIOPT score of at least 12 and identified 34

high-scoring DEGs that we grouped into broad categories. Strikingly, we observed 22 DEGs that were significantly downregulated in S0 y w versus G0 y w flies; Oseg5 and Biotinidase expression was downregulated in G0 hop^{Tum-l} versus G0 y w flies; this downregulation in space was maintained for both genes. Only two genes, veil and melt, showed significant upregulation (**Figure 4B**). This analysis revealed that human orthologs of these 34 fly genes affect many aspects of human physiology (see **Figure 4B** for details). The remaining 17 essential DEGs, with a low DIOPT value (i.e., < 12), were annotated with enzymatic, developmental, or unknown functions. The most significantly upregulated genes in hop^{Tum-l} versus y w flies were l(2)03659 (enables organic anion transporter activity) and Ir40a (involved in response to humidity changes) 36 , both maintaining differential expression in space. In addition, six DEGs, each in S0 y w flies and S0 hop^{Tum-l} flies, were either upregulated or downregulated, relative to their corresponding ground controls (**Figure 4C**).

Spaceflight activates the expression of immune genes in S0 adults; increases inflammatory tumor burden in S0 hop^{Tum-l}

A comparison of the Gene Ontology-based pathway and Biological Process enrichment terms associated with the y w versus hop^{Tum-l} transcriptional profiles provided a "big picture" view of the differential effects of space on the two strains. Both plots show that while most GO terms and almost all biological processes are affected in y w flies, only a few parameters change in both strains. Most notable of these are the Toll/Imd pathway and lysosomal pathway terms that are significantly enriched in the space samples for both genotypes, suggesting the activation of inflammation-related genes in space (**Figures S2A, B**).

Since the hop^{Tum-l} mutant fly strain carries a constitutively active JAK enzyme ³⁷, the transcriptional activation of known JAK-STAT target genes is expected in hop^{Tum-l} flies relative to y w flies without this mutation. Consistent with this expectation we found many target genes (Idgf1, SOCS36E, TotA, CG3829, CG4793, CG13559, and CG10764) to be differentially upregulated in G0 hop^{Tum-l} versus G0 y w flies. High levels of JAK-STAT pathway genes TotA, diedel, et, and CG4793 in hop^{Tum-l} versus y w were maintained in space (**Figure 5A**). Similarly, several Toll pathway components (PGRPs SA, SB1, and SD, grass, SPE) and target genes were significantly upregulated in G0 hop^{Tum-l} versus G0 y w flies (**Figures 5B-E**).

Whereas many immune genes are constitutively active in hop^{Tum-l} flies, remarkably, spaceflight activated the expression of a majority of these immune genes in y w flies (**Figures 5B-E**). The JAK-STAT pathway ligands (upd2 and upd3), several core components (SOCS36E), and target genes (TotA, Gf, mfas, and CG15211) were activated in S0 y w versus G0 y w flies (**Figure 5A**). A clear signature for Toll/Imd pathway activation was also observed in S0 y w adults. Elevated expression of pathway components (CG8046, Toll-9, **Figure 5B**), pathogen recognition receptors (PRRs, PGRPs SA, SB1, SD, **Figure 5C**), several antimicrobial peptide (AMP) genes (**Figure 5D**), and other Toll/Imd pathway target genes (**Figure 5E**) was observed in S0 y w versus G0 y w flies. Notably, some Toll/Imd pathway target genes (e.g., Drs12, 3, 5) were also activated in S0 hop^{Tum-l} versus G0 hop^{Tum-l} flies (**Figures 5D**).

To examine if the immune gene expression changes identified in space animals might have influenced tumor development in S0 hop^{Tum-l} adults (**Figure 6A**), we scored tumor number and size (small, medium, large tumors, T score; see Methods and **Figures 6B-C**). In 25-30 adults from three independent G0 and S0 cultures, the average weighted T score in G0 adults was 1.07 \pm 0.22 and 2.94 \pm 0.40 in S0 flies (**Figure 6D**), although this difference is lost in the adult G1

and S1 progeny of these G0/S0 animals (**Figure 6E**). Tumors were not detected in S0 *y w* animals, even though they showed evidence of high immune signaling.

High immune gene expression persists in naïve S1 larvae

As in the mutant hop^{Tum-l} adults, high gene expression levels of the JAK-STAT and Toll/Imd pathway genes encoding ligands, cytoplasmic mediators, and targets were recorded in naïve G1 and S1 hop^{Tum-l} larvae when compared to G1 y w and S1 y w larvae, respectively (**Figures S3A-E**). Thus, in hop^{Tum-l} larvae, the immune effects of spaceflight are evaluated in the background of constitutive immune signaling.

We assessed if naïve S1 y w or hop^{Tum-l} larvae showed any lingering effects of space observed in their S0 parents. Spaceflight-responsive differentially expressed immune genes in naïve S1 y w larvae included CG10764, LUBEL, PGRP-SB1, -SC1a, -SC1b, and AMP genes, CecB, AttC, Drs, and Drsl5 (Figures S3A-D). Similarly, naïve S1 hop^{Tum-l} larvae showed elevated expression of immune targets DptA, DptB, CecA2, Drsl3, Drsl5, and CecA1 relative to their G1 counterparts (Figure S3D). Thus, in both genetic backgrounds, immune signaling was elevated in S1 larvae, even though the affected target genes were different. Naïve S1 versus G1 hop^{Tum-l} larvae maintained the difference in inflammatory tumor burden observed in their parents $(0.08 \pm 0.03$ and 0.21 ± 0.06 , respectively, p = 0.010; Figures 7A, B), although the mitotic index in the underlying hematopoietic tissue was not significantly different $(2.74 \pm 0.93\%$ of G1 and $1.95 \pm 0.66\%$ of S1 macrophages were phospho-histone H3-positive; p = 0.53).

Tumor-encapsulation scores are higher in S1 than in G1 hop^{Tum-l} hosts

Previous studies with hop^{Tum-l} larvae have shown that Lb17 attack provokes stronger cellular immune reactions than Lh14 does. While Lb17 attack elicits encapsulation of the wasp egg due to an overabundance of circulating hemocytes (not recruited into the melanized tumors), Lh14-infected hop^{Tum-l} larvae instead develop small melanized specks 8 (see **Figure S4** for examples of immune reactions). To assess if naïve S1 versus G1 hop^{Tum-l} larval hosts differ in their ability to mount an encapsulation response, we exposed them to G0/S0 Lb17 or Lh14 wasps and computed a composite tumor-encapsulation (T + E) score for these animals, which measures their self- and wasp egg-induced encapsulation response. The experimental design consisted of scoring T + E scores from all G/S and host/parasite combinations. The following findings emerged from our comparisons of naïve versus Lb17- or Lh14-infected hop^{Tum-l} hosts.

First, naïve versus G0 or S0 Lb-infected G1 or S1 hop^{Tum-l} hosts showed a ~17-to-52-fold increase in T + E scores and scores from three of the four combinations differed significantly (**Figures 7A, B**). The T + E score in naïve versus G0/S0 Lh-infected G1 or S1 hop^{Tum-l} hosts in all four combinations similarly increased from 1.4-to-14-fold, and the increases were significantly different across all four comparisons (**Figure 7A, B**). It is noteworthy that the canonical Toll pathway target Drs is strongly upregulated in S1 hop^{Tum-l} hosts after Lb17 infection, but its expression remains unchanged after Lh14 infection (Drs, **Figure S3F, G**). This trend is characteristic of these wasps' effects on wild type hosts 8 , and suggests that the overall differences in wasp virulence were maintained in spaceflight.

Second, S1 compared to G1 hosts, infected by S0 (but not G0) wasps of both species (S0 Lb/Lh_S1 hosts versus S0 Lb/Lh_G1 hosts), were more competent at mounting an immune response $[3.64 \pm 0.46 \text{ versus } 2.11 \pm 0.72 \text{ (p} = 0.0199) \text{ for } Lb17 \text{ and } 0.76 \pm 0.03 \text{ versus } 0.11 \pm 0.72 \text{ (p} = 0.0199) \text{ for } Lb17 \text{ and } 0.76 \pm 0.03 \text{ versus } 0.11 \pm 0.72 \text{ (p} = 0.0199) \text{ for } Lb17 \text{ and } 0.76 \pm 0.03 \text{ versus } 0.11 \pm 0.72 \text{ (p} = 0.0199) \text{ for } Lb17 \text{ and } 0.76 \pm 0.03 \text{ versus } 0.11 \pm 0.72 \text{ (p} = 0.0199) \text{ for } Lb17 \text{ and } 0.76 \pm 0.03 \text{ versus } 0.11 \pm 0.72 \text{ (p} = 0.0199) \text{ for } Lb17 \text{ and } 0.76 \pm 0.03 \text{ versus } 0.11 \pm 0.72 \text{ (p} = 0.0199) \text{ for } Lb17 \text{ and } 0.76 \pm 0.03 \text{ versus } 0.11 \pm 0.72 \text{ (p} = 0.0199) \text{ for } Lb17 \text{ and } 0.76 \pm 0.03 \text{ versus } 0.11 \pm 0.72 \text{ (p} = 0.0199) \text{ for } Lb17 \text{ and } 0.76 \pm 0.03 \text{ versus } 0.11 \pm 0.72 \text{ (p} = 0.0199) \text{ ($

0.04 (p = 5.55 e-10) for Lh14; (**Figure 7A, B**)]. Thus, not only is the tumor score higher in naïve S1 compared to G1 hop^{Tum-l} larvae, but S1 hosts are also more immune reactive than G1 hosts.

Third, on ground hosts, space wasps of both species differed from ground wasps in their ability to elicit encapsulation. T + E scores in G1 hop^{Tum-l} hosts subjected to S0 or G0 parasites of the same species (S0 Lb/Lh_G1 hosts versus G0 Lb/Lh_G1 hosts) showed that for both parasites, the T + E values for S0 wasp infections were significantly lower than the corresponding values for G0 parasites [2.11 ± 0.72 versus 4.10 ± 0.65 for Lb17 (p = 0.0199); and 0.11 ± 0.04 versus 1.13 ± 0.33 (p = 0.000915) for Lb14]. The difference was not significant in space hosts (**Figures 7A, B**). These results suggest that while S1 larval progeny may be adapting to normal gravity and other terrestrial conditions, they retain altered immune physiology of their space parents, albeit transiently. S0 wasps largely maintain their inherent virulent strategies, although we could detect subtle differences in their abilities to affect host immunity relative to G0 wasps.

Lymph gland morphologies of naïve and infected G0 and S0 hosts

Upon *Lb17* attack, hemocytes in wild type lymph gland lobes divide and differentiate into lamellocytes and disperse into the hemocoel to surround the wasp egg ³⁸⁻⁴⁰. Hemocytes in the *hop* ^{Tum-l} lymph gland actively divide and differentiate in the absence of infection ³⁷. Because of the high inflammation state of space animals, we examined differences in lymph gland lobes from third-instar G0 and S0 animals. A normal lymph gland has multiple, paired lobes, consisting of hemocytes, positioned along the tubular dorsal vessel that continues into a pulsating heart, which directs the flow of the hemolymph and circulating hemocytes into the body cavity (**Figures S5A-D**). The anterior-most lobes are the largest, with hemocytes at varying

differentiation stages. The posterior lobes are smaller in size and harbor fewer differentiated cells than the anterior lobes. The margins of all lobes from naïve y w ground and space hosts were continuous with none-to-little dispersal. Like lobes from G0 naïve y w animals, lobes from S0 naïve y w animals did not exhibit any hemocyte loss or any other obvious morphological change (**Figures S5A-H**).

In contrast to naïve y w animals, all anterior lobes of naïve G0 and S0 hop^{Tum-l} larvae were dispersed due to the effect of the mutation (**Figures S5I-P**). The mutation also results in some lobes detaching from the dorsal vessel, and many GFP-positive lamellocytes were present in G0 and S0 hop^{Tum-l} samples. Some tumors were observed as small aggregates or as free-floating structures in the hemolymph made of macrophages and lamellocytes (**Figures S5J, N**). No clear difference in the posterior lobes was detected due to spaceflight in either fly strain.

G1 and S1 y w host lymph glands were unresponsive after Lb parasitization (**Figures S6G, S6A-F**). In naïve G1 hop^{Tum-l} lymph glands, GFP-expressing cells were absent (**Figures S6G, H**), whereas in S1 hosts, lamellocytes were clearly observed regardless of infection status (**Figure S6I-P**). In some samples, lamellocyte-rich tumors were associated with the anterior and posterior lobes (e.g., S1 sample, **Figures S6K, L**). In only one S1 host, the anterior lobes exhibited a strong anti-wasp response (**Figure S6O**). Thus, even though the T + E scores rise in response to Lb infection, this difference was not reflected in the lymph gland morphologies of the animals we examined.

Lh14 infection results in the gradual loss of hemocytes in all lobes. This effect is attributed to the presence of EVs in the entire lymph gland 20 . EVs were present in hematopoietic progenitor cells and dorsal vessels of G0 and S0 Lh-infected G1 and S1 y w hosts, and this association was accompanied by the loss of hematopoietic progenitors (**Figures S7A-F**).

Similarly, in G1 and S1 hop^{Tum-1} hosts, the progenitor population was reduced, and EVs were present in the lymph glands of hosts after S0 Lh infection. (G0 Lh wasps were not available for this experiment.) Lymph glands from uninfected G1 or S1 hosts do not possess EVs (**Figures S7G-N**). Thus, spaceflight does not affect the entry or distribution of Lh EVs in the hemolymphatic system.

384

385

386

387

388

389

390

391

392

393

394

395

396

397

398

399

400

379

380

381

382

383

Perturbation of Lb and Lh EV gene expression

The venom fluid containing the EVs is injected into the host during oviposition. Due to their close association with and direct effects on target hemocytes ^{17,20}, our definition of virulence proteins in this study is restricted to those that make up the EVs. Since standard annotations of wasp transcripts are not available, a custom pipeline was developed to analyze gene expression changes against corresponding transcriptomes (Figure S8A). Overall, in adult male and female wasps, the effects of spaceflight were detected (Figure S8B, C), although they were modest, and less than 1.5% of all transcripts identified showed significant change when compared to respective ground controls (293 and 310 transcripts, for Lb17 and Lh14, respectively). A majority of the transcripts were downregulated in both wasps (Figure 8A-C; Tables S2, S3). Furthermore, the intensity of gene expression change was also mild. Of the downregulated DEGs (adjusted p < 0.05), more than 80% showed log (2)-FC between -1.00 and -2.00 (228/280 in Lb17 and 250/261 in Lh14). The remaining downregulated DEGs showed log (2)-FC between -2.00 and -9.18. Only 6 of all DEGs showed a log (2)-FC > 2 for *Lb17*; this number was 16 for Lh14. These DEGs do not appear to belong to a specific functional class, and many lack clear annotations.

The identities of the proteins constituting *L. boulardi* EVs were recently published ¹⁴. Our comparative analysis indicated that *Lb* EV proteins show an overall profile similar to the *Lh* EV profile; both are enriched in mammalian extracellular vesicle proteins ¹⁵. A majority (> 98%) of the EV transcripts were identified in our RNA-Seq analysis (312/316 for *Lb17* and 398/406 for *Lh14*). In *Lb17*, 29/312 (9.89%) EV genes were significantly differentially expressed (**Figure 8D**). Of these, 28 were downregulated (**Table 1**). Two mildly downregulated genes are predicted to encode Rho-GAP superfamily proteins (GAJA01018902.1, log (2)-FC = -1.27, and GAJA01006288.1, log (2)-FC = -1.09). A RhoGAP superfamily protein called LbGAP in *Lb* EVs is implicated in wasp virulence ^{41,42}. Of the two downregulated wasp RhoGAP superfamily proteins, only one (GAJA01018902.1) showed homology to LbGAP: 69.7% nucleotide sequence identity (68% query coverage; 8e-55). For *Lh14*, only 5/398 (1.61%) transcripts were significantly differentially expressed. Of these, only one gene, lacking annotation, was about 5-fold upregulated (**Table 2**). Of the downregulated genes, three lack annotations, and one is predicted to encode a protein with a chitin-binding domain.

Spaceflight does not significantly affect wasp emergence

Spaceflight did not significantly affect the overall development of wasps. The yields per vial of each wasp species reared in space were comparable to those of ground control samples (**Figure 2E**). The relative success of parasite versus host in individual vials suggested that each *Leptopilina* species successfully disarmed both y w and hop^{Tum-l} hosts in space and also on Earth (**Figure 2D**, **E**). However, while no hop^{Tum-l} hosts escaped parasitization by Lb or Lh in either ground or space cultures, some y w flies emerged in the co-culture vials (**Figure 2D**), likely because these hosts overcame parasite infection or remained uninfected by the available

parasites. When total wasps were scored relative to all insects (% wasps/total insects in each vial; **Figure S9A**), we found no significant difference in space- versus ground-reared wasp samples. Both wasp species raised on either fly host showed equal success in flight and ground conditions (**Figure S9B**), reinforcing this conclusion.

EV morphology and *Lh14* virulence

We next investigated whether the morphology of EV particles produced by both wasp species is affected by spaceflight. In the scanning electron micrographs of gold-coated samples of G0 and S0 *Lb17* wasp venom, we observed no gross morphological difference (**Figure S10A-G**). The overall shapes and morphologies reported previously ^{9,16} were maintained in both samples. In addition to the regularly shaped, spiked particles, there were many particles with heterogeneous shapes, although most had spike-like processes. We observed small membranous protrusions on the particles from both G0 and S0 EV samples that were previously not reported. The G0 and S0 *Lh14* EV morphologies were also indistinguishable (and similar to previously reported structures ⁹), in scanning electron micrographs of gold-coated samples (**Figure S10H-S**). Overall, the *Lh14* particle morphologies were uniform, and the particles were spiked, with variable spike length.

An *ex vivo* assay was used to detect changes in G0 versus S0 *L. heterotoma* virulence. Lamellocytes from laboratory-reared hop^{Tum-l} larvae were exposed to venom fluid from G0 or S0 wasps. Venom from both wasp types promoted changes in lamellocyte shape compared to the buffer control ($6.50 \pm 0.76 \% G0$; $6.12 \pm 0.71 \% S0$; $2.99 \pm 0.06 \%$ buffer control), but there was no significant difference in the S0 versus G0 *Lh14* venom activity (**Figure S11A-C**). These results are consistent with the unremarkable difference in the overall *L. heterotoma* success (emergence) of S0 versus G0 *Lh14* wasps.

Mutant *Lh14* strains

Space-radiation-induced mutations in *D. melanogaster* have previously been reported ^{43,44}. We hypothesized that parasitoid wasps are similarly sensitive to high levels of radiation in the ISS. We therefore examined the grandsons of space-returned males (**Figure 9A**). While no heritable defects were observed for any *Lb17* or ground-raised *Lh14*, we obtained two recessive mutations in *Lh14* (**Figures 9B-G**). In the *aurum* mutant, melanization of the wings is affected, making the normal wings appear golden (horizontal arrows; **Figures 9B, 9C, 9E, 9F**; side-by-side view in panel G). This mutant is homozygous viable, and a pure-breeding stock could be established (see Methods). A second phenotypic alteration was identified in this pure-breeding *aurum* stock, where the posterior wing margin in affected individuals is angular as opposed to the wild type round shape (vertical arrows; **Figures 9D-F**). In rare cases, this *kona* mutation was incompletely penetrant, where only one wing was affected (**Figure 9F**). To our knowledge, these are the only live mutant animals in this class of wasps.

To assess if *aurum* and *kona* are unlinked, we scored over 1,000 sons of unmated double mutant heterozygous females. Roughly equal numbers of parental and recombinant classes were observed (chi-square test, p = 0.63; **Figure 9H**). Even though the *kona* strain was homozygous viable, we were unable to make a pure-breeding stock. Moreover, we did not find wasp eggs in dissected hosts, regardless of whether the infecting *kona/kona* females were unmated or mated. This result suggested that *kona/kona* females were unable to oviposit while their heterozygous counterparts were successful (**Figure 9I**). The ovipositors of *kona/kona* homozygotes showed structural defects, including branched termini instead of the sharp, needle-like ends of the wild type *Lh* ovipositor (**Figure 9J**). Abdominal dissection of *kona/kona* females revealed ovaries and

eggs that are morphologically indistinguishable from wild type or heterozygous females (**Figure S12**). Thus, it appears that oogenesis is likely unaffected in *kona* mutants, and they are sterile

due to their inability to oviposit.

DISCUSSION

American scientists first launched fruit flies into space in 1947, and since then, more than 20 spaceflight experiments with fruit flies have been conducted ⁴. Even parasitic wasps have been to space: in 1967, Biosatellite II carried *Habrobracon juglandis* into space ⁴⁵. *H. juglandis* is a small ectoparasite that attacks moths. The Biosatellite II mission reported multiple effects of spaceflight alone, or that of radiation in conjunction with spaceflight, on *D. melanogaster* and *H. juglandis* ^{45,46}. *D. melanogaster*, however, continues to be an obvious choice for space travel studies for all the advantages the model organism offers researchers on Earth. Among the most cost-effective model systems, its high fecundity and small size facilitate the study of large numbers of individual flies, which is necessary for statistically relevant experimental protocols. These previous 'fruit flies in space' studies have tackled a variety of questions, including development, aging, mating, cardiac, and neural functions, that have implications for astronaut health ^{4,47}. Despite suffering from cardiac and neurological deficits ^{33,48}, *Drosophila* born in space can largely survive the dual challenges of short-term exposure to microgravity and radiation.

Strain-specific effects on survival and transcriptional readouts in *Drosophila* are induced

by spaceflight stressors

Spaceflight conditions exerted unexpected and differential effects on our experimental Drosophila strains. While the hop^{Tum-l} flies with CI survived just as well in space as on the ground, the y w strain, free of tumors and CI, was surprisingly more vulnerable to the spaceflight stressors, and fewer y w flies emerged from the flight compared to ground cultures. Molecular analysis revealed a complex interplay between genetic and environmental conditions. Three

trend lines are noteworthy: First, specific expression profiles of Top DEGs attributed to genetic differences were maintained in space, suggesting that the gene regulatory circuits underlying these differences may be sufficiently robust and may therefore remain refractory to spaceflight.

Second, the Top DEGs include genes encoding structural proteins for the cuticle and the chorion, an observation that was also reported in a previous multigenerational study on wild type flies ⁴⁷. Some of the cuticle-related DEGs were upregulated in one of the two S0 genetic strains, but not in the other S0 strain, while other DEGs were downregulated in S0 flies of both genetic backgrounds. This result suggests that transcriptional co-regulation of promoters among Top DEG family members may be adaptive to either or both genetic and environmental variables. Chitin and its associated proteins are part of the fly's exoskeletal matrisome, and together, they support the cells they surround structurally and functionally ^{49,50}. A highly coordinated chitin synthesis and degradation program underlies insect growth. It would be interesting to assess if the cuticle or the chorion of S0 flies differ from those of G0 flies.

Third, numerous essential genes were downregulated in space in y w, but not in hop^{Tum-l} animals, suggesting that the cumulative effect of their reduced transcription may have led to their reduced viability. Thus, while increased tumor burden and alterations in gene expression in S0 hop^{Tum-l} adults did not compromise their overall survival, y w flies exhibited increased immune gene expression, remained tumor-free in space, and exhibited reduced survival. Future experiments will help clarify the differential effects of space on the expression of essential genes in these genetic strains. Many of these essential fly genes are conserved, and their human orthologs are linked to disease conditions. These results not only defied our expectation that animals with chronic disease would be more vulnerable to spaceflight but also suggested that, if

extrapolated to other animals, spaceflight's effects on individuals of distinct genetic backgrounds may not necessarily be straightforward to predict.

Elevated immune signaling in space hosts

Our previous molecular-genetic analysis of hop^{Tum-l} larvae showed that hyperactive Toll signaling in larval lamellocytes contributes to CI phenotypes ²⁴. A plethora of target genes of both the JAK-STAT and Toll pathways is constitutively active in hop^{Tum-l} mutants. Strikingly, many of the same pathway components and target genes that are constitutively active in hop^{Tum-l} mutants are also upregulated in S0 y w flies, even though the S0 y w flies remained tumor-free. A few antimicrobial peptide genes (e.g., Drs, Drsl, CecA, etc.) are further upregulated in S0 hop^{Tum-l} flies, suggesting that the increased tumor burden in S0 hop^{Tum-l} adults is fueled by ectopic JAK-STAT and Toll signaling induced in space.

Unlike their parents, however, naïve S1 larvae did not exhibit a clear and strong inflammatory gene expression readout (see S0/G0 y w column in **Figure 5D** and S1/G1 y w column in **Figure S3D**, where constitutive immune signaling does not mask the effects of space). In contrast, like their parents, many immune genes in naïve G1/S1 larvae were active in hop^{Tum-l} larvae. Even though changes in mitotic indices of host hemocytes or their lymph gland morphologies were not detected in these S1 versus G1 hop^{Tum-l} larvae, a significantly enhanced T score was observed in naïve S1 versus G1 hop^{Tum-l} larvae. This increased immune reactivity was also reflected in the enhanced T + E scores in infected S1 hop^{Tum-l} larvae, relative to their G1 counterparts. The increased tumor burden detected in naïve S1 hop^{Tum-l} larvae did not persist in S1 hop^{Tum-l} adults. Collectively, these observations suggest that, with re-adaptation to normal gravity, the inflammatory effects of spaceflight are transient and reversible. The highly inflamed

state of hop^{Tum-l} animals provided physiological insights into the modest changes in wasp virulence due to spaceflight.

544

545

546

547

548

549

550

551

552

553

554

555

556

557

558

559

560

561

562

563

564

542

543

Wasp success, wasp virulence, and gene expression changes

We hypothesized that stress from spaceflight could compromise the development of either of the two partners: the fly or the parasite. Because of the complete dependence of the parasite on the host, either situation would be detrimental to parasite development. In an alternative scenario, if the effects of spaceflight on fly hosts are modest, then endoparasite development should not be affected. Wasps of both species developed successfully in the ISS environment; the more virulent Lh14 species was equally successful in both conditions, while Lb17 survival was marginally compromised in space. This difference in Lb17 versus Lh14 success may have to do with their dissimilar virulence strategies, with Lb17 being less successful on D. melanogaster than Lh14 8. Global gene expression changes in space-raised parasites were remarkably mild, and less than 1.5% of the adult parasite transcripts were affected. Consistent with parasite emergence results, the transcription of many more genes was affected in S0 Lb17 than in S0 Lh14. Thus, even though radiation in space led to germline mutations in one of the two parasites, the overall detrimental effects of microgravity were not sufficiently strong to block parasite development. We speculate that the notable overall success of both parasites in space may be due to their endoparasitoid life histories: developing internally, the preimaginal stages remain protected from the environmental challenges in space. Parasites have varied life histories and distinct survival strategies in the context of host physiology. With increased travel to space, it is inevitable that parasites will unintentionally hitch a ride with their hosts. With plans for the colonization of other planets, multigenerational experiments on "short life cycle" organisms such as D.

melanogaster and their associated flora and fauna will become important. Innovative and sophisticated hardware designed for multigenerational studies will be helpful in this regard.

The virulence properties of both parasites also appeared to be largely maintained in space. This conclusion is based on (a) comparable yields of parasites in space versus ground cultures; (b) relatively stronger effects of Lb17 on the T + E score compared to Lh14; and (c) stronger transcriptional activation of Drosomycin (Drs) in S1 hosts after Lb17 infection but not after Lh14 infection (**Figures S3F, G**). It is intriguing that S0 wasps of both species were less effective at increasing the T + E score in both G1 and S1 hop^{Tum-l} hosts. This result suggests that the space environment did affect wasp physiology or virulence; the latter interpretation is consistent with reported increases in microbial virulence in space 31,32 .

A clear molecular explanation for differences in S0 versus G0 wasps was not apparent from the molecular analysis of wasp EV gene transcription. Transcript levels of only 29/312 Lb17 EV genes were significantly affected with all but one gene being downregulated. Only one of the two predicted RhoGAP superfamily genes shares structural similarity with the known LbGAP virulence protein 42 , and even its expression is weakly downregulated in space. The transcription of only 5/398 Lh14 EV transcripts was differentially affected, with only one gene (lacking annotation) showing ~ 5 -fold upregulation. None of these genes is currently implicated in Lh14 virulence. Furthermore, in an ex vivo assay, Lh14 venom from S0 wasps was no different in its ability to distort lamellocytes than Lh14 venom from G0 wasps. The abundance and distribution of G0 and S0 Lh14 EVs in the dorsal vessel and lymph gland lobes of infected animals further suggests that the integrity of S0 Lh14 EVs is comparable to that of controls. It is possible that the cumulative effects of differential gene expression changes contribute to

differences between S0 and G0 wasps. Alternatively, S0 wasps may differ in their oviposition behavior, affecting the quantity of venom introduced into the host.

589

590

591

592

593

594

595

596

597

598

599

600

601

602

603

604

605

606

607

608

609

587

588

Mutant wasps

Haplodiploidy in Hymenoptera makes it convenient to conduct mutational studies in space, as haploid sons (developing from unfertilized eggs of mutated females) would exhibit dominant or recessive mutant phenotypes. In our study, male wasps were used to evaluate the effects of radiation on their germline, while female wasps were used in virulence assays. Screening grandsons of S0 Lh14 males developed in space resulted in the isolation of two visible mutants, one of which is homozygous viable, while the other is homozygous female-sterile. Dosimetry measurements on SpaceX-14 recorded an average absorbed dose rate of 0.3 mGy/day, or 9.6 mGy for the 32-day duration in the ISS. Being in low Earth orbit, the ISS is protected by the Earth's magnetosphere ⁵¹. Yet, chronic exposure to these radiation levels likely resulted in DNA damage in the germline of the parasites reared in space. Despite efforts to shield the Space Station from the damaging consequences of radiation ⁵², our results support previous studies showing that animals in the ISS are at risk for DNA damage and physiological dysfunction ¹. Given the success of this mission, systematic studies designed to compare the effects of radiation on Drosophila and Leptopilina may be particularly insightful, as both species yield high numbers of progeny and mutant phenotypes can be scored in the F1 generation. The risks of radiation increase considerably with the planned manned lunar missions and other deep space missions for long-term colonization ^{1,53}. Future model organism studies can help assess the hazardous effects of radiation on soma versus germline genomes and inspire ways to avert these risks with innovative shielding designs. The isolation of mutant wasp lines will advance our understanding

of wasp genomics, genetics, and host-parasite biology. The space environment is likely to have as yet unknown impacts on animal immune function; refining our understanding of host-parasite systems with new genetic tools on Earth will broaden our understanding of immune function in space. Studies of other animal and plant hosts and their natural parasites in modeled microgravity and/or radiation will provide insights into their effects on host defense and parasite virulence.

LIMITATIONS OF THE STUDY

Spaceflight experiments with live organisms are constrained by the weather, the logistics of the launch and retrieval protocols, the duration of the mission, the physical conditions within the ISS module, and available crew time. This study faced all these constraints. Although the 34-day mission duration aligned well with the overall goals of our experiment, by the end of the mission, the number of G0/S0 larvae was insufficient to set up infections with G0/S0 wasps. (Available G0/S0 larvae were dissected to examine lymph gland hemocyte morphologies (**Figure S5**).) It is quite likely that the effects of infection on the T + E values in G0/S0 larval hosts infected with G0/S0 wasps would be stronger than what we observed in G1/S1 hosts. The availability of fresh fly media for culturing naïve G0/S0 adult flies, born in space or on ground, would have ensured sufficient numbers of larval hosts for these infection experiments, a strong consideration for designing future experiments.

629	ACKNOWLEDGEMENTS
630	We are grateful to Edina Blazevic, Jackson Chen, Amy Gresser, Ye He, Waleed Khalid, Kevin
631	Martin, Leo Mazur, Jorge Morales, and Zubaidul Razzak for assistance with experiments or
632	analysis. Kristen Peach and Jack Miller provided the radiation data, and Amy Gresser designed
633	the FFL-03 emblem in the Graphical Abstract. S. A. Tasnim Ahmed and Asif Siddiq helped with
634	assembling figures. San-huei Lai Polo helped with data curation on OSDR. Research was funded
635	by NASA (NNX15AB42G), the National Science Foundation (1121817 and 2022235), the
636	National Institutes of Health (1F31GM111052-01A1), and PSC-CUNY (63816-00 51 and
637	66619-00 54). The sponsors or funders did not play any role in the study design, data collection
638	and analysis, decision to publish, or preparation of the manuscript.
639	
640	AUTHOR CONTRIBUTIONS
641	Conceptualization, Methodology, Investigation, Formal Analysis, Visualization, Resources,
642	Writing – Review and Editing: All authors; Software: ASB; Data Curation: ASB, JC, SG;
643	Supervision, Writing - Original Draft: SG; Funding Acquisition, Supervision: SB, SG.
644	
645	DECLARATION OF INTERESTS
646	The authors declare no competing interests.
647	
648	INCLUSION AND DIVERSITY
649	We support inclusive, diverse, and equitable conduct of research.
650	

MAIN FIGURE TITLES AND LEGENDS

651

652

(bottom left) imaged together with parasitoid wasps (bottom right). Female wasps have shorter 653 654 antennae than males (right). (B) Vented fly box (VFB) with 15 holding slots for fly vials. (C) Six VFBs in one cargo transfer bag (CTB). Samples in the CTB were placed in the ISS by the crew. 655 The ISS flight conditions were mirrored at the Kennedy Space Center laboratory, where ground 656 control samples were housed for the duration of the mission. (D) The FFL-03 experimental 657 design consisted of two fly-only cultures and four fly/wasp co-cultures, as shown. See STAR 658 659 Methods for more details. Figure 2. Survival of flies and wasps in ground control (G0) and space (S0) samples. (A-C) 660 The average numbers of adult male (A), adult female (B), and all adult (C) flies per vial in naïve 661 v w and hop^{Tum-l} cultures. The number of animals, averaged from 14 vials, is shown below. Bars 662 show standard error. y w males per vial in G0 and S0 samples = 86 ± 3 and 39 ± 5 ; p $\leq 2.23 \times 10^{-5}$ 663 ⁸. hop^{Tum-l} males per vial in G0 and S0 samples = 44 ± 5 and 57 ± 3 ; p = 0.03. y w females per 664 vial in G0 and S0 samples = 105 ± 4 and 63 ± 4 ; p = 1.03×10^{-8} . hop^{Tum-l} females per vial in G0 665 and S0 samples = 53 ± 7 and 51 ± 3 ; p = 0.74. Total y w adults per vial in G0 and S0 samples = 666 260 ± 8 and 151 ± 10 ; p = 5.38×10^{-10} . Total hop^{Tum-l} adults per vial in G0 and S0 samples = 122 667 \pm 15 and 129 \pm 6; p = 0.38. (D, E) The number of G0 adult flies (D) and wasps (E) per vial in 668 fly-wasp co-cultures. G0 y w from Lb infections = 7 ± 7 ; S0 y w from Lb infections = 36 ± 14 ; p 669 = 0.07. G0 y w from Lh infections = 10 ± 9 ; S0 y w from Lh infections = 0.36 ± 0.17 ; p = 0.33. 670 G0 *Lb* on *y w* hosts = 38 ± 5 ; S0 *Lb* on *y w* hosts = 41 ± 5 ; p = 0.31. G0 *Lb* on hop^{Tum-l} hosts = 14671 \pm 4; S0 *Lb* on *hop*^{Tum-l} hosts = 15 \pm 3; p = 0.78. G0 *Lh* on *y w* hosts = 75 \pm 7; S0 *Lh* on *y w* hosts 672

Figure 1. The FFL-03 experimental design. (A) *D. melanogaster* adults (top left) and larva

 $= 84 \pm 9$; p = 0.48. G0 *Lh* on hop^{Tum-l} hosts = 10 ± 2 ; S0 *Lh* on hop^{Tum-l} hosts = 14 ± 3 ; p = 0.26. 673 674 See also Figure S9. Figure 3. Differential expression of Top DEGs in S0/G0 adult flies. (A, B) Top DEGs 675 upregulated (A) or downregulated (B) in G0 hop^{Tum-l} vs. G0 v w. Most genes in panel A that 676 maintain differential expression in space are Toll pathway target genes 54,55 (TotM and Tep1 677 family members, SPH93, and CG18563). Lectin-24A is predicted to bind galactose, and its 678 human homolog is associated with the 3MC syndrome 3 ⁵⁶. Notable DEGs in panel (B) with 679 disease-relevant human orthologs are CG32379, CG32318, and CG30059⁵⁷. (C, D) 680 Comparisons showing differential expression of upregulated (C) and downregulated (D) genes in 681 S0 y w versus G0 y w. Cuticle-related and chorion-family genes are included in these profiles. 682 The fly histone H1s (orthologous to the human H1 gene, implicated in acute lymphoblastic 683 leukemia ⁵⁸) and *CG6431*, a triacylglycerol hydrolase (orthologous to several human disease 684 genes implicated in cardiovascular disease and type-2 diabetes), are downregulated (D). (E) 685 Genes in hop^{Tum-l} whose expression is activated in space. Cuticle-related and chorion-family 686 687 genes are included in this profile. CG3108 is predicted to enable metallocarboxypeptidase activity, whose human orthologs are implicated in familial febrile seizures 11 and familial 688 temporal lobe epilepsy 5 57 . (F) Genes in hop^{Tum-l} whose expression is downregulated in space. 689 Cuticle-related and flight-related genes are included. Flight-related genes are CG34327 690 (associated with abnormal flight), flightin (fln), and Troponin C isoform 4 (TpnC4). See also 691 Figure S1. 692 Figure 4. Differential expression of essential genes in S0/G0 adult flies. (A) The expression of 693 137 genes essential to fly viability that were differentially expressed (adjusted p < 0.05 and 694

 $|\log 2FC| > 1$) in one or more comparisons is shown. (B) Expression of 34 genes pertinent to

human health. The DIOPT category and score-relevant human disease or trait linked to the human ortholog were determined using the *Drosophila* RNAi Screening Center Integrative Ortholog Prediction Tool ⁵⁹. The disease/trait category for the fly gene refers to at least one human disease or trait linked to one or more human ortholog. MS = musculoskeletal, DN = development/neurological, MO = metabolic-/obesity-related, S = skin-related, P = pulmonary, IA = infection and/or autoimmune, and C = coronary-/cardiac-related. (C) The differential expression of essential genes with no human ortholog or none-to-low disease relevance. See also Figure S1. Figure 5. Differentially expressed immune signaling genes in S0/G0 adult flies. (A) JAK-STAT pathway components and target genes are shown based on fold-induction. Genes were grouped based on their annotation in FlyBase ⁵⁷ as follows: *Upd2* and *Upd3* are ligands; *CycD*, CycE, and Cdk2 are positive regulators; diedel, Socs36E, and et are negative regulators. The target genes are: TotA, Idgf1, pirk, mfas, CG3829, CG4793, CG13559, CG10764, CG15211, and Gf. (B-E) Differentially expressed Toll pathway components: core components (B), pathogen recognition receptors (C), antimicrobial peptides (D), and other targets (E). Only significantly affected DEGs (adjusted p < 0.05 and |log 2FC| > 1, in one or more comparisons) are shown. See also Figures S1 and S2. Figure 6. Tumor burden in naïve G0/S0 hop^{Tum-l} fly adults. (A) Experimental design for space and ground hop^{Tum-l} flies for post-flight experiments. The progeny of 300 females and 150 adult males were raised either in the ISS or at KSC (see Methods) at 22°C, and then at 25°C, once returned to the laboratory. Tumors were scored in larval and adult samples. (B-C) Representative G1 hop^{Tum-l} adult female (B) and male (C), showing tumor size classes: small, medium, and large. (D-E) Weighted average number of tumors per animal in adult fly samples retrieved from

696

697

698

699

700

701

702

703

704

705

706

707

708

709

710

711

712

713

714

715

716

717

719 ground (G0) and space (S0) (D) and values from their ground (G1) and space (S1) adult progeny (E). The weighted tumor numbers per animal in G0 and S0 adults were 1.07 ± 0.22 and $2.94 \pm$ 720 0.40, respectively (mean \pm standard error; p = 0.015, student t-test; * indicates p < 0.05). The 721 weighted average tumor numbers per animal in G1 and S1 hop^{Tum-l} adult males were 5.09 ± 0.08 722 and 5.07 ± 0.33 , respectively (mean \pm standard error; p = 0.95, student t-test). See also Figures 723 S1 and S2. 724 Figure 7. Cellular immunity in G1 and S1 hop^{Tum-l} larvae, post parasitization. (A) Tumor 725 (T) scores of uninfected (UI) and tumor and encapsulation (T + E) scores of G0/S0 *Lb*- or G0/S0 726 *Lh*-infected G1/S1 hop^{Tum-l} larvae. Value above each bar indicates the mean \pm standard error. (B) 727 Summary of the statistical analysis of pairwise comparisons of T or T + E scores (see Methods). 728 Lb17 wasp infection rows are shaded for clarity. p-values < 0.05 (Mann-Whitney U-test for 729 730 unpaired samples) were considered significant (bold). See also Figures S3, S4, S6, and S7. Figure 8. Differential expression of EV genes. (A, B) Enhanced volcano plots for DEGs in 731 Lb17 (A) and Lh14 (B) S0 vs. G0 wasp samples. Numerical identifiers correspond to EV genes 732 733 in Tables 1 and 2, with their corresponding accession numbers. (C) Number of transcripts from adult male and female wasps, showing fluctuation in space. The term "all transcripts" refers to 734 the number of transcript sequences in the *Lb17* (GAJA00000000) and *Lh14* (GAJC00000000) 735 transcriptomes that aligned with the corresponding RNA-Seq reads ⁶⁰. The term "all DE 736 transcripts" refers to the number of differentially expressed transcripts in spaceflight vs. ground 737 control samples (Tables S2 and S3). A majority of transcripts were downregulated. See Methods 738 and Figure S8 for more details. (D) Transcripts coding for EV proteins in the RNA-Seq samples 739 show that 312 Lb17 EV and 398 Lh14 EV transcripts were identified for each wasp. Of these, 740 741 only 29 Lb17 and 5 Lh14 transcripts were differentially expressed in S0 vs. G0 samples. Their

also Figures S8, S10, and S11. Figure 9. Mutant strains of L. heterotoma. (A) Steps employed for the isolation of mutant wasps. (B-F) Phenotypes of mutant wasps (C-F), identified from space samples compared to wild type (B) Lh wasps. Males of wild type, aurum (pigmentation of the wing blade and of wing veins affected), and kona (wing shape affected) wasps are shown. Horizontal arrows point to differences in melanization in wild type versus aurum mutants. The color difference is subtle but consistent. Vertical arrows point to the angular wing shape of the kona mutant as compared to the rounded wild type wing blade. Double mutants in panels (E) and (F) possess both mutant traits. The shape of the left wing in panel (F) is wild type in appearance, while the right one (arrow) is angular. Samples in panels B-F were photographed at the same time. (G) A side-byside comparison of wild type (left) and aurum (right) wings shows a clear difference in the melanization of wing veins. (H) The aurum and kona loci appear to be unlinked, as F2 males from unmated heterozygous females were scored in roughly equal proportions. (I) Homozygous kona females are unable to oviposit based on observations of more than 30 hosts dissected. (The number of hosts scored is indicated in parenthesis.) (J) Representative ovipositor morphologies from wild type and mutant wasps. Homozygous kona females with defective ovipositors show areas of compromised integrity or have branched ends (arrows) compared to the continuous ovipositors with sharp ends from wild type control wasps (+/+). Posterior is to the top. Scale bar = 300 μ m. See also Figure S12.

identities, fold-change values, and conserved protein domains are shown in Tables 1 and 2. See

742

743

744

745

746

747

748

749

750

751

752

753

754

755

756

757

758

759

760

761

MAIN TABLES AND LEGENDS

Table 1. Lb17 EV transcripts whose expression is significantly altered (adjusted p < 0.05 and |log2FC| > 1) in S0 wasps compared to G0 wasps. Conserved domains and motifs were detected via the Conserved Domain Database 61 . GenBank accession numbers and E-values of the domain or protein family are shown. Transcripts are organized by log (2)-FC in their expression. ID refers to the Lb identifier for each transcript labeled in the Volcano Plot in Figure 8A.

ID	Accession	Conserved domain	Log (2)-FC S0 vs. G0	Adjusted p-value S0 vs. G0
1	GAJA01001411.1	CYP4 cd20628 (0E+00)	-6.87725	0.00026306
2	GAJA01001411.1	ycf1 superfamily cl42951 (1.59E-04)	-2.53668	0.00020300
3	GAJA01017388.1 GAJA01015791.1	None	-2.45226	0.00021388
4	GAJA01013791.1 GAJA01018823.1	PLN02872 superfamily cl28691 (2.42E-38)	-2.44316	1.71E-06
5	GAJA01018823.1 GAJA01012169.1	None	-2.43751	0.01366223
6	GAJA01012109.1	LRR 8 pfam13855 (4.09E-08)	-2.35265	0.00318438
7	GAJA01009829.1 GAJA01006376.1	ZnMc superfamily cl00064 (1.72E-28)	-2.23343	0.00318438
8	GAJA01000370.1	TIL cd19941 (3.57E-03)	-2.23343	0.0362285
9	GAJA01020203.1 GAJA01000968.1	None	-2.22716	0.00809954
10	GAJA01000908.1 GAJA01006002.1	None	-2.22710	0.03823238
11	GAJA01000002.1 GAJA01012568.1	None	-2.2178	3.62E-06
12	GAJA01012308.1 GAJA01020069.1	None	-2.17438	0.04720412
13	GAJA01018222.1	PBP_GOBP pfam01395 (8.21E-20)	-2.07279	5.15E-07
14	GAJA01008705.1	CAP_euk cd05380 (4.17E-39)	-2.01981	0.00043155
15	GAJA01016048.1	None	-1.98327	3.90E-05
16	GAJA01014376.1	None	-1.95966	0.00030382
17	GAJA01015285.1	None	-1.93316	0.00119667
18	GAJA01020187.1	serpin42Da-like cd19601 (5.03E-116)	-1.93082	0.03067199
19	GAJA01019354.1	Amino_oxidase pfam01593 (1.15E-64)	-1.82038	0.0035116
20	GAJA01005947.1	nuc_hydro superfamily cl0026 (8.92E-81)	-1.74632	6.09E-13
21	GAJA01008032.1	NADB_Rossman superfamily (1.00E-130)	-1.54859	0.03714499
22	GAJA01011758.1	None	-1.54458	0.00149792
23	GAJA01019353.1	Amino_oxidase pfam01593 (1.15E-64)	-1.32183	0.00449535
24	GAJA01019883.1	MYSc_Myh1_insects_crustaceans cd14909 (0E+00)	-1.30444	1.74E-11
25	GAJA01018902.1	RhoGAP superfamily cl02570 (1.14E-51)	-1.27277	0.04705272
26	GAJA01008333.1	PTZ00184 superfamily cl33172 (2.73E-22)	-1.26373	0.0008629
27	GAJA01016214.1	RT_like superfamily cl02808 (7.14E-03)	-1.26184	0.02510846
28	GAJA01006288.1	RhoGAP superfamily cl02570 (1.11E-22)	-1.09051	0.00805544
29	GAJA01013892.1	S10_plectin pfam03501 (1.28E-64)	1.020586	0.0253683

Table 2. $\mathit{Lh14}$ EV transcripts whose expression is significantly altered in S0 wasps compared to G0 wasps (adjusted p < 0.05 and |log2FC| > 1). Transcripts are organized by log (2)-FC in gene expression. Conserved domain(s) predicted from the Conserved Domain Database 61 search results are also shown. ID refers to the Lh identifier for each transcript labeled in the Volcano Plot in Figure 8B.

7	7	4

ID	Accession	Conserved domain	Log (2)-FC S0 vs. G0	Adjusted p-value S0 vs. G0
1	GAJC01017287.1	None	-1.23674	0.00096682
2	GAJC01017061.1	Chitin_bind_4 pfam00379 (3.07E-19)	-1.11582	0.03116203
3	GAJC01000522.1	None	-1.09305	0.01189165
4	GAJC01000520.1	None	-1.02435	0.00556429
5	GAJC01012741.1	None	4.993669	0.00937726

777 STAR METHODS

RESOURCE AVAILABILITY

779	Lead	contact

778

782

785

786

787

788

789

792

793

794

795

796

Further information and requests for resources and reagents should be directed to and will be fulfilled by the lead contact, Shubha Govind (sgovind@ccny.cuny.edu).

Materials availability

This study generated two mutant strains of *Leptopilina heterotoma*. Mutant strains will be shared by the lead contact upon request.

Data and code availability

- Original transcriptomic data (raw read counts and FASTQ files) from bulk RNA-Seq
 experiments on hosts and parasites have been deposited in and can be accessed from
 NASA's publicly available Open Science Data Repository
 (https://osdr.nasa.gov/bio/repo). Accession numbers are listed in the key resources table.
- Version D of NASA GeneLab's bioinformatics pipeline, available on GitHub, was used
 to process *Drosophila* RNA-Seq reads. A DOI is listed in the key resource table.
 - A modified version of the *Drosophila* pipeline was used to analyze *L. boulardi* and *L. heterotoma* reads. Those scripts are available with the supplemental material Data S1 (L.boulardi_ L.heterotoma_RNAseq_processing_scripts.zip).
 - Microscopy data and any additional information required to reanalyze the data reported in this paper are available from the lead contact upon request.

797

798

799

EXPERIMENTAL MODEL AND STUDY PARTICIPANT DETAILS

Experimental design and sample preparation

D. melanogaster strains y^l w^l and y w hop^{Tum-l} msn-GAL4; UAS-mCD8-GFP $(hop^{Tum-l}$ msn > GFP) 24 , and wasp species L. boulardi strain 17 (Lb17) and L. heterotoma strain 14 (Lh14) 8 , were included in the ground control and flight experiments. The hop^{Tum-l} strain carries a dominant point mutation in the human Janus kinase (JAK) homolog, hopscotch 22 . This mutation confers constitutive JAK-STAT signaling, which drives hematopoietic proliferation and differentiation in larval stages; small, melanized tumors form that can be scored in adult flies. In this strain, the misshapen (msn) promoter directs Gal4 expression to lamellocytes 62 . Expression of the UAS-mCD8-GFP transgene helps visualize lamellocytes, which make up the bulk of the tumors.

Extensive pre-flight testing was done to estimate the diet volume and insect numbers for optimal growth during the 34-day flight period. Six conditions (two fly-only cultures, four fly/wasp co-cultures) were distributed among six VFBs (**Figure 1**). The fly-only cultures were reared in polystyrene vials containing $12 \text{ ml} \pm 1 \text{ ml}$ fly food, while the co-culture vials contained $10 \text{ ml} \pm 1 \text{ ml}$ fly food. The difference in fly food volume accommodated the respective life histories of the two insect species; unlike flies that depend on fly food medium, wasps consume the growing fly larvae and pupae. This volume of fly food supported insect growth for 34 days while keeping carbon dioxide production to a minimum.

Prior to launch, y w fly-only cultures were initiated with 8 female and 5 male flies. The hop^{Tum-l} cultures were similarly initiated with 20 female and 10 male flies. Fly-wasp co-cultures were set up simultaneously by first adding the flies to vials for three days, whereupon the flies were removed and adult wasps introduced. For the y w co-cultures, 30 adult females and 15 adult males were added to each polystyrene vial for egg-laying. For hop^{Tum-l} egg-lays, 35 females and

fifteen males were used. Fifteen egg-lays were made for each genotype, and 15 female and 15 male wasps were added to each egg-lay a day prior to launch.

Mission and hardware details

Six VFBs, each with 15 vials, were placed inside a CTB before the launch of the SpaceX-14 mission to the ISS (**Figure 1**). The mission was launched at 20:30 UTC (Coordinated Universal Time) on April 2nd, 2018. Wasp infection modifies fly development; it takes 20-25 days for wasps to develop into adults, while naïve flies complete their development in 10-15 days. Weather-related issues delayed the original mission time from 31 days to 34 days. The ISS crew installed the samples into the Columbus Module endcone with the CTB lid open to promote air exchange between the VFBs and cabin air, where they remained until approximately two days prior to their return to Earth. Samples remained at ambient temperature (~22°C). Temperature and humidity data in each VFB were collected throughout the flight mission. The radiation dosimeter on the ISS was the COL1A2 Radiation Assessment Detector, ISS-RAD, that detects charged particles ⁶³. Insects remained in the VFBs throughout the mission until their return on the Dragon capsule.

A full-scale, near-synchronous ground control was conducted that was staggered 48 hours from launch, using the environmental data streamed to a Space Station Processing Facility Environmental Simulator at the Kennedy Space Center (KSC). The ground control samples were manually set to recapitulate the temperature and humidity conditions of the space samples. While the temperatures between space and ground samples were similar for the duration of the experiment, the relative humidity of space samples was higher by 20-25% than that of ground samples. This was attributed to reduced convection in the microgravity environment, making it

more difficult for moisture to evaporate quickly. The Dragon capsule was unberthed at 13:22 UTC on May 5th, 2018, and splashdown in the Pacific Ocean occurred on the same day at 20:00, off the coast of Long Beach, CA, from where samples were flown to New York. Ground control samples were similarly collected from KSC and flown to New York.

Condition of insect cultures

Visual inspection of the cultures indicated that most of the fly food in all vials was consumed, and there was no apparent evidence of mold or other microbial infection in any culture vial. G0 and S0 fly-only vials of both genetic backgrounds did not contain sufficient early instar larvae to set up wasp infections. (G1/S1 larval hosts were used instead for infection experiments.) Almost all adult wasps retrieved from G0/S0 cultures developed under corresponding conditions, while adult fly samples contained individuals of mixed age and from 2-3 generations. For all studies, appropriate numbers of animals were randomly selected from different vials.

METHOD DETAILS

Survival studies

Animals in each vial were sorted and scored under a dissecting microscope immediately upon arrival. For fly-only cultures, statistical analysis was performed on counts after excluding counts from vials where sample counts were incomplete. For co-cultures, statistical analysis was performed on the number of flies and wasps after excluding vials where either no insects developed or where sample counts were incomplete. The percentage of female wasps was obtained by dividing the number of female wasps by the total number of wasps in each vial.

Dissections, staining, and imaging

Depending on sample availability, 5-15 animals were dissected to examine lymph glands.

Methods for larval lymph gland dissections, staining, and imaging were previously published ⁶⁴⁻⁶⁷. Lymph glands were counter-stained with rhodamine-labeled phalloidin (R415 Life Technologies) and Hoechst 33258 pentahydrate (Invitrogen). For *Lh*-infected G1 or S1 larvae, primary mouse anti-p40 antibody ^{9,20} (1:1000) was used. Fixed and stained samples were imaged on the Laser Scanning Zeiss 710 or 800 confocal microscopes controlled with Zeiss Zen imaging software in the CCNY core facilities. Images were processed with Photoshop software. Whole insects were imaged with a Leica MZFLIII attached to an Optronics camera. Images were collected using the Magnafire-SP software.

Mitotic index

Three-day egg-lays of G0/S0 *hop* ^{Tum-l} adult flies (described above) were set up at 25°C. Three to five wandering third-instar larvae were used per hemocyte smear for each replicate; three biological replicates were performed. Samples were incubated with rabbit anti-phospho-histone H3 antibody (1:200, EMD Millipore), which was visualized with goat anti-rabbit alkaline phosphatase-linked secondary antibody (1:5000, Thermo Scientific). Antibody binding was visualized by alkaline phosphatase staining (125 μg/ml BCIP and 250 μg/ml NBT, from Promega). The percentage of phospho-histone H3-positive macrophages was calculated by dividing the number of phospho-histone H3-positive macrophages by the total number of macrophages over six visual fields. Cells were scored using a Zeiss Axioplan light microscope.

Adult tumorigenesis

Tumors in randomly chosen G0 and S0 *hop*^{Tum-l} adults (20 males and 5-10 females, ~22°C) were scored 6.5 days (25°C) after their return. The G1 and S1 progeny of these G0 and S0 *hop*^{Tum-l} flies was reared at 27°C, and their abdominal tumors were similarly scored 18.5 days post egglay ²⁴. Using a dissecting microscope, abdominal tumors were categorized as follows: small (< 0.5 body segment), medium (0.5-1 body segment), and large (> 1 body segment). Small-, medium-, and large-sized tumors were arbitrarily weighed as 1, 2, and 3, respectively, and all tumors in each animal were recorded. The average number of tumor structures per animal was determined by dividing the sum of all tumors in each replicate by the total number of animals scored. Three biological replicates were performed for both S0/G0 and S1/G1 comparisons. A student t-test was used to determine if the averages of two data sets differed significantly from each other.

Infection and larval host immunity assay

Egg-lays of G0/S0 *hop*^{Tum-l} flies were set up with the same number of flies used in flight. Larval progeny, raised at 25°C for 3 days, were exposed to 10 male and 10 female G0 and S0 *Lb17* or *Lh14* wasps for 8 hours. For each condition, hosts of the same strain were taken from more than one vial to randomize samples and ensure robust egg-laying. Similarly, wasps of the same species from different vials were combined for infections. Each experiment was replicated 3-4 times.

Infected larvae were randomly selected and examined under a dissecting microscope 3-5 days later for the presence of either melanotic tumors or melanized parasite-induced encapsulation reactions. hop^{Tum-l} tumors and parasite capsules differ in shape; tumors are globular, while capsules are typically sickle-shaped and surround a wasp egg or wasp larva.

These structures can fragment into smaller, melanized pieces, making it difficult to distinguish them. Regardless of their identity, they were classified based on size: (a) specks (similar in appearance to melanized crystal cells), (b) small melanized structures, or (c) large melanized structures. To quantify spaceflight's effects on these reactions, an arbitrary score was assigned as follows: 1-3 specks, 4-8 specks, and > 8 specks were assigned a value of 0.5, 0.75, or 1, respectively. Small- and large-melanized structures were assigned a value of 1 and 4, respectively. Where clear encapsulation reactions (with evidence of a wasp egg) were observed, the structure was also assigned a value of 4. A composite tumor and encapsulation (T + E) score was calculated from 16-29 G1/S1 *Lb17*- or *Lh14*-infected *hop*^{Tum-l} larvae. Uninfected G1/S1 *hop*^{Tum-l} larvae (70-89 animals) served as controls. Pairwise comparisons of the average T + E scores were made using the Mann-Whitney U-test for unpaired samples.

Bulk RNA-Seq sample preparation methods

For RNA-Seq experiments (technique reviewed in ⁶⁸), samples were flash-frozen in dry ice and stored at -80°C. Bulk RNA-Seq analysis was performed on RNA prepared from four replicates of (a) ground control (G0) and space-flown (S0) adult flies; (b) G0 and S0 adult wasps; and (c) G1 and S1 larvae. The RNA/protein purification plus kit from Norgen Biotek Corp. was used for RNA preparation, and the extracted total RNA was stored in Norgen RNA isolation kit elution buffer.

For adult flies, three males and females each, of (a) G0 y w; (b) S0 y w; (c) G0 hop^{Tum-l}; (d) S0 hop^{Tum-l} were used for extraction. RNA preparations of G0 and S0 Lb17 and Lh14 wasps were made from three females and three males. Larval RNA was isolated from G1 and S1 y w animals. In addition, RNA was also extracted from hop^{Tum-l} larvae as follows: (a) uninfected G1;

(b) uninfected S1; (c) G0 *Lb*-infected G1 hosts; (d) S0 *Lb*-infected G1 hosts; (e) G0 *Lb*-infected S1 hosts; (f) S0 *Lb*-infected S1 hosts; (g) G0 *Lh*-infected G1 hosts; (h) S0 *Lh*-infected G1 hosts; (i) G0 *Lh*-infected S1 hosts; and (j) S0 *Lh*-infected S1 hosts.

The RNA from G0 and S0 adult flies and wasps was processed at Genewiz, Inc. as follows: After poly (A)+ extraction, libraries for adult flies and wasps were prepared using the non-stranded NEBNext Ultra RNA Library Prep Kit E7775, following the manufacturer's instructions (NEB, Ipswich, MA, USA). The libraries were validated using the Agilent TapeStation. Libraries were sequenced on the Illumina HiSeq 4000 machine for HiSeq 2x150bp, single index, at Genewiz. Data output was ~300-350 million raw paired-end reads per lane.

The total RNA prepared from G1 and S1 larval samples (stored at -80°C) was processed as follows at NASA's GeneLab Samples Processing Laboratory. The RNA concentration was determined using a Qubit 4.0 Fluorometer, and 400 ng of each sample was used for poly (A)+ extraction. RNA-Seq sequencing libraries were prepared using the E7775 NEBNext Ultra RNA Library Prep Kit, as above. The libraries were validated by using Agilent TapeStation D1000 tape. Quantification was performed using the Qubit 4.0 Fluorometer. Libraries were pooled and sequenced on the Illumina iSeq 100 sequencer to confirm library balancing and screen for ribosomal RNA. The final library pool was sequenced on Illumina NovaSeq 6000 sequencer using S1 Reagent Kit v1.5 (300 cycles, 2 lanes).

Processing of *Drosophila* RNA-Seq data

The reads from adult fly and larval fly RNA were analyzed using version D of NASA GeneLab's

RNA-Seq processing pipeline

(https://github.com/nasa/GeneLab_Data_Processing/blob/master/RNAseq/Pipeline_GL-DPPD-

7101_Versions/GL-DPPD-7101-D.md). For this, the raw fastq files of the adult fly RNA-Seq reads obtained from Genewiz were transferred to GeneLab. Raw fastq files of both sample sets were assessed for percent rRNA (0.30–0.42% rRNA in adults; 0.20–2.73% rRNA in larvae) using HTStream SeqScreener (version 1.3.2) and filtered using Trim Galore! (version 0.6.7) powered by Cutadapt (version 2.6). Raw and trimmed fastq file quality was evaluated with FastQC (version 0.11.9), and MultiQC (version 1.11) was used to generate MultiQC reports.

D. melanogaster STAR and RSEM references were built using STAR (version 2.7.8a) and RSEM (version 1.3.1), respectively, Ensembl release 101, genome version BDGP6.28 (Drosophila_melanogaster.BDGP6.28.dna.toplevel.fa) and the following gtf annotation file: Drosophila_melanogaster.BDGP6.28.101.gtf. Trimmed reads were aligned to the Drosophila melanogaster STAR reference with STAR (version 2.7.8a). A majority (90.08%-94.47%) of trimmed reads mapped uniquely to the fly reference genome. Aligned reads were assessed for strandedness using the RSeQC Infer Experiment (version 4.0.0) and determined to be unstranded. Then aligned reads from all samples were quantified using RSEM (version 1.3.1), with strandedness set to none.

RSEM raw gene counts were imported to R (version 4.0.3) with tximport (version 1.18.0) and normalized with DESeq2 (version 1.30.0) ⁶⁹ median of ratios method. Differential expression analysis was performed in R (version 4.0.3) using DESeq2 (version 1.30.0); all groups were compared pairwise using the Wald test, and the likelihood ratio test was used to generate the F statistic p-value. False discovery rate (adjusted p-value) corrections were performed using Benjamini-Hochberg multiple testing adjustment. Gene annotations were assigned using the following Bioconductor and annotation packages: STRINGdb (v2.2.0),

PANTHER.db (v1.0.10), and org.Dm.eg.db (v3.12.0). Genes were considered differentially expressed if adjusted p < 0.05 and |log2FC| > 1.

984

985

986

987

988

989

990

991

992

993

994

995

996

997

998

999

1000

1001

1002

1003

1004

982

983

Analysis of *Drosophila* RNA-Seq results

Global analyses: Principal Component Analysis (PCA) was performed in R (version 4.0.3) using log (2)-transformed count data from unnormalized and normalized counts. PCA plots were generated for each set of count data using ggplot2 (version 3.3.3). Volcano plots were created using EnhancedVolcano (version 1.8.0), with adjusted p < 0.05 and $|\log 2FC| > 1$ cutoff values specified. KEGG enrichment analyses for adult samples: DEGs in adult fly samples (adjusted p-value < 0.05 and |log2FC| > 1) were used for analysis. Gene ontology (GO) and KEGG enrichment analyses were performed using the Bioconductor package ClusterProfiler v 3.18.0 70 and the Drosophila database (org.Dm.eg.db version 3.13). EnrichGO and EnrichKEGG functions were used to determine functionally enriched GO categories for KEGG pathways and molecular function ⁷¹. Results were visualized by R package⁷². Analysis of Top, Essential, and Pathway DEGs: The most highly modulated Top DEGs in the adult fly samples were identified by sorting log (2)-FC for each comparison and then filtering genes that met the adjusted p-value significance p < 0.05 and |log 2FC| > 1. From this list, the top 50 upregulated or downregulated genes were identified for each comparison, yielding ~280 genes. Annotations and other functional information for these ~280 genes were examined in FlyBase ⁵⁷ and genes with clear orthologs or paralogs and known or predicted functions (172 genes) were retained. Clustering of these 172 Top DEGs revealed six major expression profiles. The magnitude of log (2)-FC for these genes, in both directions, ranged from ~3- to 12-fold.

For Essential DEGs, a list of 1,024 genes that were identified experimentally in P-element insertion screens was compiled ⁷³⁻⁷⁶. Of these 1,024 genes, 137 were differentially expressed in at least one of four comparisons. The DIOPT-DIST tool ⁵⁹, which predicts human orthologs of fly genes and diseases or traits associated with the human orthologs identified through GWAS or OMIM databases, was used to determine the disease relevance of these essential genes. Genes in the JAK-STAT, Toll, and Imd pathways were compiled from KEGG and/or FlyBase. Additional pathway target genes were added from the primary literature ^{54,77,78}.

For larval samples, gene set enrichment analysis of larval RNA-Seq results did not highlight immune changes, and hence the results of this analysis were not included here. Gene expression changes were examined in the context of signaling pathways as was done for the adult RNA-Seq results above.

Processing of parasite RNA-Seq reads

Raw fastq files were filtered using Trim Galore! (version 0.6.7) powered by Cutadapt (version 3.7). Raw and trimmed fastq file quality was evaluated with FastQC (version 0.11.9), and MultiQC (version 1.12) was used to generate MultiQC reports. *L. heterotoma* Bowtie2 and RSEM indices were built using Bowtie2 (version 2.5.0) and RSEM (version 1.3.1), respectively, and the *Lh14* GAJC contig transcriptome reference from NCBI (https://sra-download.ncbi.nlm.nih.gov/traces/wgs03/wgs_aux/GA/JC/GAJC01/GAJC01.1.fsa_nt.gz). *L. boulardi* Bowtie2 and RSEM indices were built using Bowtie2 (version 2.5.0) and RSEM (version 1.3.1), respectively, with *Lb17* GAJA contig transcriptome reference from NCBI (https://sra-download.ncbi.nlm.nih.gov/traces/wgs03/wgs_aux/GA/JA/GAJA01/GAJA01.1.fsa_nt.gz).

Trimmed reads were aligned to the respective wasp parasite species Bowtie2 transcriptome reference with Bowtie2 (version 2.5.0), and aligned reads from all samples were quantified using RSEM (version 1.3.1), with strandedness set to none. Quantification data was imported to R (version 4.1.2) with tximport (version 1.22.0) and normalized with DESeq2 (version 1.34.0) using the median of ratios method. Normalized transcript counts were subject to differential expression analysis in R (version 4.1.2) using DESeq2 (version 1.34.0); all groups were compared using the Wald test, and the likelihood ratio test was used to generate the F statistic p-value. The numbers of significantly differentially expressed transcripts (adjusted p < 0.05 and $|\log 2FC| > 1$) for Lb17 and Lh14 were 293 and 310, respectively. The presence of conserved protein domains or motifs in these differentially expressed Lb17 and Lh14 DEGs was performed via CDD searches (database version CDD v3.20 - 59693 PSSMs; and expect value threshold 0.01) (**Tables S2, S3**).

Analysis of parasite RNA-Seq results

Global analyses: Principal Component Analysis was performed in R (version 4.1.2) using log (2)-transformed count data from unnormalized and normalized counts. PCA plots were generated for each set of count data using ggplot2 (version 3.3.5). Volcano plots were created using EnhancedVolcano (version 1.12.0) with an adjusted p-value < 0.05 and |log2FC| > 1 cutoff values specified.

Identification and analysis of parasite EV transcripts: Proteins from purified Lb17 EVs have not been characterized, but the composition of purified EVs from the Lb Gotheron (LbG) strain is published ¹⁴. To identify differentially expressed Lb17 EV transcripts in space corresponding to these previously characterized 383 LbG EV proteins, we queried the LbG EV protein sequences

against all 293 differentially expressed *Lb17* transcripts in space (**Table S2**; *LbG* EV query sequences were kindly provided by J. Varaldi, University of Lyon). For this, NCBI's tblastn tool was used at default settings (BLOSUM62; gap costs existence extension 1, filtered for low complexity regions, January 2023). Results where E-value ≤ 1 e-30, query coverage ≥ 50 %, and percent identity of ≥ 50 % were scored as high confidence homologs and included 27 sequences. Two sequences did not meet these criteria but were added to our results (**Table 1**), either due to their high log (2)-FC value (GAJA01001411.1; E = 3.00 e-100, query coverage 96%, and % identity 32.49), or due to interesting homology (GAJA01009829.1; E = 4.00 e-30, query coverage 57%, and % identity 32.69).

An estimate of the overall Lb17 EV proteome size was obtained as follows: the 383 LbG sequences were used to tblastn-search the GAJA00000000 sequences 60 . This search identified 316 non-redundant EV protein-encoding GAJA sequences (E \leq 1 e-50, query coverage \geq 70%, percent identity \geq 70%; NCBI BLAST+ (v 2.7.1) $^{15,79-81}$. Some homologs were not identified due to strain differences; nevertheless, the analysis revealed that most of the LbG EV proteins are expressed in the Lb17 female abdomen. Since the Lh14 EV proteome is already characterized 11,12 , tblastn analyses were not necessary, and EV genes were filtered from the 310 Lh14 DEGs (**Table 2**).

SEM preparation of venom EVs and imaging

Thirty venom glands of G0 and S0 wasps were dissected in 100 µl of ice-cold PBS and fixed in 100 µl of 4% glutaraldehyde in 0.1M sodium cacodylate buffer, pH 7.4 (Electron Microscopy Sciences). Venom glands were processed for scanning electron microscopy imaging as follows:

Ten drops of 2% osmium tetroxide aqueous solution (Electron Microscopy Sciences) were added to the sample on ice for 20 minutes. The sample was filtered on a wet 25-mm polycarbonate

Whatman membrane filter (0.1 µm pore size), covered with a second wet filter, and suctioned with the sample in between the filters. The filters were clamped between O-rings and quickly immersed in ice-cold distilled water. The filters were then rinsed in distilled water five times, three minutes for each rinse. This was followed by dehydration in a graded (10%, 30%, 50%, 70%, 80%, 90%, 95%, 100%) series of ethanol for 5 minutes each. The filters were then critical point dried (Balzers, CPD 030) in liquid carbon dioxide five times, 3-5 minutes each. Dehydrated and dried samples were mounted on aluminum SEM specimen mount stubs (Electron Microscopy Sciences) using conductive carbon adhesive tabs (Electron Microscopy Sciences) and stored in a 60°C oven for 2 hours or longer. Samples on the filter were coated with gold/palladium (Leica, EM ACE600) right before being observed on the Zeiss SUPRA 55VP scanning electron microscope. These procedures were carried out at the CCNY and CUNY ASRC core facilities. Figures were assembled in Adobe Photoshop program versions 23.4.1 or 2020 v21.

Virulence assay for *Lh14* venom

Forty *hop*^{Tum-l} larvae were bled in 200 μl of 7% bovine serum albumin. 50 μl of this hemolymph preparation was aliquoted into individual chambers of a 4-chamber slide and allowed to incubate at room temperature for 1 hour. Venom was extracted from G0 and S0 *Lh14* wasps, and protein was quantified using the Bradford method. An appropriate volume of the venom extract containing 30 μg of venom protein was added to the slide chamber with *hop*^{Tum-l} hemocytes. Phosphate-buffered saline (20 mM, pH 7.4) was used as a control. After incubation for 4 hours at 25°C, excess liquid was removed by aspiration, hemocytes were air-dried at room temperature and fixed with 4% paraformaldehyde for 10 min. After washing, cells were stained successively

with rhodamine-labeled phalloidin (R415 Life Technologies) and Hoechst 33258 pentahydrate (Invitrogen) for 15 min each at room temperature. Samples were washed three times with PBS, and stained cells were mounted in Vectashield for confocal microscopy. Lamellocytes with bipolar morphology (i.e., spindle-shaped GFP-positive lamellocytes with two pointed ends) were manually scored. Experiments were replicated three times and the student t-test statistic was applied to determine the significance.

Isolation and characterization of *L. heterotoma* mutants

G0/S0 *Lb17* and *Lh14* male wasps were mated with females from lab cultures, and their grandsons were examined for viable mutations affecting wing color, wing venation, wing morphology, eye color, eye morphology, and antennal morphology. Mutant grandsons were not obtained from the G0/S0 *Lb17* or G0 *Lh14* screens. One *Lh14* grandson with golden wings (instead of the normal grey wings) was identified. This *aurum* male was mated with "lab" females; the progeny was "selfed" to obtain additional mutant males. For a pure-breeding stock, putative heterozygous unmated females were collected by placing pupae into Falcon 3072 96-well plates (Becton Dickinson) 1-3 days prior to their emergence. Strips of Scotch Tape (0.9 cm wide) were used to seal the wells. The *aurum* strain was homozygous viable, and a pure-breeding stock was established.

A second mutant phenotype was observed in the *aurum* wasp culture. The posterior wing margins of this *aurum* wasp were angular instead of the normal round ends. This mutant, *kona*, was similarly homozygous viable but a pure-breeding stock could not be established as *kona* females could not infect hosts. To establish this, 14 unmated, or 11 *kona* male-mated,

heterozygous or homozygous *kona* females, were introduced to *y w* hosts. Ten males were used for the matings. Larval hosts were dissected to assess the presence of eggs.

To examine if *aurum* and *kona* mutations assort independently, unmated *aurum* females were mated with *kona* males. Thirty-six unmated double heterozygous females were used for two rounds of *y w* infections. Over 1,000 male progeny of the four expected genotypes were scored.

Ovaries from wild type, heterozygous, or homozygous *kona* females were fixed in ethanol, mounted in 50% glycerol, and imaged on a Nikon Eclipse TE2000-U microscope attached to a Diagnostic Instruments Inc. camera and NIS Elements Imaging Software 64.0 bit 3.22.14. Ovipositors of 10 wild type and 30 homozygous *kona* females were gently pulled out using sharp forceps, briefly dipped in 70% ethanol and PBS, fixed in 4% paraformaldehyde, and washed in PBS, before mounting in Vectashield. Images were acquired with a Leica Aperio CS2 microscope.

QUANTIFICATION AND STATISTICAL ANALYSIS

Sample size, experimental replication, and data analysis of results are also described in the corresponding sections above and/or the corresponding figure legend. For Figures 2 and S9, each experimental vial was considered a replicate, and statistical analysis of insect survival in space relative to ground after their return to the lab was performed in Microsoft Excel 2016. The mean numbers (\pm standard error) of flies and/or wasps from 14 vials were calculated in Microsoft Excel (2016). Student t-test statistic was applied, and the difference between the corresponding space versus ground samples was significant if p < 0.05. For the data in Figures 6D and 6E, the weighted average number of tumors per animal in S0 versus G0 flies, or S1 versus G1 flies, was calculated in Microsoft Excel. The mean \pm standard error was calculated, and a student t-test was

used to determine biological significance. For Figure 7B, the non-parametric Mann-Whitney Utest for unpaired samples was performed to compare all conditions pairwise. p-values < 0.05 were considered significant. For Figure 9H, more than 1,000 F2 males were scored from unmated dihybrid females, and the raw numbers obtained are shown. A standard chi-square test was applied to accept the null hypothesis. For Figure 9I, at least 30 larvae per condition were dissected and scored for signs of infection. For Figure S11, the means of the proportion of bipolar cells in the *L. heterotoma* virulence assay were compared in experimental versus control samples using Excel and a student t-test. Between 129 and 1,146 lamellocytes were scored per replicate. For differential gene expression analysis in R using DESeq2, all groups were compared using the Wald test. To generate the F statistic p-value and false discovery rate (adjusted p-value), the likelihood ratio test was used. Corrections for multiple testing adjustment were performed using Benjamini-Hochberg. Genes were considered differentially expressed if adjusted p < 0.05 and |log2FC| > 1.

1156 **SUPPLEMENTAL ITEMS Supplemental Information.** Figures S1-S12 and Table S1. 1157 **Table S2.** Lb17 transcripts, differentially expressed in space, related to Figure 8 and Table 1. 1158 1159 All 293 *Lb17* transcripts, differentially expressed (adjusted p < 0.05 and |log2FC| > 1) in space are listed. The GAJA number is the NCBI accession number of the L. boulardi transcript. The 1160 conserved protein domain (top hit), its accession ID and E-value are shown next. Values in bold 1161 identify genes included in Table 1. 1162 **Table S3.** *Lh14* transcripts, differentially expressed in space, related to Figure 8 and Table 2. 1163 All 310 *Lh14* transcripts, differentially expressed (adjusted p < 0.05 and |log2FC| > 1) in space 1164 are listed. The GAJC number is the NCBI accession number of the *L. heterotoma* transcript. The 1165 conserved protein domain (top hit), its accession ID and E-value are shown next. Values in bold 1166 1167 identify genes included in Table 2. **Data S1.** Scripts for modified pipelines for processing the L. boulardi and L. heterotoma RNA-1168 Seq reads. Related to Figure 8, Figure S8, Tables S2 and S3, and Star Methods. 1169 1170

1171 REFERENCES

1172

Afshinnekoo, E., Scott, R.T., MacKay, M.J., Pariset, E., Cekanaviciute, E., Barker, R., Gilroy, S.,
 Hassane, D., Smith, S.M., Zwart, S.R., et al. (2020). Fundamental Biological Features of
 Spaceflight: Advancing the Field to Enable Deep-Space Exploration. Cell 183, 1162-1184.
 10.1016/j.cell.2020.10.050.

- Marcu, O., Lera, M.P., Sanchez, M.E., Levic, E., Higgins, L.A., Shmygelska, A., Fahlen, T.F., Nichol,
 H., and Bhattacharya, S. (2011). Innate immune responses of Drosophila melanogaster are
 altered by spaceflight. PLoS One 6, e15361. 10.1371/journal.pone.0015361.
- Taylor, K., Kleinhesselink, K., George, M.D., Morgan, R., Smallwood, T., Hammonds, A.S., Fuller,
 P.M., Saelao, P., Alley, J., Gibbs, A.G., et al. (2014). Toll mediated infection response is altered by
 gravity and spaceflight in Drosophila. PLoS One 9, e86485. 10.1371/journal.pone.0086485.
- lyer, J., Mhatre, S.D., Gilbert, R., and Bhattacharya, S. (2022). Multi-system responses to altered
 gravity and spaceflight: Insights from Drosophila melanogaster. Neurosci Biobehav Rev *142*,
 104880. 10.1016/j.neubiorev.2022.104880.
- Lue, C.H., Buffington, M.L., Scheffer, S., Lewis, M., Elliott, T.A., Lindsey, A.R.I., Driskell, A.,
 Jandova, A., Kimura, M.T., Carton, Y., et al. (2021). DROP: Molecular voucher database for identification of Drosophila parasitoids. Mol Ecol Resour *21*, 2437-2454. 10.1111/1755-0998.13435.
- Kim-Jo, C., Gatti, J.L., and Poirie, M. (2019). Drosophila Cellular Immunity Against Parasitoid
 Wasps: A Complex and Time-Dependent Process. Front Physiol *10*, 603.
 10.3389/fphys.2019.00603.
- 1193 7. Ehlers, S., and Schaible, U.E. (2012). The granuloma in tuberculosis: dynamics of a host-pathogen collusion. Front Immunol *3*, 411. 10.3389/fimmu.2012.00411.
- Schlenke, T.A., Morales, J., Govind, S., and Clark, A.G. (2007). Contrasting infection strategies in generalist and specialist wasp parasitoids of Drosophila melanogaster. PLoS Pathog *3*, 1486-1197 1501. 06-PLPA-RA-0488 [pii]10.1371/journal.ppat.0030158.
- 1198 9. Chiu, H., Morales, J., and Govind, S. (2006). Identification and immuno-electron microscopy 1199 localization of p40, a protein component of immunosuppressive virus-like particles from 1200 Leptopilina heterotoma, a virulent parasitoid wasp of Drosophila. J Gen Virol *87*, 461-470. 1201 10.1099/vir.0.81474-0.
- 1202 10. Rizki, R.M., and Rizki, T.M. (1984). Selective destruction of a host blood cell type by a parasitoid wasp. Proc Natl Acad Sci U S A *81*, 6154-6158.
- 11. Heavner, M.E., Ramroop, J., Gueguen, G., Ramrattan, G., Dolios, G., Scarpati, M., Kwiat, J.,
 1205 Bhattacharya, S., Wang, R., Singh, S., and Govind, S. (2017). Novel Organelles with Elements of
 1206 Bacterial and Eukaryotic Secretion Systems Weaponize Parasites of Drosophila. Curr Biol *27*,
 1207 2869-2877 e2866. 10.1016/j.cub.2017.08.019.
- Wey, B., Heavner, M.E., Wittmeyer, K.T., Briese, T., Hopper, K.R., and Govind, S. (2020). Immune
 Suppressive Extracellular Vesicle Proteins of Leptopilina heterotoma Are Encoded in the Wasp
 Genome. G3 (Bethesda) 10, 1-12. 10.1534/g3.119.400349.
- 1211 13. Colinet, D., Schmitz, A., Cazes, D., Gatti, J.-L., Poirie, M. (2010). The origin of intraspecific variation of virulence in an eukaryotic immune suppressive parasite. PLoS Pathog *6*, e1001206.
- 1213 14. Di Giovanni, D., Lepetit, D., Guinet, B., Bennetot, B., Boulesteix, M., Couté, Y., Bouchez, O., Ravallec, M., and Varaldi, J. (2020). A behavior-manipulating virus relative as a source of adaptive genes for Drosophila parasitoids. Mol Biol Evol. 10.1093/molbev/msaa030.
- 1216 15. Wey, B. (2021). PhD Thesis: Insights into Leptopilina Spp. Immune-Suppressive Strategies Using Mixed-omics and Molecular Approaches. https://academicworks.cuny.edu/gc_etds/4162.

- 1218 16. Gueguen, G., Rajwani, R., Paddibhatla, I., Morales, J., and Govind, S. (2011). VLPs of Leptopilina 1219 boulardi share biogenesis and overall stellate morphology with VLPs of the heterotoma clade. 1220 Virus Res *160*, 159-165. 10.1016/j.virusres.2011.06.005.
- 17. Wan, B., Poirie, M., and Gatti, J.L. (2020). Parasitoid wasp venom vesicles (venosomes) enter
 1222 Drosophila melanogaster lamellocytes through a flotillin/lipid raft-dependent endocytic
 1223 pathway. Virulence 11, 1512-1521. 10.1080/21505594.2020.1838116.
- 12.4 18. Chiu, H., and Govind, S. (2002). Natural infection of D. melanogaster by virulent parasitic wasps
 1225 induces apoptotic depletion of hematopoietic precursors. Cell Death Differ *9*, 1379-1381.
 1226 10.1038/sj.cdd.4401134.
- 1227 19. Rizki, T.M., Rizki, R.M., Carton, Y. (1990). *Leptopilina heterotoma* and *L. boulardi:* strategies to avoid cellular defense responses of *Drosophila melanogaster*. Exp Parasitol *70*, 466-475.
- 1229 20. Ramroop, J.R., Heavner, M.E., Razzak, Z.H., and Govind, S. (2021). A parasitoid wasp of
 1230 Drosophila employs preemptive and reactive strategies to deplete its host's blood cells. PLoS
 1231 Pathog 17, e1009615. 10.1371/journal.ppat.1009615.
- 1232 21. Rizki, T.M., and Rizki, R.M. (1994). Parasitoid-induced cellular immune deficiency in Drosophila.

 1233 Ann N Y Acad Sci *712*, 178-194.
- Luo, H., Hanratty, W.P., and Dearolf, C.R. (1995). An amino acid substitution in the Drosophila
 hopTum-l Jak kinase causes leukemia-like hematopoietic defects. EMBO J 14, 1412-1420.
- Harrison, D.A., Binari, R., Nahreini, T.S., Gilman, M. and Perrimon, N. (1995). Activation of a
 Drosophila Janus kinase (JAK) causes hematopoietic neoplasia and developmental defects.
 EMBO J. 14, 2857-2865.
- Panettieri, S., Paddibhatla, I., Chou, J., Rajwani, R., Moore, R.S., Goncharuk, T., John, G., and
 Govind, S. (2019). Discovery of aspirin-triggered eicosanoid-like mediators in a Drosophila
 metainflammation blood tumor model. J Cell Sci 133. 10.1242/jcs.236141.
- 1242 25. Qiu, P., Pan, P.C., and Govind, S. (1998). A role for the Drosophila Toll/Cactus pathway in larval hematopoiesis. Development *125*, 1909-1920.
- 1244 26. Govind, S. (1996). Rel signalling pathway and the melanotic tumour phenotype of Drosophila. 1245 Biochem Soc Trans *24*, 39-44.
- Hanratty, W.P., and Ryerse, J.S. (1981). A genetic melanotic neoplasm of Drosophila melanogaster. Dev Biol. *83*, 238-249. https://doi.org/10.1016/0012-1606(81)90470-X.
- 1248 28. Rizki, R.M., and Rizki, T.M. (1974). Basement membrane abnormalities in melanotic tumor formation of Drosophila. Experientia *30*, 543-546.
- 29. Banerjee, S., Biehl, A., Gadina, M., Hasni, S., and Schwartz, D.M. (2017). JAK-STAT Signaling as a
 Target for Inflammatory and Autoimmune Diseases: Current and Future Prospects. Drugs 77,
 521-546. 10.1007/s40265-017-0701-9.
- 30. Barnabei, L., Laplantine, E., Mbongo, W., Rieux-Laucat, F., and Weil, R. (2021). NF-kappaB: At the
 Borders of Autoimmunity and Inflammation. Front Immunol *12*, 716469.
 10.3389/fimmu.2021.716469.
- 1256 31. Nickerson, C.A., Ott, C.M., Mister, S.J., Morrow, B.J., Burns-Keliher, L., and Pierson, D.L. (2000).
- Microgravity as a novel environmental signal affecting Salmonella enterica serovar Typhimurium virulence. Infect Immun *68*, 3147-3152. 10.1128/IAI.68.6.3147-3152.2000.
- 1259 32. Gilbert, R., Torres, M., Clemens, R., Hateley, S., Hosamani, R., Wade, W., and Bhattacharya, S.
- 1260 (2020). Spaceflight and simulated microgravity conditions increase virulence of Serratia
 1261 marcescens in the Drosophila melanogaster infection model. NPJ Microgravity 6, 4.
- 1262 10.1038/s41526-019-0091-2.
- 1263 33. Mhatre, S.D., Iyer, J., Petereit, J., Dolling-Boreham, R.M., Tyryshkina, A., Paul, A.M., Gilbert, R., 1264 Jensen, M., Woolsey, R.J., Anand, S., et al. (2022). Artificial gravity partially protects space-

- induced neurological deficits in Drosophila melanogaster. Cell Rep *40*, 111279. 1266 10.1016/j.celrep.2022.111279.
- de Cicco, D.V., and Spradling, A.C. (1984). Localization of a cis-acting element responsible for the developmentally regulated amplification of Drosophila chorion genes. Cell *38*, 45-54. 10.1016/0092-8674(84)90525-7.
- 1270 35. Cornman, R.S. (2009). Molecular evolution of Drosophila cuticular protein genes. PLoS One *4*, e8345. 10.1371/journal.pone.0008345.
- 1272 36. Enjin, A., Zaharieva, E.E., Frank, D.D., Mansourian, S., Suh, G.S., Gallio, M., and Stensmyr, M.C.
 1273 (2016). Humidity Sensing in Drosophila. Curr Biol *26*, 1352-1358. 10.1016/j.cub.2016.03.049.
- Hanratty, W.P., and Dearolf, C.R. (1993). The Drosophila Tumorous-lethal hematopoietic oncogene is a dominant mutation in the hopscotch locus. Mol Gen Genet *238*, 33-37.
- 1276 38. Lanot, R., Zachary, D., Holder, F., and Meister, M. (2001). Postembryonic hematopoiesis in Drosophila. Dev Biol *230*, 243-257. 10.1006/dbio.2000.0123.
- 1278 39. Louradour, I., Sharma, A., Morin-Poulard, I., Letourneau, M., Vincent, A., Crozatier, M., and
 1279 Vanzo, N. (2017). Reactive oxygen species-dependent Toll/NF-kappaB activation in the
 1280 Drosophila hematopoietic niche confers resistance to wasp parasitism. Elife 6.
 1281 10.7554/eLife.25496.
- 1282 40. Sorrentino, R.P., Carton, Y., and Govind, S. (2002). Cellular immune response to parasite infection in the Drosophila lymph gland is developmentally regulated. Dev Biol *243*, 65-80. 1284 10.1006/dbio.2001.0542.
- 1285 41. Colinet, D., Schmitz, A., Depoix, D., Crochard, D., and Poirie, M. (2007). Convergent use of
 1286 RhoGAP toxins by eukaryotic parasites and bacterial pathogens. PLoS Pathog *3*, e203. 07-PLPA1287 RA-0581 [pii]10.1371/journal.ppat.0030203.
- Labrosse, C., Stasiak, K., Lesobre, J., Grangeia, A., Huguet, E. (2005). A RhoGAP protein as a main immune suppressive factor in the *Leptopilina boulari* (Hymenoptera, Figitidae)-*Drosophila melanogaster* interaction. Insect. Biochem. Mol. Biol. *35*, 92-103.
- 1291 43. Ikenaga, M., Yoshikawa, I., Kojo, M., Ayaki, T., Ryo, H., Ishizaki, K., Kato, T., Yamamoto, H., and 1292 Hara, R. (1997). Mutations induced in Drosophila during space flight. Biol Sci Space *11*, 346-350. 10.2187/bss.11.346.
- Filatova, L.P., Vaulina, E.N., Grozdova, T., Prudhommeau, C., and Proust, J. (1983). Some results
 of the effect of space flight factors on Drosophila melanogaster. Adv Space Res *3*, 143-146.
 10.1016/0273-1177(83)90184-9.
- Honor 1297 45. Buckhold, B. (1969). Biosatellite II--physiological and somatic effects on insects. Life Sci Space Res 7, 77-83.
- 1299 46. Thimann, K.V. (1968). Biosatellite II experiments: preliminary results. Proc Natl Acad Sci U S A *60*, 347-361. 10.1073/pnas.60.2.347.
- 1301 47. Ogneva, I.V., Belyakin, S.N., and Sarantseva, S.V. (2016). The Development Of Drosophila
 1302 Melanogaster under Different Duration Space Flight and Subsequent Adaptation to Earth
 1303 Gravity. PLoS One *11*, e0166885. 10.1371/journal.pone.0166885.
- 48. Walls, S., Diop, S., Birse, R., Elmen, L., Gan, Z., Kalvakuri, S., Pineda, S., Reddy, C., Taylor, E.,
 1305 Trinh, B., et al. (2020). Prolonged Exposure to Microgravity Reduces Cardiac Contractility and
 1306 Initiates Remodeling in Drosophila. Cell Rep *33*, 108445. 10.1016/j.celrep.2020.108445.
- 1307 49. Merzendorfer, H., and Zimoch, L. (2003). Chitin metabolism in insects: structure, function and regulation of chitin synthases and chitinases. J Exp Biol *206*, 4393-4412. 10.1242/jeb.00709.
- Davis, M.N., Horne-Badovinac, S., and Naba, A. (2019). In-silico definition of the Drosophila melanogaster matrisome. Matrix Biol Plus *4*, 100015. 10.1016/j.mbplus.2019.100015.
- Hassler, D.M., Zeitlin, C., Wimmer-Schweingruber, R.F., Ehresmann, B., Rafkin, S., Eigenbrode, J.L., Brinza, D.E., Weigle, G., Bottcher, S., Bohm, E., et al. (2014). Mars' surface radiation

- environment measured with the Mars Science Laboratory's Curiosity rover. Science *343*, 1244797. 10.1126/science.1244797.
- Hellweg, C.E., and Baumstark-Khan, C. (2007). Getting ready for the manned mission to Mars: the astronauts' risk from space radiation. Naturwissenschaften *94*, 517-526. 10.1007/s00114-006-0204-0.
- 1318 53. Cucinotta, F.A., To, K., and Cacao, E. (2017). Predictions of space radiation fatality risk for exploration missions. Life Sci Space Res (Amst) *13*, 1-11. 10.1016/j.lssr.2017.01.005.
- De Gregorio, E., Spellman, P.T., Tzou, P., Rubin, G.M., and Lemaitre, B. (2002). The Toll and Imd pathways are the major regulators of the immune response in Drosophila. EMBO J *21*, 2568-2579. 10.1093/emboj/21.11.2568.
- Buchon, N., Broderick, N.A., Poidevin, M., Pradervand, S., and Lemaitre, B. (2009). Drosophila
 intestinal response to bacterial infection: activation of host defense and stem cell proliferation.
 Cell Host Microbe 5, 200-211. S1931-3128(09)00028-6 [pii]10.1016/j.chom.2009.01.003.
- 1326 56. Rooryck, C., Diaz-Font, A., Osborn, D.P., Chabchoub, E., Hernandez-Hernandez, V., Shamseldin,
 1327 H., Kenny, J., Waters, A., Jenkins, D., Kaissi, A.A., et al. (2011). Mutations in lectin complement
 1328 pathway genes COLEC11 and MASP1 cause 3MC syndrome. Nat Genet 43, 197-203.
 1329 10.1038/ng.757.
- 1330 57. Gramates, L.S., Agapite, J., Attrill, H., Calvi, B.R., Crosby, M.A., Dos Santos, G., Goodman, J.L.,
 1331 Goutte-Gattat, D., Jenkins, V.K., Kaufman, T., et al. (2022). Fly Base: a guided tour of highlighted
 1332 features. Genetics 220. 10.1093/genetics/iyac035.
- Davis, C.F., and Dorak, M.T. (2010). An extensive analysis of the hereditary hemochromatosis gene HFE and neighboring histone genes: associations with childhood leukemia. Ann Hematol 89, 375-384. 10.1007/s00277-009-0839-y.
- Hu, Y., Flockhart, I., Vinayagam, A., Bergwitz, C., Berger, B., Perrimon, N., and Mohr, S.E. (2011).
 An integrative approach to ortholog prediction for disease-focused and other functional studies.
 BMC Bioinformatics 12, 357. 10.1186/1471-2105-12-357.
- Goecks, J., Mortimer, N.T., Mobley, J.A., Bowersock, G.J., Taylor, J., Schlenke, T.A. (2013).
 Integrative approach reveals composition of endoparasitoid wasp venoms. PLoS One 8, e64125.
- Lu, S., Wang, J., Chitsaz, F., Derbyshire, M.K., Geer, R.C., Gonzales, N.R., Gwadz, M., Hurwitz, D.I.,
 Marchler, G.H., Song, J.S., et al. (2020). CDD/SPARCLE: the conserved domain database in 2020.
 Nucleic Acids Res 48, D265-D268. 10.1093/nar/gkz991.
- Tokusumi, T., Sorrentino, R.P., Russell, M., Ferrarese, R., Govind, S., and Schulz, R.A. (2009).

 Characterization of a lamellocyte transcriptional enhancer located within the misshapen gene of Drosophila melanogaster. PLoS One *4*, e6429. 10.1371/journal.pone.0006429.
- Zeitlin C, C.A., Beard KB, Abdelmelek M., Hayes BM, Johnson AS, Stoffle N, Rios RR. (2023).
 Results from the Radiation Assessment Detector on the International Space Station: Part 1, the
 Charged Particle Detector. Life Sciences in Space Research *In press*.
- Gueguen, G., Kalamarz, M.E., Ramroop, J., Uribe, J., Govind, S. (2013). Polydnaviral ankyrin
 proteins aid parasitic wasp survival by coordinate and selective inhibition of hematopoietic and
 immune NF-kappa B signaling in insect hosts. PLoS Pathog *9* e1003580.
- Small, C., Ramroop, J., Otazo, M., Huang, L.H., Saleque, S., and Govind, S. (2014). An unexpected link between notch signaling and ROS in restricting the differentiation of hematopoietic progenitors in Drosophila. Genetics *197*, 471-483. genetics.113.159210
 [pii]10.1534/genetics.113.159210.
- Kalamarz, M.E., Paddibhatla, I., Nadar, C., Govind, S. (2012). Sumoylation is tumor-suppressive
 and confers proliferative quiescence to hematopoietic progenitors in Drosophila melanogaster
 larvae. Biol Open 1, 161-172. doi: 10.1242/bio.2012043.

- 1360 67. Paddibhatla, I., Lee, M.J., Kalamarz, M.E., Ferrarese, R., and Govind, S. (2010). Role for
 1361 sumoylation in systemic inflammation and immune homeostasis in Drosophila larvae. PLoS
 1362 Pathog 6, e1001234. 10.1371/journal.ppat.1001234.
- 1363 68. Stark, R., Grzelak, M., and Hadfield, J. (2019). RNA sequencing: the teenage years. Nat Rev Genet 20, 631-656. 10.1038/s41576-019-0150-2.
- Love, M.I., Huber, W., and Anders, S. (2014). Moderated estimation of fold change and dispersion for RNA-seq data with DESeq2. Genome Biol *15*, 550. 10.1186/s13059-014-0550-8.
- 1367 70. Yu, G., Wang, L.G., Han, Y., and He, Q.Y. (2012). clusterProfiler: an R package for comparing biological themes among gene clusters. OMICS *16*, 284-287. 10.1089/omi.2011.0118.
- 1369 71. Consortium, G.O. (2021). The Gene Ontology resource: enriching a GOld mine. Nucleic Acids Res 49, D325-D334. 10.1093/nar/gkaa1113.
- 1371 72. Wickham, H. (2016). ggplot2: Elegant Graphics for Data Analysis. Use R!,. 2nd ed. Springer
 1372 International Publishing: Imprint: Springer,.
- Spradling, A.C., Stern, D., Beaton, A., Rhem, E.J., Laverty, T., Mozden, N., Misra, S., and Rubin,
 G.M. (1999). The Berkeley Drosophila Genome Project gene disruption project: Single P-element
 insertions mutating 25% of vital Drosophila genes. Genetics 153, 135-177.
 10.1093/genetics/153.1.135.
- Salzberg, A., Prokopenko, S.N., He, Y., Tsai, P., Pal, M., Maroy, P., Glover, D.M., Deak, P., and
 Bellen, H.J. (1997). P-element insertion alleles of essential genes on the third chromosome of
 Drosophila melanogaster: mutations affecting embryonic PNS development. Genetics 147, 1723 1741. 10.1093/genetics/147.4.1723.
- 1381 75. Bourbon, H.M., Gonzy-Treboul, G., Peronnet, F., Alin, M.F., Ardourel, C., Benassayag, C., Cribbs, D., Deutsch, J., Ferrer, P., Haenlin, M., et al. (2002). A P-insertion screen identifying novel X-linked essential genes in Drosophila. Mech Dev *110*, 71-83. S0925477301005664 [pii].
- 1384 76. Oh, S.W., Kingsley, T., Shin, H.H., Zheng, Z., Chen, H.W., Chen, X., Wang, H., Ruan, P., Moody, M., and Hou, S.X. (2003). A P-element insertion screen identified mutations in 455 novel essential genes in Drosophila. Genetics *163*, 195-201. 10.1093/genetics/163.1.195.
- Hanson, M.A., and Lemaitre, B. (2020). New insights on Drosophila antimicrobial peptide
 function in host defense and beyond. Curr Opin Immunol *62*, 22-30. 10.1016/j.coi.2019.11.008.
- 1389 78. Bina, S., Wright, V.M., Fisher, K.H., Milo, M., and Zeidler, M.P. (2010). Transcriptional targets of
 1390 Drosophila JAK/STAT pathway signalling as effectors of haematopoietic tumour formation.
 1391 EMBO Rep 11, 201-207. 10.1038/embor.2010.1.
- 79. Altschul, S.F., Gish, W., Miller, W., Myers, E.W., and Lipman, D.J. (1990). Basic local alignment search tool. J Mol Biol *215*, 403-410. 10.1006/jmbi.1990.9999S0022-2836(05)80360-2 [pii].
- Johnson, M., Zaretskaya, I., Raytselis, Y., Merezhuk, Y., McGinnis, S., and Madden, T.L. (2008). NCBI BLAST: a better web interface. Nucleic Acids Res *36*, W5-9. 10.1093/nar/gkn201.

1399

1396 81. Camacho, C., Coulouris, G., Avagyan, V., Ma, N., Papadopoulos, J., Bealer, K., and Madden, T.L. (2009). BLAST+: architecture and applications. BMC Bioinformatics *10*, 421. 10.1186/1471-2105-10-421.



Key resources table

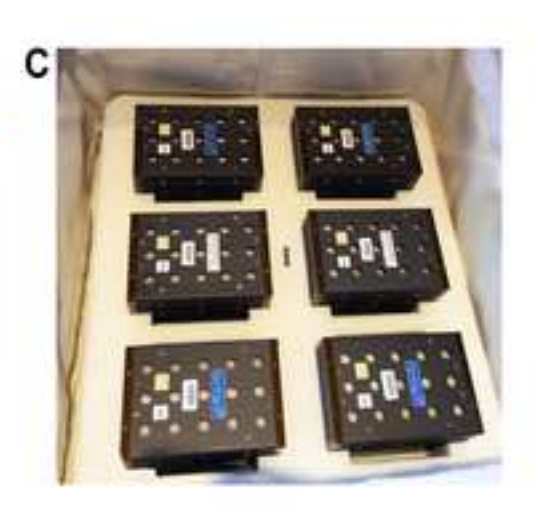
REAGENT or RESOURCE	SOURCE	IDENTIFIER
Antibodies		
rabbit anti-phospho-histone H3 antibody	EMD Millipore	Catalog # 06-570
mouse anti-p40 antibody	Chiu et al., 2006	PMID: 16432035
Chemicals, peptides, and recombinant proteins	•	
5-bromo 4-chloro 3-indoyl phosphate (BCIP)	Promega	Catalog # S381C
nitroblue tetrazolium (NBT)	Promega	Catalog # S380C
paraformaldehyde (crystalline)	Sigma	Catalog # P6148
rhodamine-labeled phalloidin	Life Technologies	Catalog # R415
vectashield mounting medium	Vector Labs	Catalog # H100
Hoechst 33258 pentahydrate	Invitrogen	Catalog # H-1398
4% glutaraldehyde in 0.1M sodium cacodylate buffer, pH 7.4	Electron Microscopy Sciences	Catalog # 16539-06
2% osmium tetroxide	Electron Microscopy Sciences	Catalog # 19150
Biological samples		
G0 and S0 adult <i>y w</i> and <i>hop</i> ^{Tum-l} flies (genotypes below)	This study	N/A
G0 and S0 <i>y w</i> and <i>hop</i> ^{Tum-l} larvae	This study	N/A
G1 and S1 <i>y w</i> and <i>hop</i> ^{Tum-l} larvae	This study	N/A
G0 and S0 Leptopilina boulardi 17 adult wasps	This study	N/A
G0 and S0 Leptopilina heterotoma 14 adult wasps	This study	N/A
Critical commercial assays	•	
RNA extraction RNA/Protein Purification plus kit	Norgen	Catalog # 48200
Non-stranded NEBNext Ultra RNA Library Prep Kit for RNA-Seq sequencing libraries	New England Biolabs	Catalog # E7775
Deposited data	•	
Drosophila RNA-Seq data	NASA Open Science Data Repository	GeneLab ID: GLDS-583; OSDR ID: OSD-588; https://osdr.nasa.gov/bio/repo/data/studies/OSD-588; DOI: 10.26030/v9rh-5a70
Leptopilina boulardi RNA-Seq data	NASA Open Science Data Repository	GeneLab ID: GLDS-587; OSDR ID: OSD-610; https://osdr.nasa.gov/bio/repo/data/studies/OSD-610; DOI: 10.26030/9ee4-6s36



Leptopilina heterotoma RNA-Seq data	NASA Open Science Data Repository	GeneLab ID: GLDS-586; OSDR ID: OSD-609; https://osdr.nasa.gov/bio/repo/data/studies/OSD-609; DOI: 10.26030/5rjq-a347
Experimental models: Organisms/strains		
$y^1 w^1$	Bloomington Stock Center	BDSC:1495
y w hop ^{Tum-I} msn-Gal4; UAS-mCD8-GFP (hop ^{Tum-I} msn > GFP	Panettieri et al., 2019	PMID: 31562189
L. boulardi strain 17 (Lb17)	Schlenke et al., 2007	PMID: 34051038
L. heterotoma strain 14 (Lh14)	Schlenke et al., 2007	PMID: 34051038
Wing color mutant: L. heterotoma14 aurum	This study	Lh14 aurum
Wing shape and ovipositor mutant: <i>L. heterotoma14 kona</i>	This study	Lh14 kona
Software and algorithms		
Adobe Photoshop Creative Cloud v20-v24	Adobe	https://www.adobe.c om/
Pipeline for <i>Drosophila</i> RNA-Seq data	NASA GeneLab: Open Science for Life in Space	GL-DPPD-7101-D; https://github.com/na sa/GeneLab Data P rocessing/blob/mast er/RNAseq/Pipeline GL-DPPD- 7101 Versions/GL- DPPD-7101-D.md
Slurm and R scripts to process and analyze Leptopilina boulardi RNA-Seq data and Leptopilina heterotoma RNA-Seq data	This study, supplement	Data S1
Other	1	
25 mm polycarbonate Whatman membrane filter (0.1 μm pore size)	Whatman	Catalog # 110605
SEM specimen mount stubs	Electron Microscopy Sciences	Catalog # 75110
Illumina HiSeq 4000 (Genewiz)	Illumina, San Diego	https://www.Illumina. com
Illumina NovaSeq 6000 sequencer using S1 Reagent Kit v1.5 (GeneLab)	Illumina, San Diego	https://www.Illumina. com





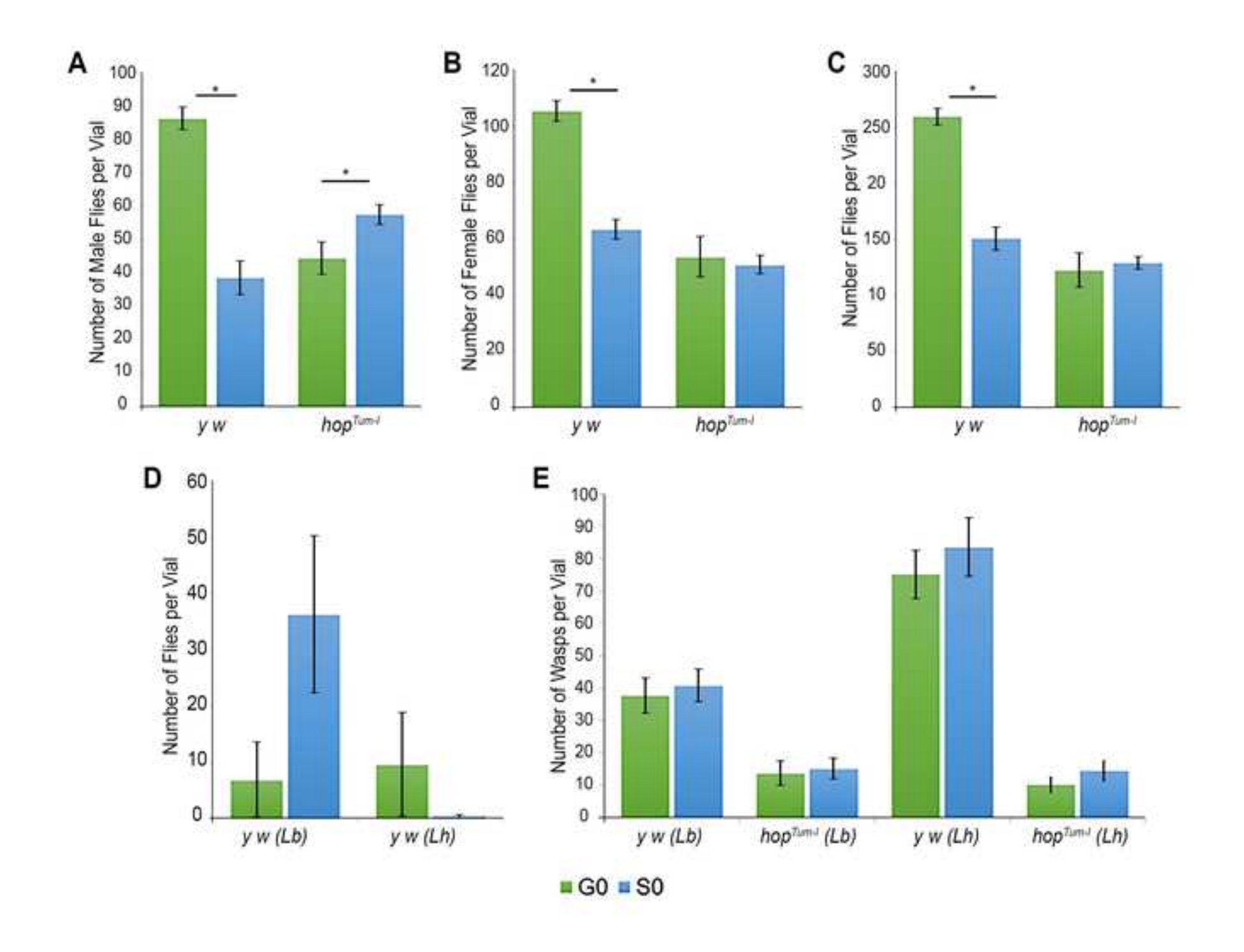


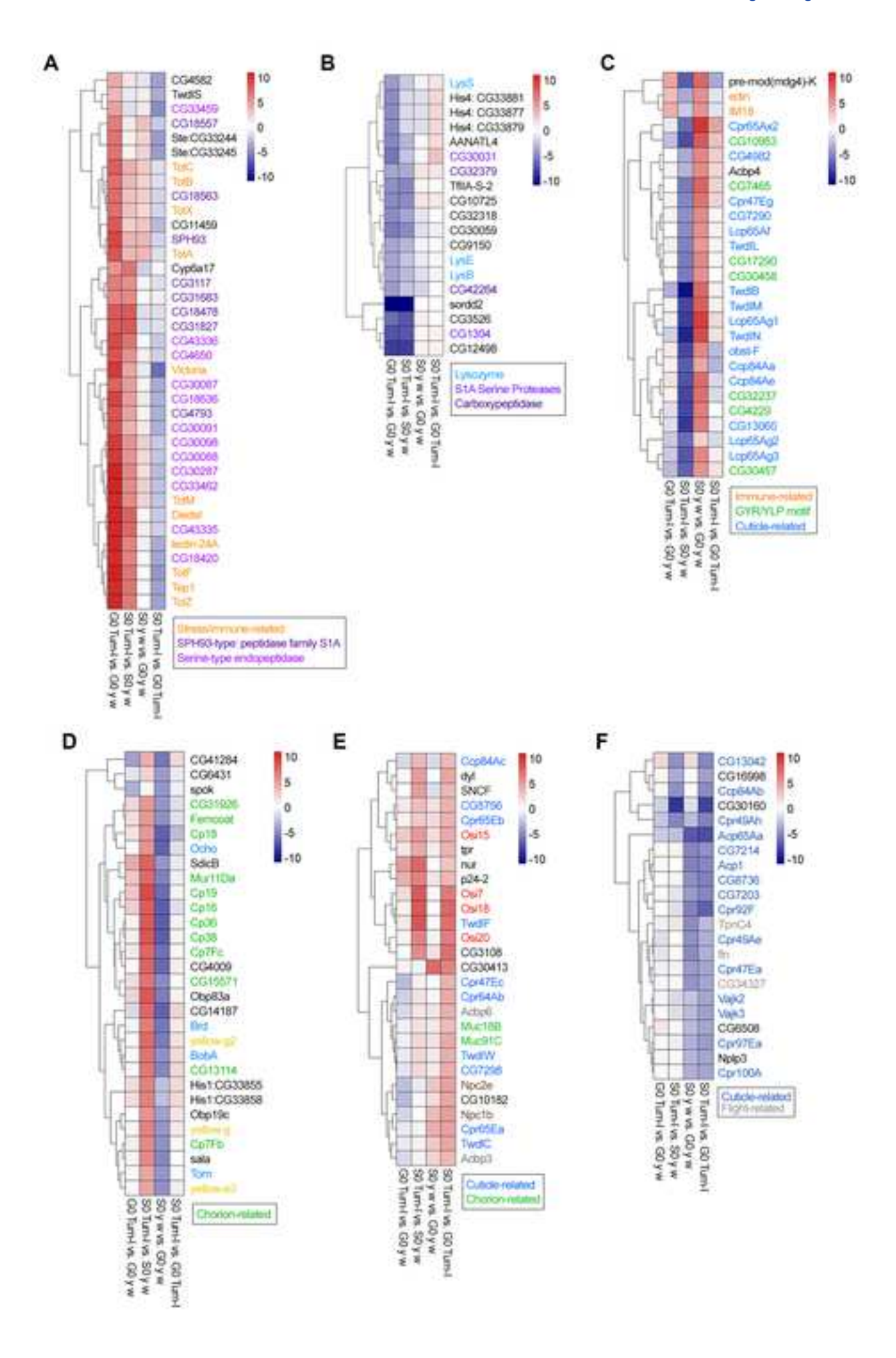
Ply-only Cultures (15 replicates)

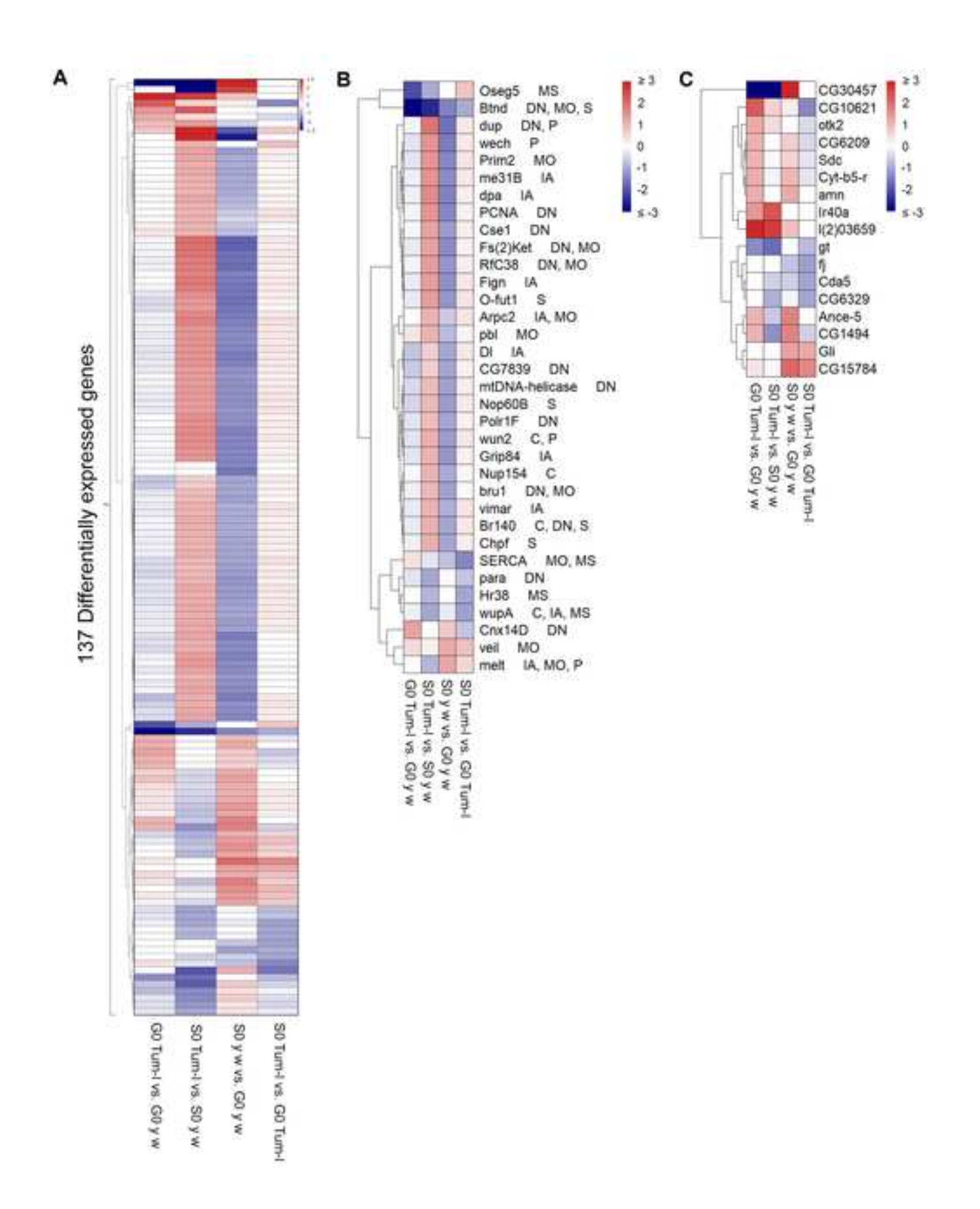
Control Immune-activated yw hop^{Tumel}

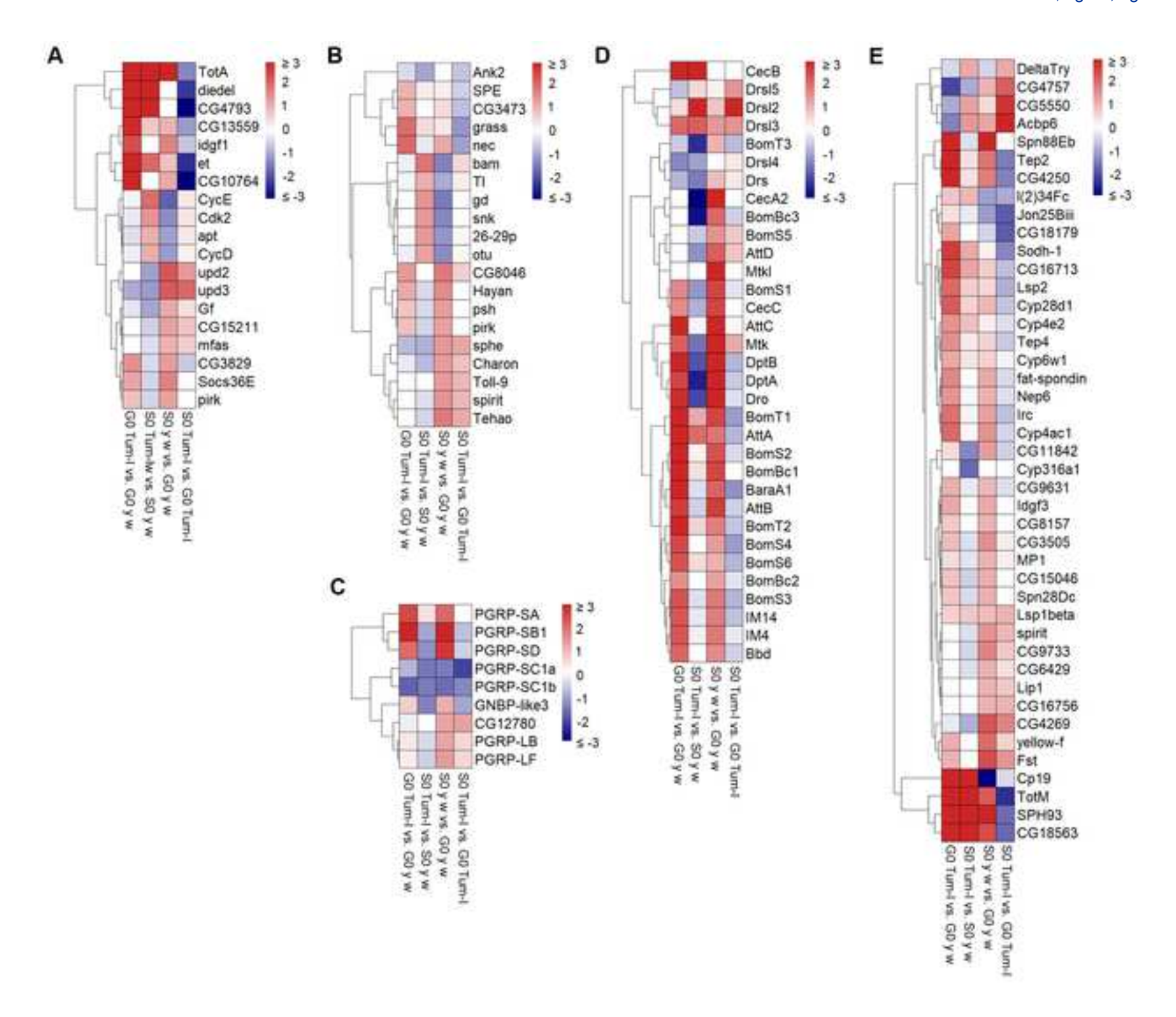
yw hop^{Tumel}

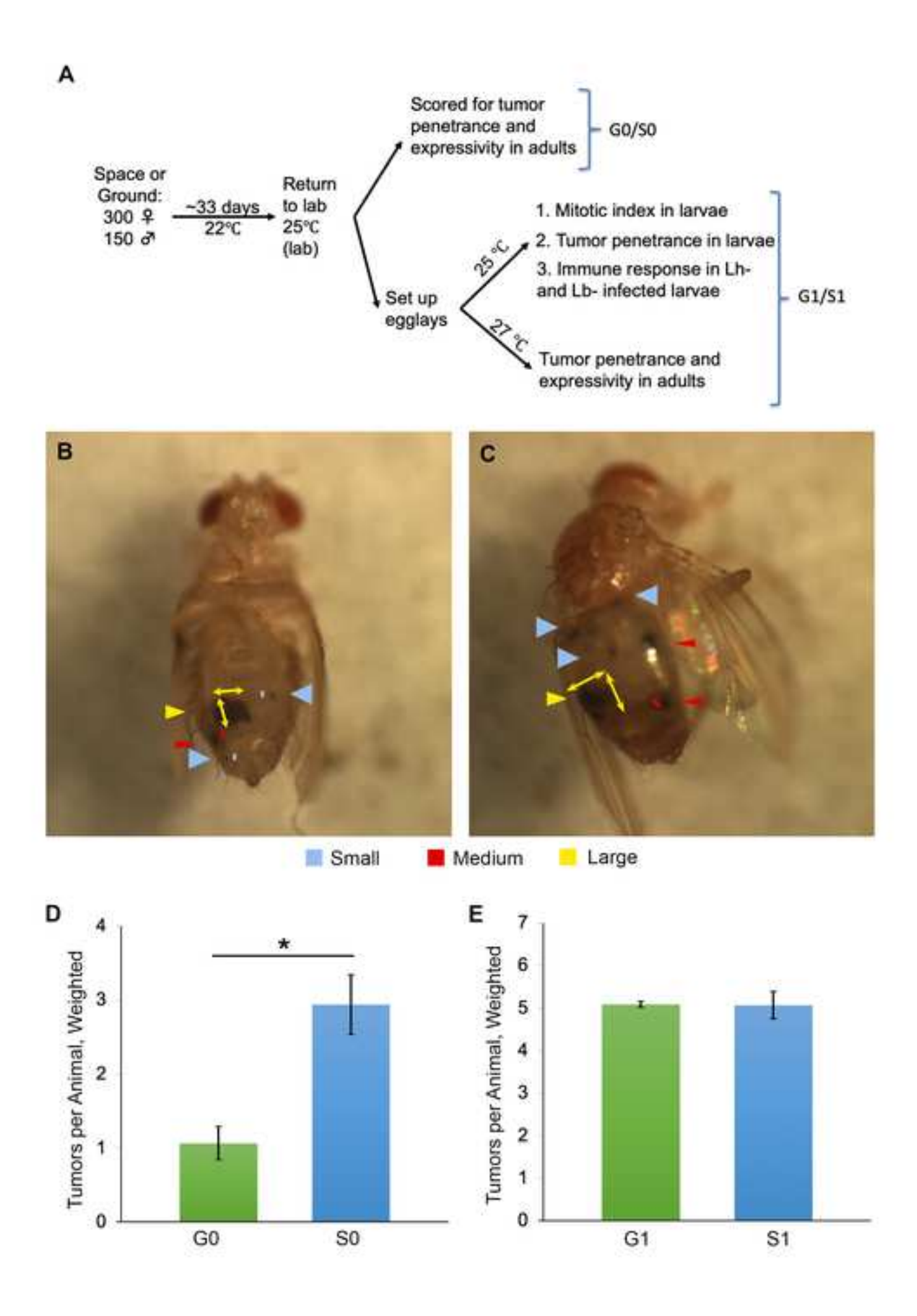
(Lb17) (Lb17) (Lh14) (Lh14)

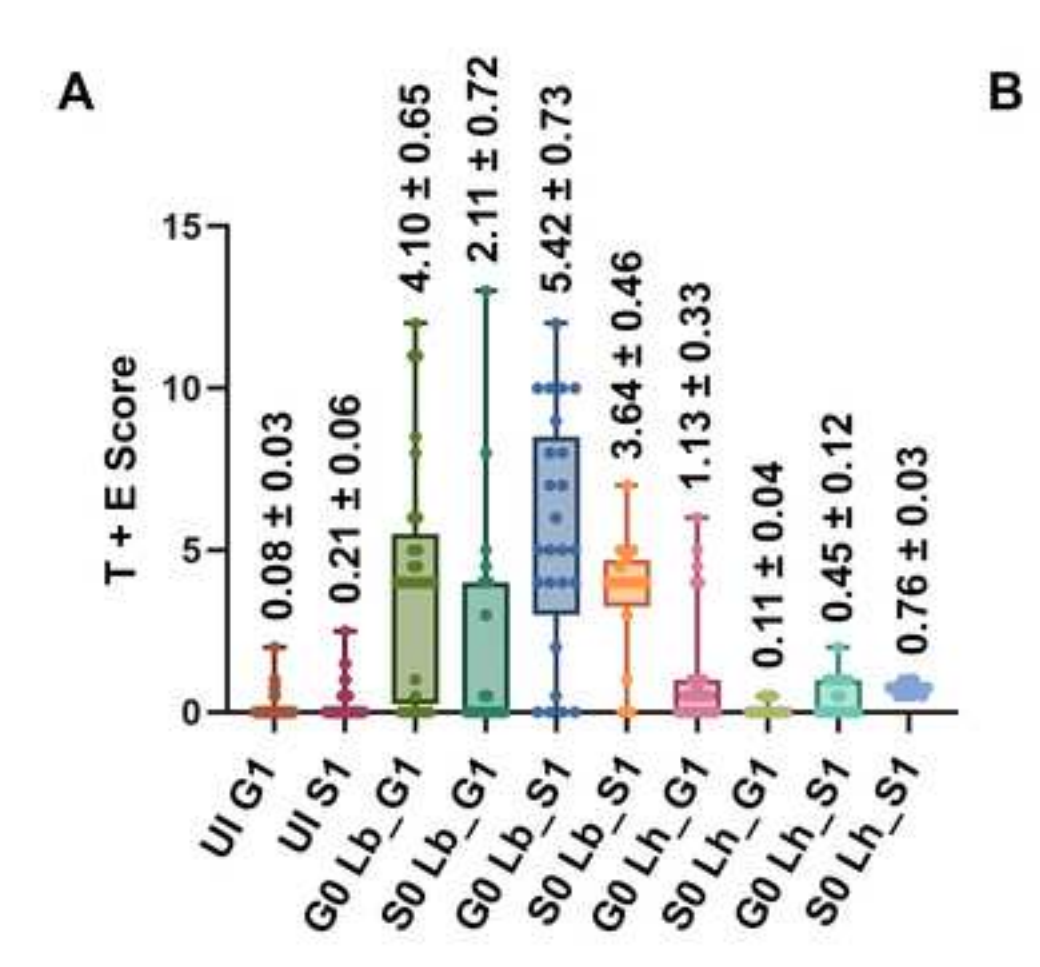




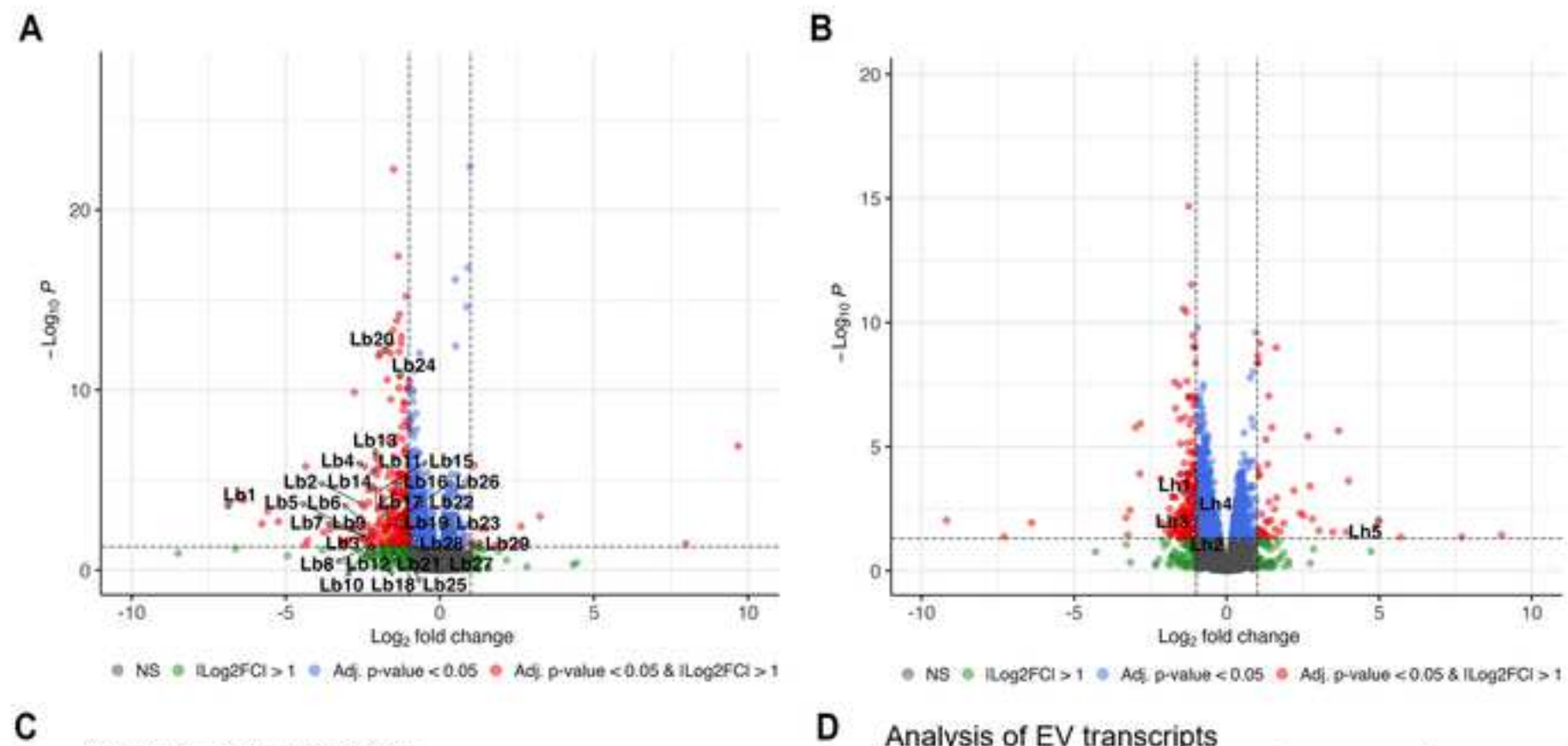








Comparison	p-value
UI S1 hosts vs. UI G1 hosts	0.01
G0 Lb_G1 hosts vs. UI G1 hosts	1.4E-14
S0 Lb_G1 hosts vs. UI G1 hosts	0.00001
G0 Lb_S1 hosts vs. UI S1 hosts	5.3E-09
S0 Lb_S1 hosts vs. UI S1 hosts	0.09729
G0 Lh_G1 hosts vs. UI G1 hosts	5E-11
S0 Lh_G1 hosts vs. UI G1 hosts	1.5E-09
G0 Lh_S1 hosts vs. UI S1 hosts	0.03582
S0 Lh_S1 hosts vs. UI S1 hosts	1.7E-10
G0 Lb_S1 hosts vs. G0 Lb_G1 hosts	0.14011
S0 Lb_S1 hosts vs. S0 Lb_G1 hosts	0.0199
G0 Lh_S1 hosts vs. G0 Lh_G1 hosts	0.37765
S0 Lh_S1 hosts vs. S0 Lh_G1 hosts	5.5E-10
S0 Lb_G1 hosts vs. G0 Lb_G1 hosts	0.01975
S0 Lb_S1 hosts vs. G0 Lb_S1 hosts	0.06352
S0 Lh_G1 hosts vs. G0 Lh_G1 hosts	0.00092
S0 Lh_S1 hosts vs. G0 Lh_S1 hosts	0.04575

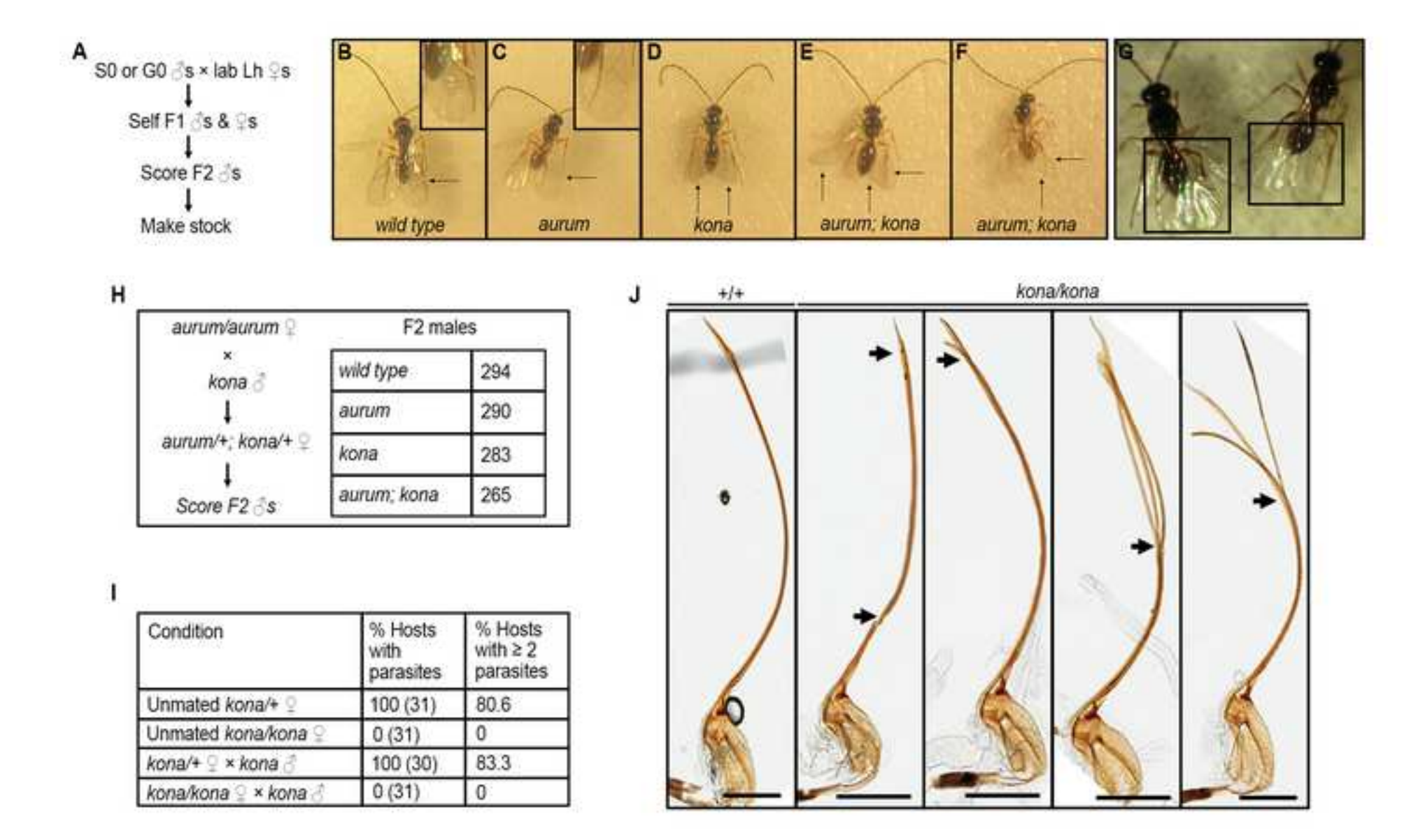


Analysis of all transcripts

Wasp	All transcripts	0.0000000000000000000000000000000000000	% DE transcripts	Down	Up
Lb17	19,836	293	1.48	280 (95.56%)	13 (4.43%)
Lh14	24,170	310	1.28	261 (84.19%)	49 (15.8%)

Analysis of EV transcripts

Wasp	EV transcripts analyzed		transcripts	expressed EV	% DE EV transcripts/ all DE transcripts
Lb17	316	312	98.73	29	9.89
Lh14	406	398	98.03	5	1.61



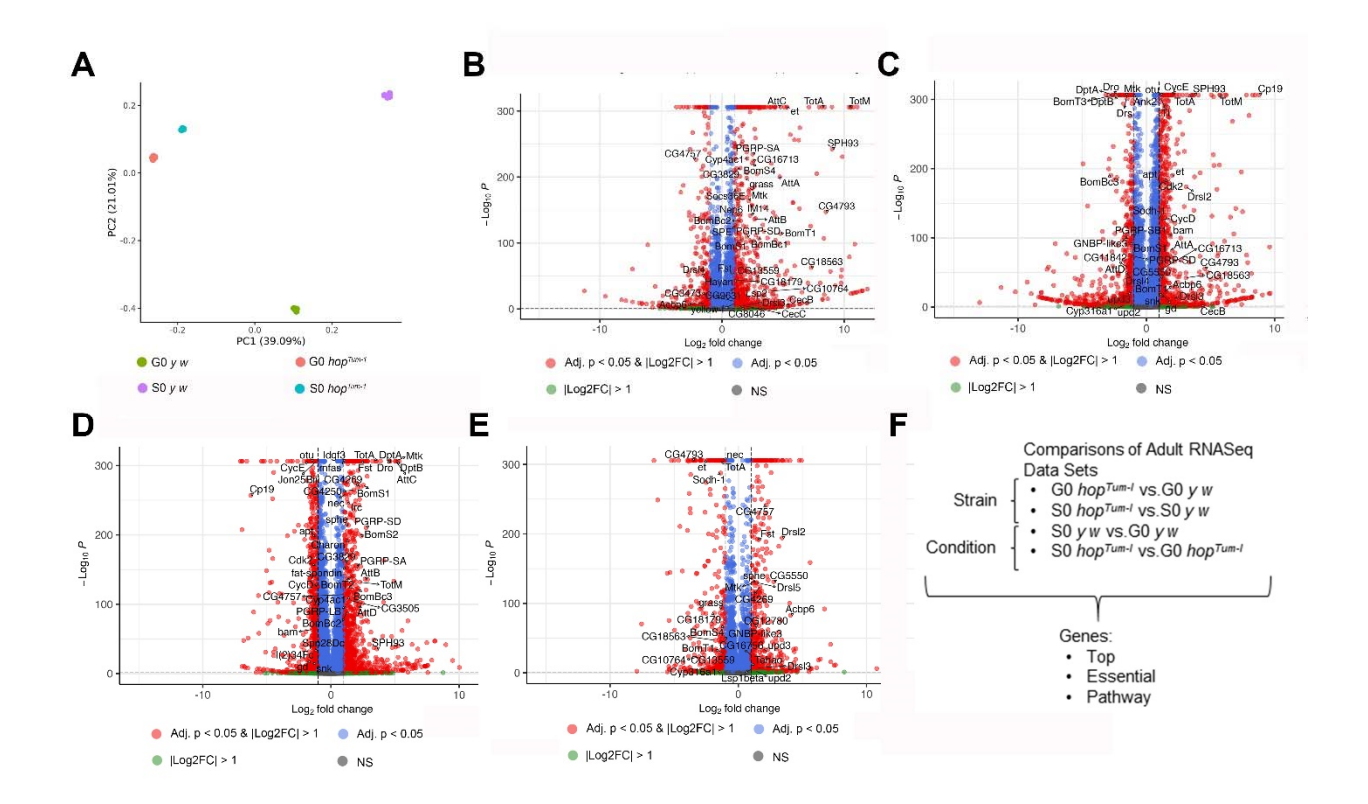


Figure S1. RNA-Seq analysis of adult fly samples, related to Figures 3-6.

(A) Principal component analysis for 16 samples with the log (2)-fold-transformed normalized gene-level counts data.

(B-E) Enhanced volcano plots comparing DEGs from adult fly samples. (B) G0 hop^{Tum-l} vs. G0 y w; (C) S0 hop^{Tum-l} vs. S0 y w; (D) S0 y w vs. G0 y w; (E) S0 hop^{Tum-l} vs. G0 hop^{Tum-l} . Each dot represents the average value from four replicates for a single gene. Red colors indicate upregulated and downregulated genes with adjusted p < 0.05 and |log2FC| > 1 cutoff values; blue dots indicate genes with adjusted p < 0.05 and |log2FC| < 1. Multiple comparisons were accounted for by calculation of a Benjamini–Hochberg false discovery rate-adjusted p-value (i.e., q-value). Dashed horizontal lines mark a q-value of 0.05 and dashed vertical lines indicate a log 2-FC of 1 and -1. Gene symbols correspond to differentially expressed immune genes.

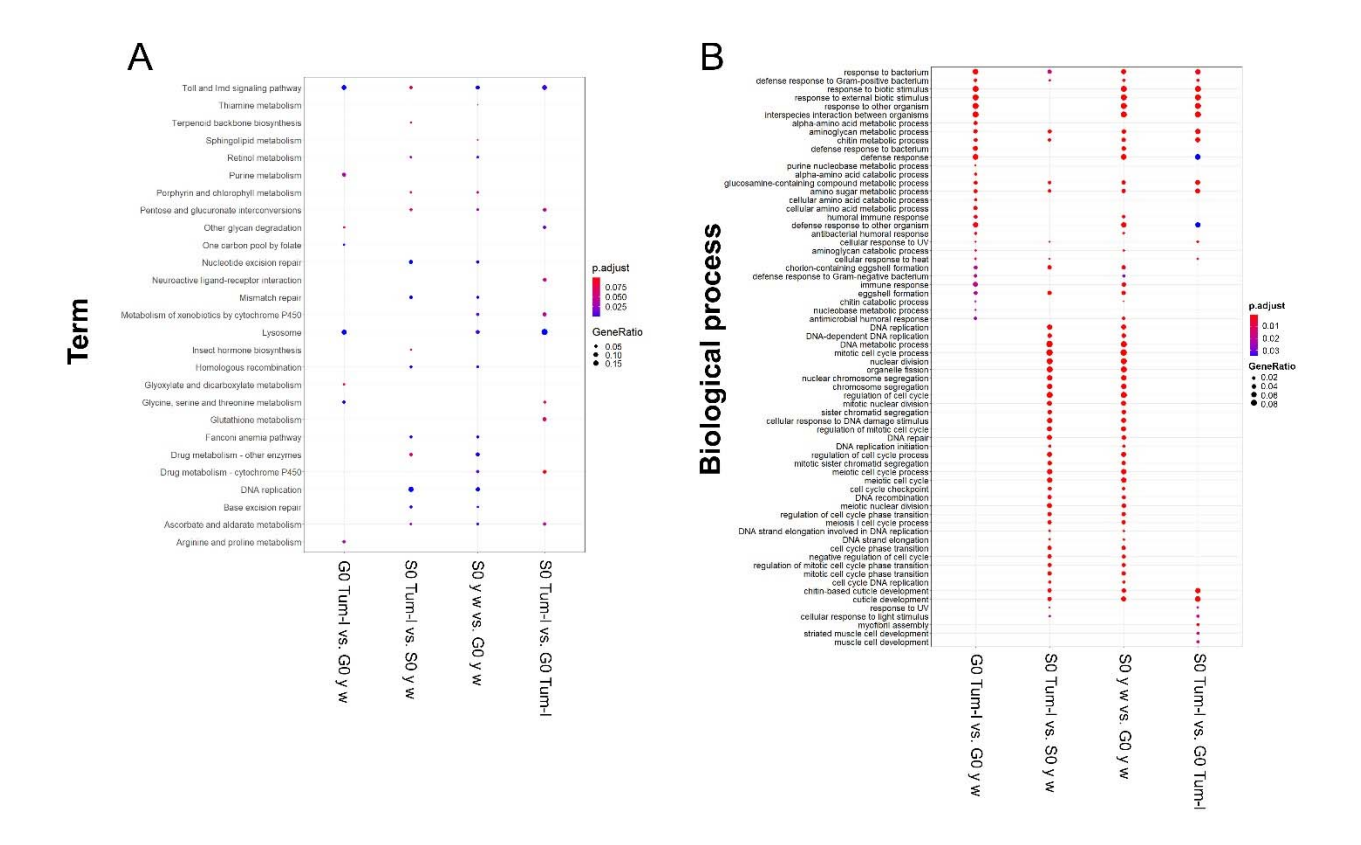


Figure S2. Enrichment analysis of differentially expressed genes in G0 and S0 adult flies, related to Figures 3-6.

(A) Enrichment analysis of KEGG pathways visualized by dot plot (adjusted p-value < 0.1). The size of the dot is based on the gene count enriched in the pathway, while the color of the dot represents pathway significance. Experimental conditions analyzed are (a) G0 hop^{Tum-l} versus G0 y w (G0 Tum-l vs. G0 y w); (b) S0 hop^{Tum-l} versus S0 y w (S0 Tum-l vs. S0 y w); (c) S0 y w versus G0 y w (S0 y w); and (d) S0 hop^{Tum-l} versus G0 hop^{Tum-l} (S0 Tum-l vs. G0 Tum-l).

(B) Gene ontology enrichment for biological process. Dot plot representing top 20 significantly enriched gene ontology terms (adjusted p-value < 0.05) in biological processes for experimental conditions shown in panel A. Enrichment is represented as gene ratio, which indicates the number of genes differentially expressed in the experimental versus control condition, for each biological process indicated on the left.

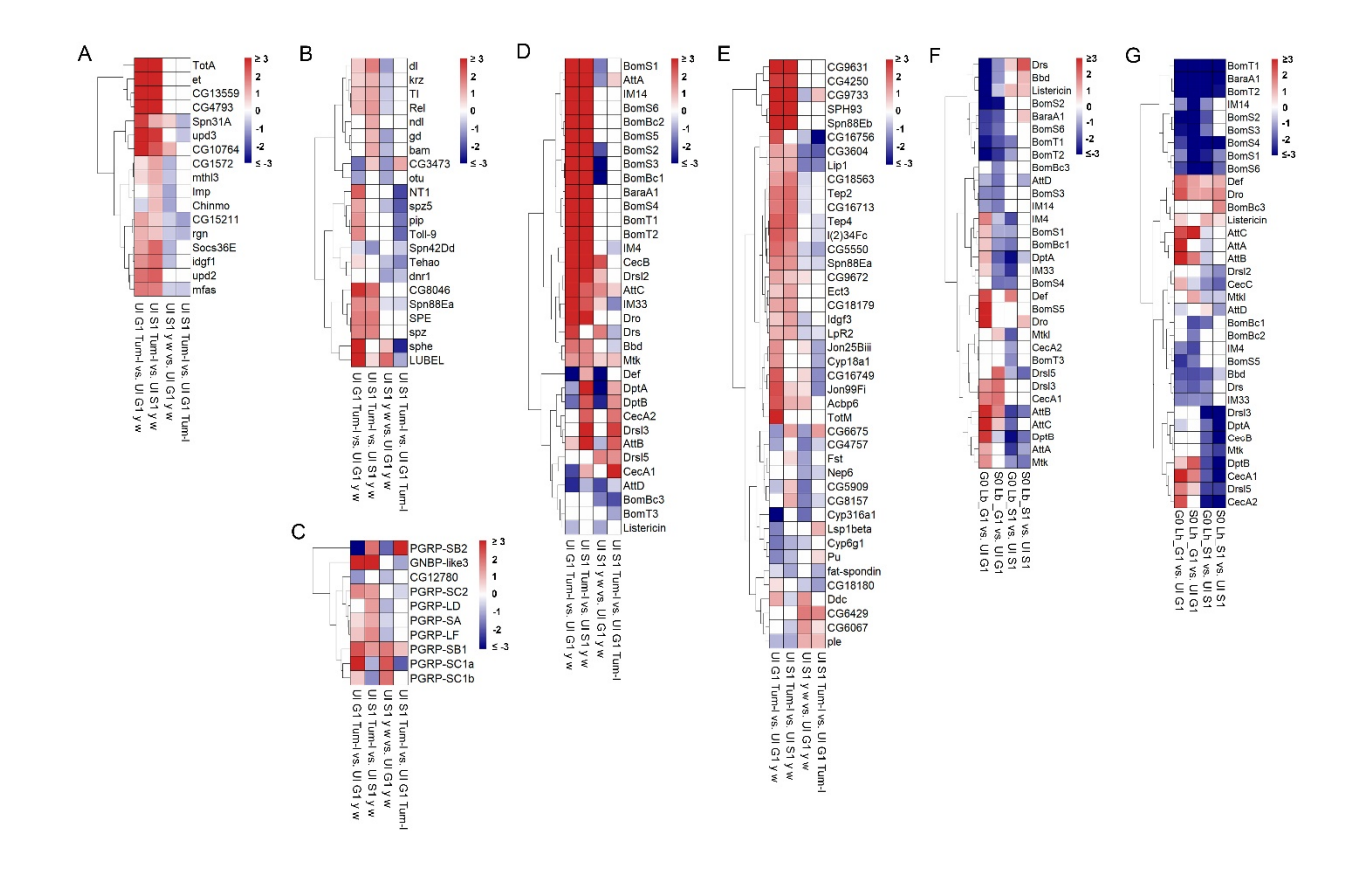


Figure S3. Differentially expressed immune signaling genes in naïve and wasp-infected G1 and S1 larvae, related to Figure 7.

- (A) JAK-STAT pathway components and target genes in naïve S1 and G1 y w or hop^{Tum-l} larvae are shown based on fold-induction. Genes were grouped based on their annotation in FlyBase 1 . Pathway genes that were significantly differentially expressed (adjusted p < 0.05 and |log2FC| > 1) in at least one of the four comparisons are shown.
- (B-E) Genes in the Toll/Imd pathway in naïve S1 and G1 y w or hop^{Tum-l} larvae that are differentially expressed (adjusted p < 0.05 and |log2FC| > 1) in at least one of the four comparisons are indicated. Core pathway components (B), Pattern Recognition Receptor genes (C), antimicrobial peptide genes (D), and other targets (E).

(**F**, **G**) Heat maps of AMP target immune genes comparing gene expression in G1 or S1 *hop*^{Tum-l} hosts, parasitized with either G0/S0 *L. boulardi* (F), or G0/S0 *L. heterotoma* (G) relative to uninfected controls.

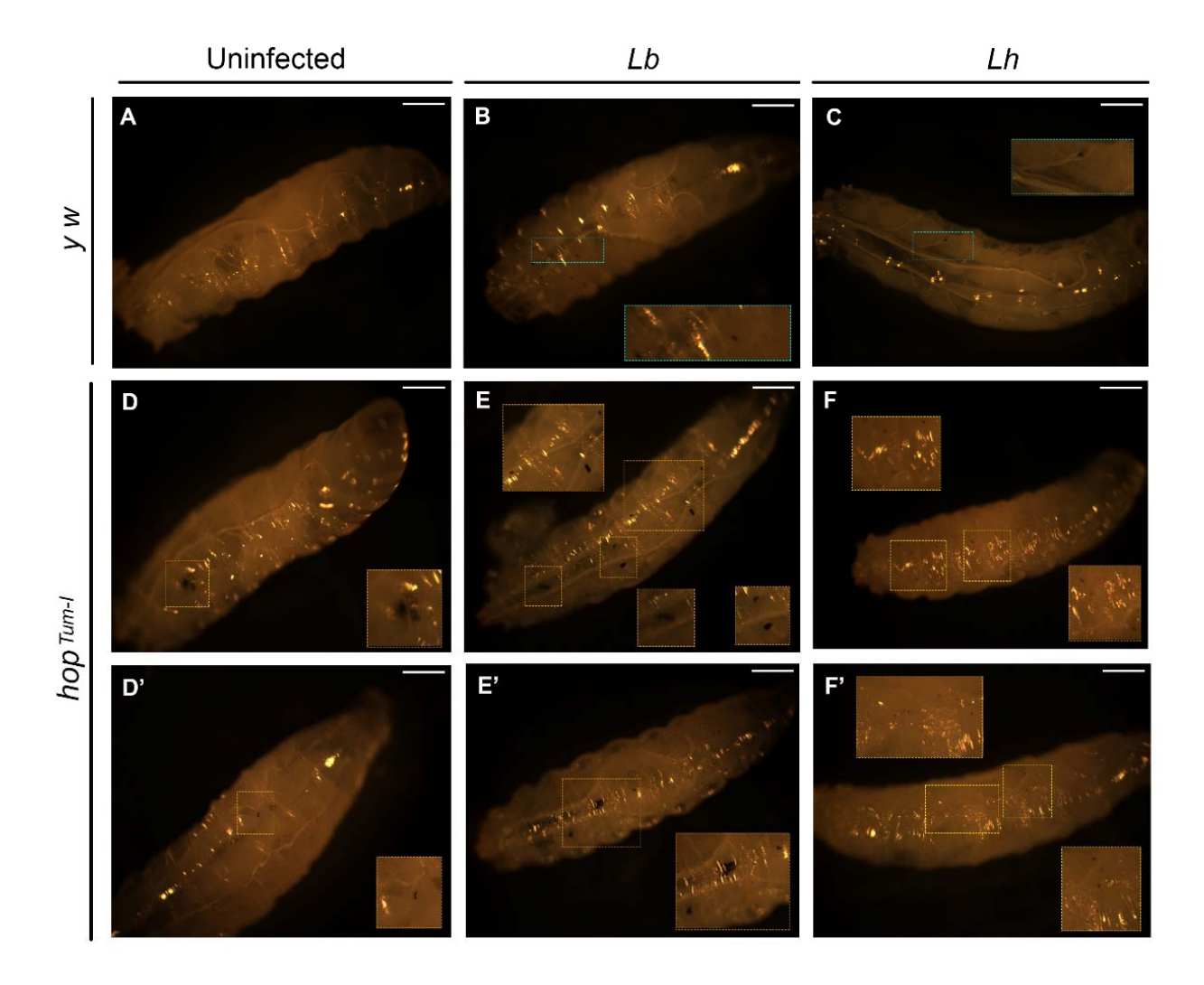


Figure S4. Immune reactions observed after wasp infection, related to Figure 7.

(A-C) Cellular encapsulation reactions in Lb- or Lh-infected G1 or S1 y w larvae. Fewer reactions are evident in Lh- versus Lb-infected y w larvae.

(D-F') Examples of tumors and encapsulation reactions in *Lb*- or *Lh*-infected G1 or S1 hop^{Tum-l} hosts. These melanized structures have similar features of varying sizes as shown. Select areas with immune reactions are enlarged and shown as insets. Scale bars = 1 mm.

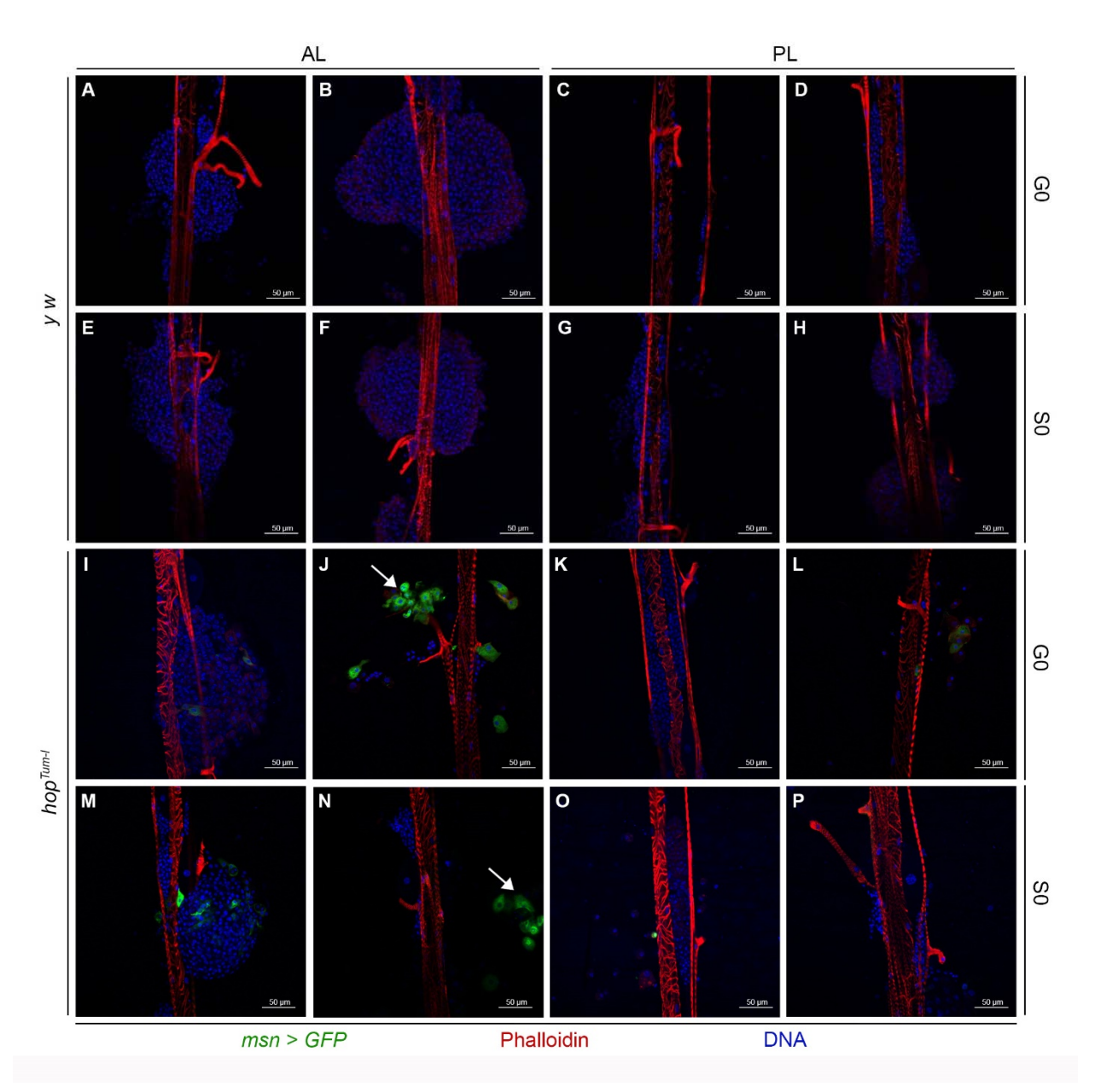


Figure S5. Lymph glands of naïve G0 and S0 hosts, related to Figure 7.

(A-H) Representative lymph glands from G0 (A-D) and S0 (E-H) y w larvae. Anterior (A, B, E, F) and posterior lobes (C, D, G, H) of y w lymph glands. n = 12 lymph glands, each condition. (I-P) Representative lymph glands from G0 (I-L) and S0 (M-P) hop^{Tum-l} msn > GFP larvae. Anterior (I, J, M, N) and posterior (K, L, O, P) lobes. n = 12 for each condition.

Scale bars 50 μm . AL refers to anterior lobes, PL to posterior lobes. Arrows in panels J and N indicate GFP-positive lamellocyte aggregates.

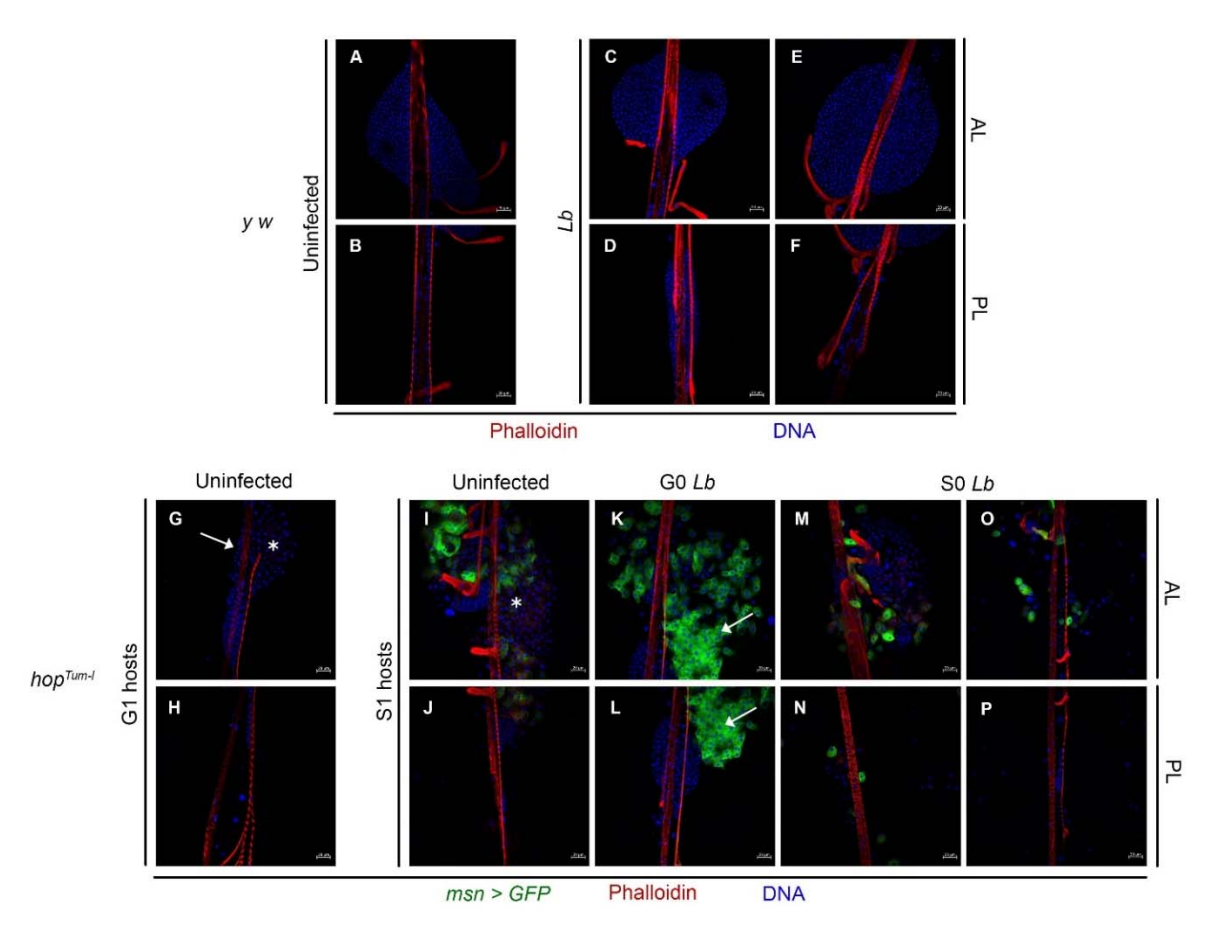


Figure S6. Lymph glands of naïve and *Lb*-parasitized G1 and S1 hosts, related to Figure 7.

- (A, B) Lymph glands of naïve G1 y w larvae.
- (C-F) Lymph glands of Lb-infected G1 (C, D) and Lb-infected S1 (E, F) y w hosts.
- **(G, H)** Lymph glands of naïve G1 *hop*^{Tum-l} hosts. Arrow in panel G shows absence of the left lobe and asterisk shows a reduced right lobe, likely due to release of differentiated hemocytes in the mutant background (compare with right lobe of panel I, as indicated by asterisk).
- (I-P) Lymph glands of S1 hop^{Tum-l} hosts. Naïve hosts (I, J). S1 hosts infected with G0 Lb (K, L) or S0 Lb (M-P). Arrow in panels K and L refer to tumor-containing, GFP-expressing lamellocytes. Anterior (AL) and posterior (PL) lobes are as shown. Scale bars 50 μ m. (n = 3 naïve y w, 8 G0 Lb-infected y w, and 3 S0 Lb-infected y w larvae).

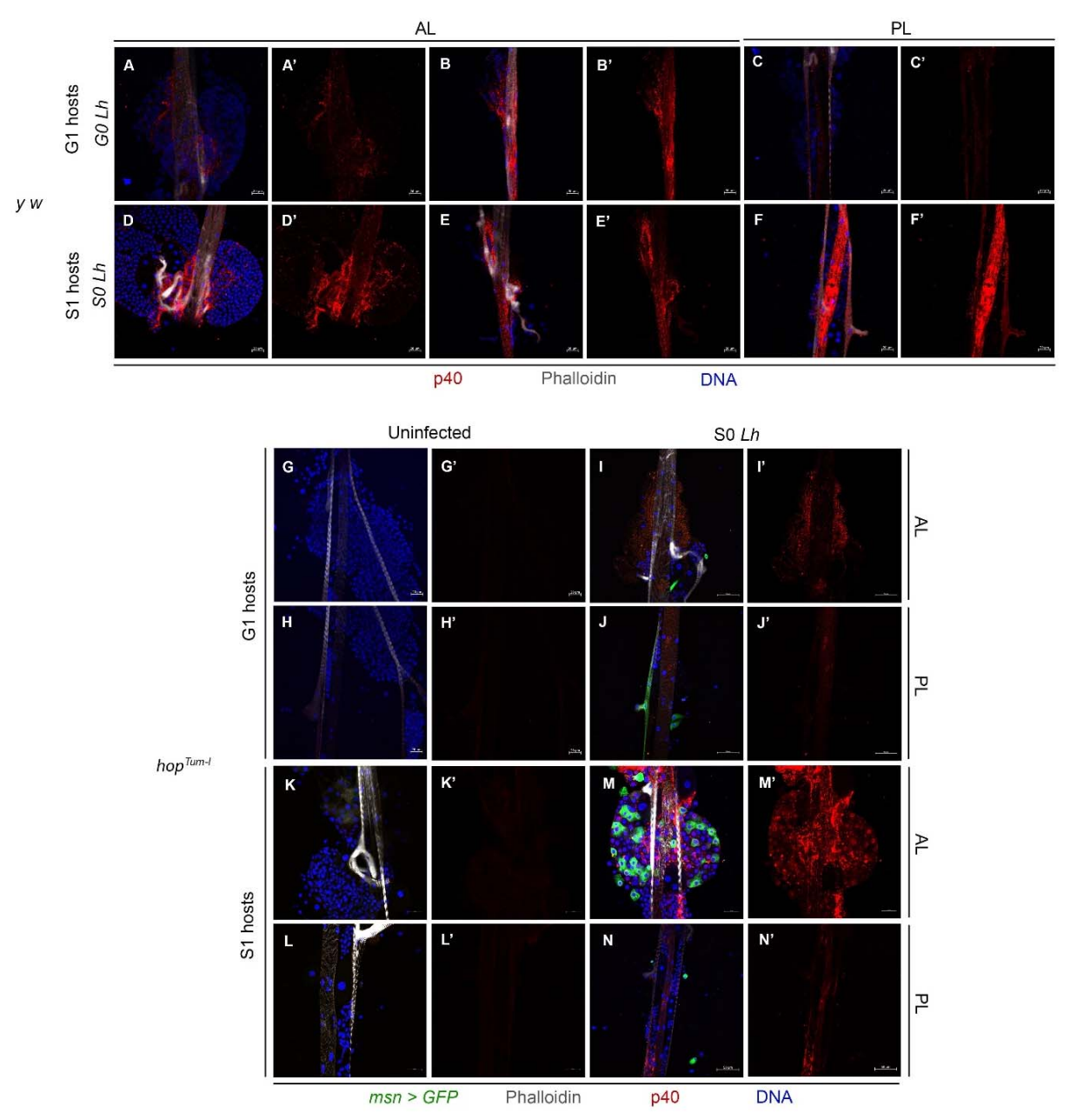


Figure S7. Lymph glands of naïve and Lh-infected G1 and S1 hosts, related to Figure 7.

(A-F') Lymph glands of *Lh*-infected G1 (A-C) and *Lh*-infected S1 (D-F) y w hosts.

(G-J') Lymph glands of naïve G1 hop^{Tum-l} hosts (G, H), or infected by S0 Lh (I, J).

(K-N') Lymph glands of naïve S1 hop^{Tum-l} hosts (K, L), or parasitized by S0 Lh (M, N). Primed panels show red-only channel to visualize EV distribution in the lymph glands.

Anterior (AL) and posterior (PL) lobes are as shown. Scale bars 50 µm.

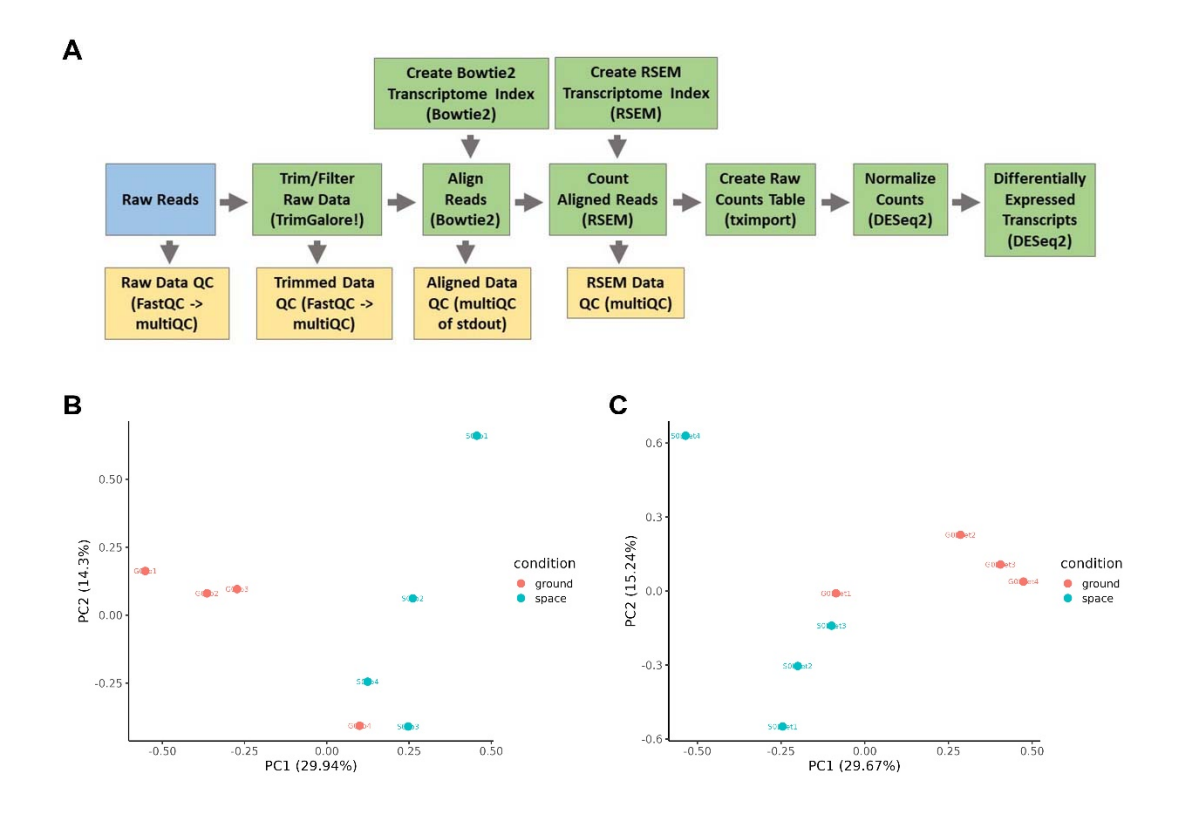


Figure S8. Evaluation of wasp parasite gene expression, related to Figure 8.

(A) Bioinformatics pipeline used for aligning RNA-Seq reads to available abdominal transcript sequences in the *Lb17* (GAJA00000000) and *Lh14* (GAJC00000000) transcriptomes 2 .

Differentially expressed transcripts in G0 and S0 *Lb17* and G0 and S0 *Lh14* were then identified (see Methods for more details).

(**B**, **C**) Principal component analysis of normalized counts from RNA-Seq samples of *Lb17* (B), and *Lh14* (C), obtained from ground and spaceflight conditions, as indicated.

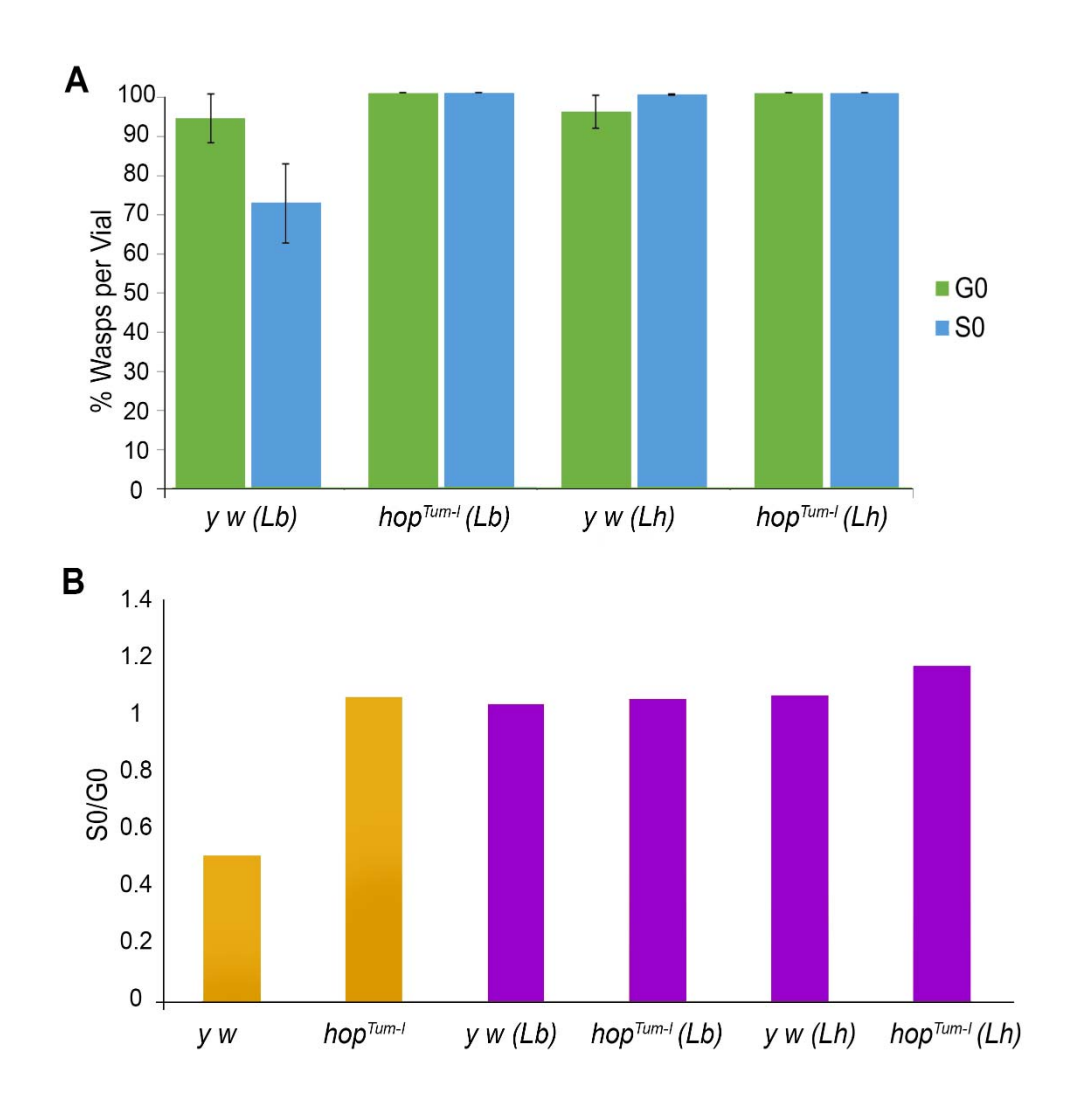


Figure S9. Survival of G0 and S0 adult flies and wasps, related to Figures 2 and 8.

- (A) Percentage of wasps relative to total insects scored per vial. For raw data, see legend of Figure 2D, E. The p-values for S0 versus G0 wasps are: Lb17 = 0.08 and Lh14 = 0.31 (Student t-test). No flies were observed in the hop^{Tum-l} co-cultures.
- **(B)** Ratio of S0/G0 flies in fly-only cultures (orange) and wasps in co-cultures (purple). Insects were scored from all replicates.

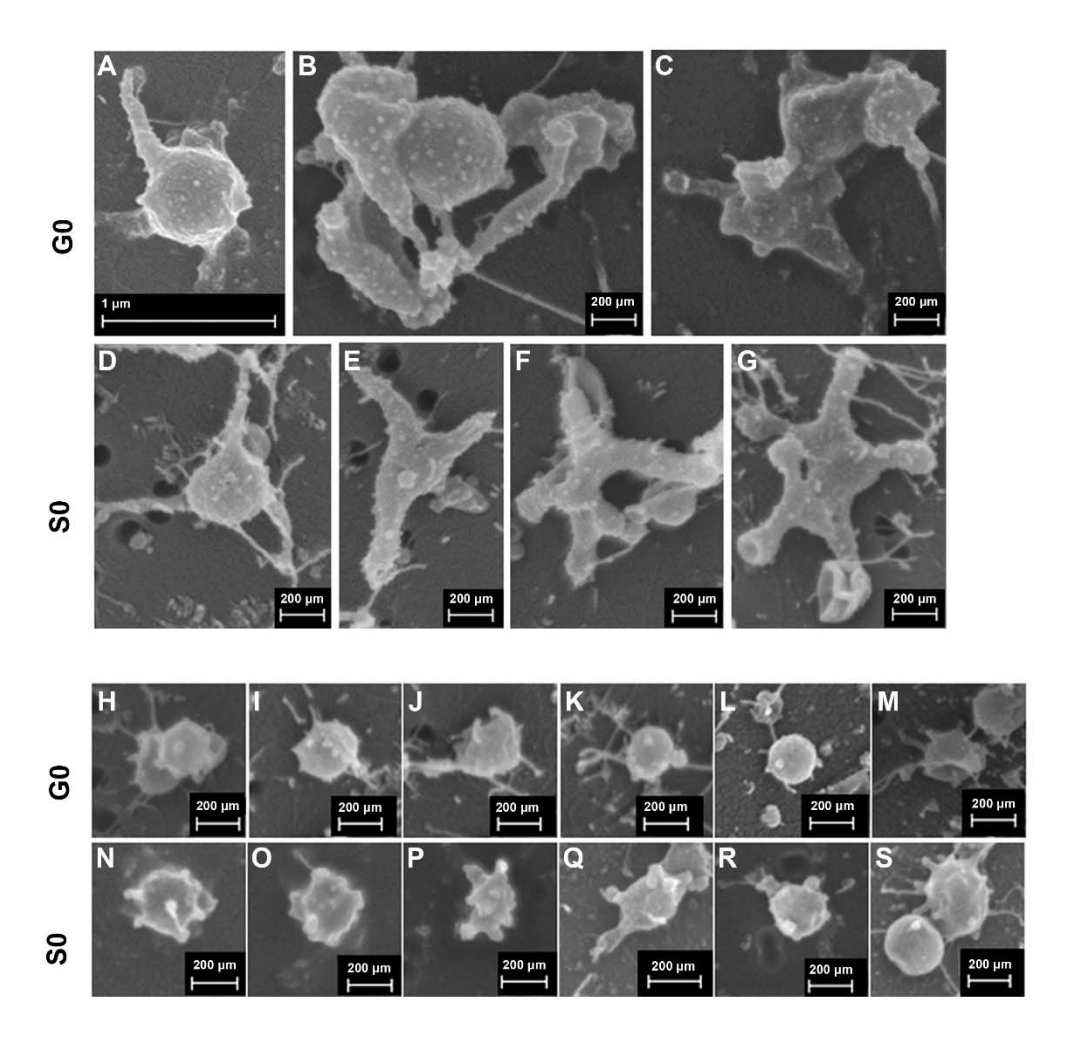


Figure S10. Extracellular vesicle-like particles from *L. boulardi* and *L. heterotoma*, related to Figures 2 and 8.

(A-S) Scanning electron micrographs of EVs from G0 *Lb* (A-C), S0 *Lb* (D-G), G0 *Lh* (H-M), and S0 *Lh* (N-S).

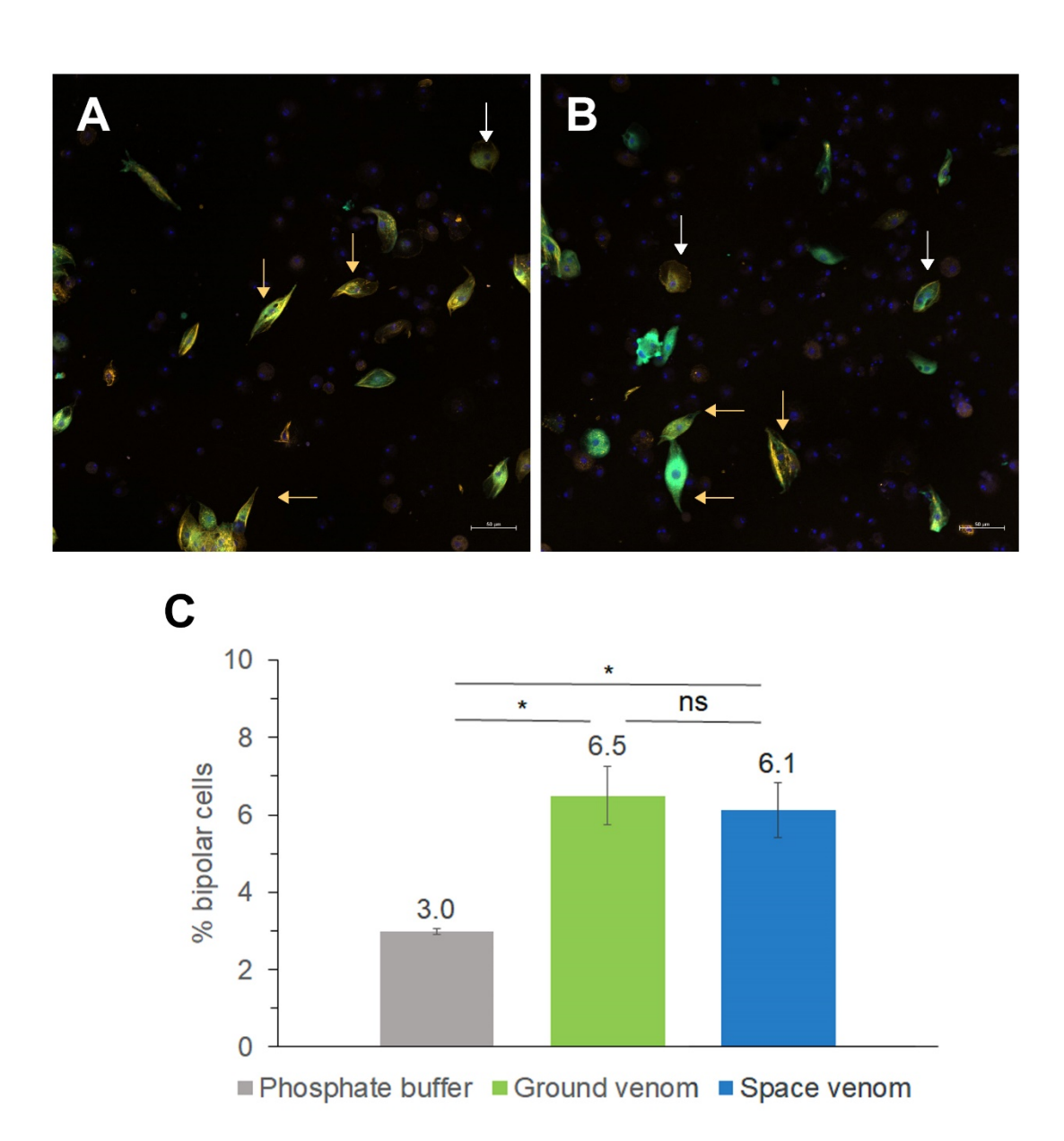


Figure S11. Assessing *L. heterotoma* venom activity *in vitro*, related to Figures 2 and 8.

(A-B) Confocal images of hemocytes from $hop^{Tum-l} msn > GFP$ larvae. Lamellocytes are GFP-positive; macrophages are GFP-negative. Normal Lh venom activity modifies a typical discoidal lamellocyte (white arrows) to assume a bipolar shape (yellow arrows). Hemocytes were incubated with venom from G0 (A) and S0 Lh14 wasps (B), respectively. Scale bars 50 μ m.

(C) Percent hemocytes with bipolar morphology after venom treatment (data are from 3-4 replicates). Differences between buffer control and G0/S0 venom activities are significant (indicated by *, Student t-test; p = 0.02 for both comparisons). G0/S0 venom effects on host lamellocytes are not significantly different (ns, p = 0.73). For phosphate buffer control, 129-347 lamellocytes were scored per replicate. The number of lamellocytes scored per replicate for G0 and S0 venom ranged from 290 to 721 and from 239 to 1,146, respectively.

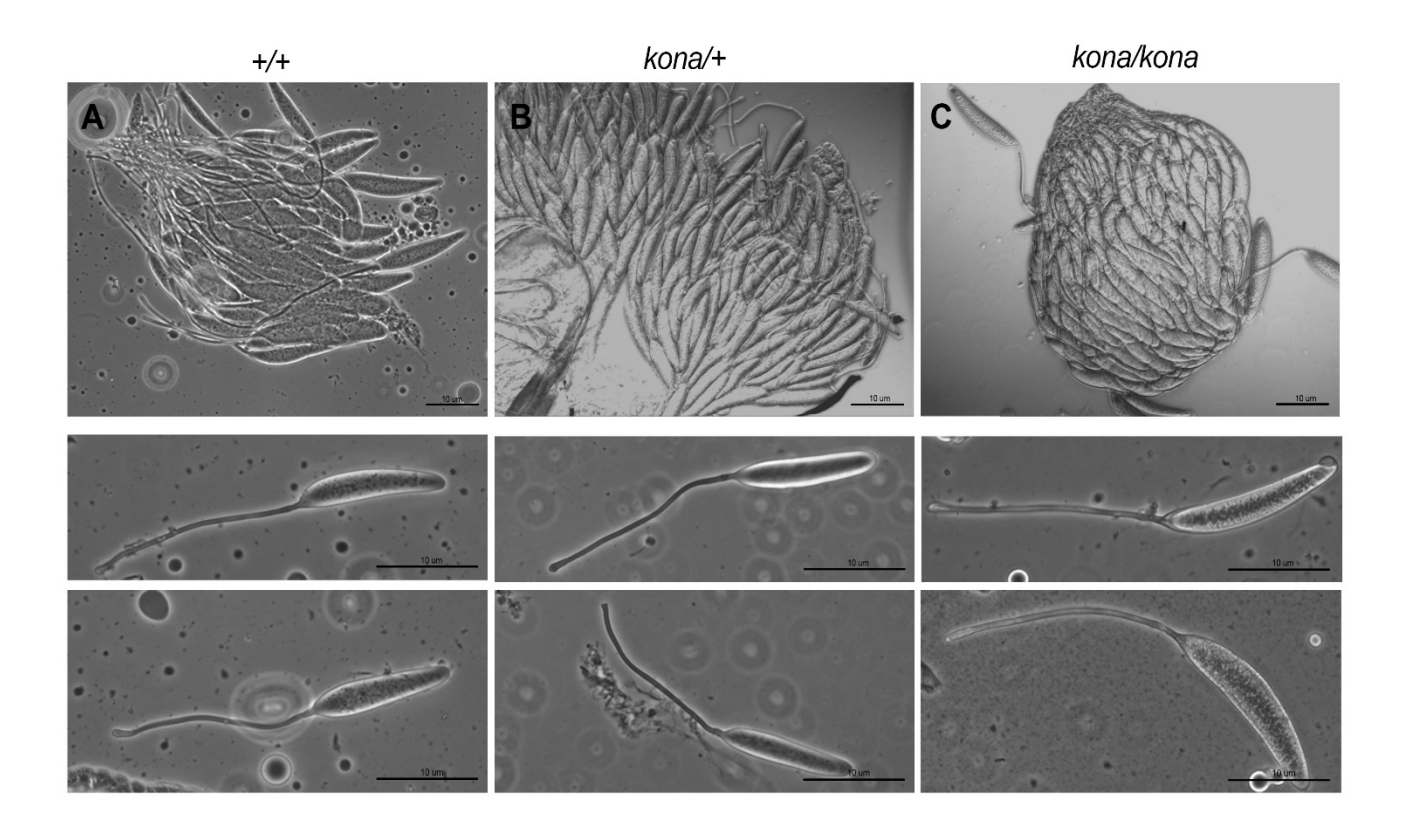


Figure S12. Ovaries from *L. heterotoma*, related to Figure 9.

(A-C) Ovaries and eggs from wild type (A), heterozygous (B), and homozygous *kona* mutant (C) wasps. Scale bars = 10 microns.

Table S1. Overall gene expression changes observed in naïve S0/G0 adult flies (top) and naïve S1/G1 larvae (bottom), related to Figures 3-5 and Figure S1.

The number and percent of expressed genes that are differentially expressed (DEGs, adjusted p < 0.05 and |log2FC| > 1) and either up- or down-regulated are shown. A total of 15,628 genes were expressed in adult flies and 16,123 genes were expressed in larvae. A *Drosophila* gene was considered expressed if the sum of raw counts across all samples was > 10.

Adult Comparisons	Change	# Genes	% Genes	% DEGs
•	up	1049	6.71	
G Tum-l vs. G y w	down	466	2.98	9.69
C. Trust 1 and C. and a	up	1061	6.79	14.02
S Tum-l vs. S y w	down	1131	7.24	14.03
Carrage Carrage	up	1221	7.81	12.22
Sywvs.Gyw	down	845	5.41	13.22
S Tum-l vs. G	up	538	3.44	6.78
Tum-l	down	521	3.33	0.78

Larval	Change	#	%	%
Comparisons	change	Genes	Genes	DEGs
G Tum-l vs. G y w	up	1984	12.31	29.29
G Tum-t Vs. G y W	down	2739	16.99	29.29
S. Tarre 1 va S and	up	1092	6.77	10.06
S Tum-l vs. S y w	down	530	3.29	10.00
Samuel Carrie	up	609	3.78	5.07
Sywvs.Gyw	down	208	1.29	5.07
S Tum-l vs. G	up	2345	14.54	21.17
Tum-l	down	1068	6.62	21.17

References

- 1. Gramates, L.S., Agapite, J., Attrill, H., Calvi, B.R., Crosby, M.A., Dos Santos, G., Goodman, J.L., Goutte-Gattat, D., Jenkins, V.K., Kaufman, T., et al. (2022). Fly Base: a guided tour of highlighted features. Genetics *220*. 10.1093/genetics/iyac035.
- 2. Goecks, J., Mortimer, N.T., Mobley, J.A., Bowersock, G.J., Taylor, J., Schlenke, T.A. (2013). Integrative approach reveals composition of endoparasitoid wasp venoms. PLoS One 8, e64125.

Supplemental Videos and Spreadsheets

Click here to access/download **Supplemental Videos and Spreadsheets**Table S2_12-03.xlsx

Supplemental Videos and Spreadsheets

Click here to access/download **Supplemental Videos and Spreadsheets**Table S3_12-03.xlsx

Supplemental File Sets

Click here to access/download

Supplemental File Sets

L.boulardi_

L.heterotoma_RNAseq_processing_scripts.zip



CELL PRESS DECLARATION OF INTERESTS POLICY

Transparency is essential for a reader's trust in the scientific process and for the credibility of published articles. At Cell Press, we feel that disclosure of competing interests is a critical aspect of transparency. Therefore, we require a "declaration of interests" section in which all authors disclose any financial or other interests related to the submitted work that (1) could affect or have the perception of affecting the author's objectivity or (2) could influence or have the perception of influencing the content of the article.

What types of articles does this apply to?

We require that you disclose competing interests for all submitted content by completing and submitting the form below. We also require that you include a "declaration of interests" section in the text of all articles even if there are no interests to declare.

What should I disclose?

We require that you and all authors disclose any personal financial interests (e.g., stocks or shares in companies with interests related to the submitted work or consulting fees from companies that could have interests related to the work), professional affiliations, advisory positions, board memberships (including membership on a journal's advisory board when publishing in that journal), or patent holdings that are related to the subject matter of the contribution. As a guideline, you need to declare an interest for (1) any affiliation associated with a payment or financial benefit exceeding \$10,000 p.a. or 5% ownership of a company or (2) research funding by a company with related interests. You do not need to disclose diversified mutual funds, 401ks, or investment trusts.

Authors should also disclose relevant financial interests of immediate family members. Cell Press uses the Public Health Service definition of "immediate family member," which includes spouse and dependent children.

Where do I declare competing interests?

Competing interests should be disclosed on this form as well as in a "declaration of interests" section in the manuscript. This section should include financial or other competing interests as well as affiliations that are not included in the author list. Examples of "declaration of interests" language include:

"AUTHOR is an employee and shareholder of COMPANY."

"AUTHOR is a founder of COMPANY and a member of its scientific advisory board."

NOTE: Primary affiliations should be included with the author list and do not need to be included in the "declaration of interests" section. Funding sources should be included in the "acknowledgments" section and also do not need to be included in the "declaration of interests" section. (A small number of front-matter article types do not include an "acknowledgments" section. For these articles, reporting of funding sources is not required.)

What if there are no competing interests to declare?

If you have no competing interests to declare, please note that in the "declaration of interests" section with the following wording:

"The authors declare no competing interests."



CELL PRESS DECLARATION OF INTERESTS FORM

If submitting materials via Editorial Manager, please complete this form and upload with your initial submission. Otherwise, please email as an attachment to the editor handling your manuscript.

Please complete each section of the form and insert any necessary "declaration of interests" statement in the text box at the end of the form. A matching statement should be included in a "declaration of interests" section in the manuscript.

"declaration of interests" section in the manuscript.
Institutional affiliations
We require that you list the current institutional affiliations of all authors, including academic, corporate, and industrial, on the title page of the manuscript. <i>Please select one of the following:</i>
■ All affiliations are listed on the title page of the manuscript.
☐ I or other authors have additional affiliations that we have noted in the "declaration of interests" section of the manuscript and on this form below.
<u>Funding sources</u> We require that you disclose all funding sources for the research described in this work. <i>Please confirm</i> the following:
All funding sources for this study are listed in the "acknowledgments" section of the manuscript.*
*A small number of front-matter article types do not include an "acknowledgments" section. For these, reporting funding sources is not required.
Competing financial interests We require that authors disclose any financial interests and any such interests of immediate family members, including financial holdings, professional affiliations, advisory positions, board memberships receipt of consulting fees, etc., that:
(1) could affect or have the perception of affecting the author's objectivity, or

Please select one of the following:

	members.
	the manuscript and on this form below, and we have noted interests of our immediate family
	We, the authors, have noted any financial interests in the "declaration of interests" section of
X	we, the authors and our immediate family members, have no financial interests to declare.

(2) could influence or have the perception of influencing the content of the article.



Advisory/management and consulting positions

We require that authors disclose any position, be it a member of a board or advisory committee or a paid consultant, that they have been involved with that is related to this study. We also require that members of our journal advisory boards disclose their position when publishing in that journal. *Please select one of the following:*

	e authors and our immediate family members, have no positions to declare and are embers of the journal's advisory board.				
consul	thors and/or their immediate family members have management/advisory or ting relationships noted in the "declaration of interests" section of the manuscript and form below.				
<u>Patents</u> We require that y Please select one	ou disclose any patents related to this work by any of the authors or their institutions. of the following:				
🗷 We, th	e authors and our immediate family members, have no related patents to declare.				
interes	e authors, have a patent related to this work, which is noted in the "declaration of its" section of the manuscript and on this form below, and we have noted the patents nediate family members.				
Please insert any "declaration of interests" statements in this space. This exact text should also be included in the "declaration of interests" section of the manuscript. If no authors have a competing interest, please insert the text, "The authors declare no competing interests."					
The authors declare no competing interests.					
On behalf of all authors, I declare that I have disclosed all competing interests related to this work. If any exist, they have been included in the "declaration of interests" section of the manuscript.					
Name:	Shubha Govind				
N. 4 - 1 - 1 - 1 - 1 - 1 - 1 - 1 - 1 - 1 -					
Manuscript number	ISCIENCE-D-23-03001R2				
(if available):					